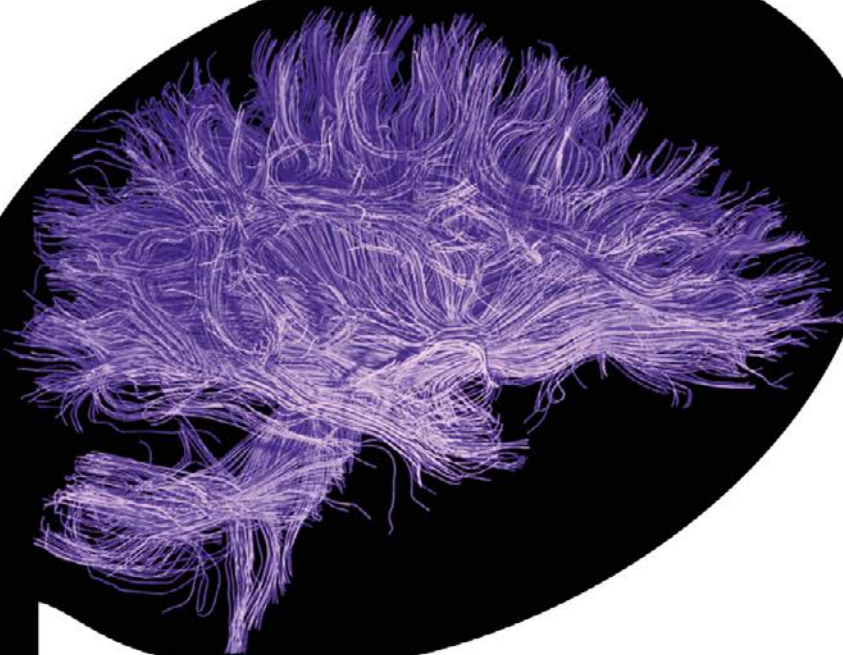




Turun yliopisto
University of Turku



NEURAL BASIS OF ACQUIRED AMUSIA AND ITS RECOVERY

Aleksi J. Sihvonen



Turun yliopisto
University of Turku

NEURAL BASIS OF ACQUIRED AMUSIA AND ITS RECOVERY

Aleksi J. Sihvonen

University of Turku

Faculty of Medicine

Department of Clinical Medicine

Neurology

Doctoral Programme in Clinical Research

Supervised by

Seppo Soinila, M.D., Ph.D.

Professor of Neurology

Division of Clinical Neurosciences

Turku University Hospital

Department of Neurology

University of Turku

Turku, Finland

Teppo Särkämö, Ph.D.

Docent, Psychologist

Cognitive Brain Research Unit

Department of Psychology and Logopedics

Faculty of Medicine

University of Helsinki

Helsinki, Finland

Reviewed by

David Copland, Ph.D.

Professor

UQ Centre for Clinical Research

Faculty of Medicine

University of Queensland

Queensland, Australia

Daniela Sammler, Ph.D.

Group Leader

Otto Hahn Group Neural Bases of Intonation in
Speech and Music

Max Planck Institute for Human Cognitive and
Brain Sciences

Leipzig, Germany

Opponent

Thomas Münte, M.D., Ph.D.

Professor of Neurology

Department of Neurology

University of Lübeck

Lübeck, Germany

Cover image by Aleks J. Sihvonen

The originality of this thesis has been checked in accordance with the University of Turku quality assurance system using the Turnitin OriginalityCheck service.

ISBN 978-951-29-7262-3 (PRINT)

ISBN 978-951-29-7263-0 (PDF)

ISSN 0355-9483 (Print)

ISSN 2343-3213 (Online)

Suomen Yliopistopaino Oy - Juvenes Print – Turku, Finland, 2018

To my family

ABSTRACT

Aleksi J. Sihvonen

NEURAL BASIS OF ACQUIRED AMUSIA AND ITS RECOVERY

From: University of Turku, Faculty of Medicine, Department of Clinical Medicine, Neurology, Doctoral Programme in Clinical Research

Annales Universitatis Turkuensis, Medica-Odontologica, 2018, Turku, Finland

Suomen Yliopistopaino Oy - Juvenes Print – Turku, Finland, 2018

In acquired amusia, the healthy music processing system in the brain is disrupted due to focal brain damage. This creates an exceptional opportunity to investigate the critical neural architectures of music processing. Yet, the neural basis of acquired amusia has remained largely unexplored.

In this multimodal magnetic resonance imaging (MRI) study of stroke patients with a 6-month follow-up, we systematically explored the neural basis of music processing by determining the lesions patterns, structural grey and white matter changes, and brain activation and functional network connectivity changes associated with acquired amusia and its recovery.

We found that damage to the right temporal areas, insula, and putamen forms the crucial neural substrate for acquired amusia after stroke. Longitudinally, persistent amusia was associated with further atrophy in the right superior temporal regions, located more anteriorly for rhythm-amusia and more posteriorly for pitch-amusia. In addition, persistent amusia was associated with structural damage and later degeneration in multiple right frontotemporal and frontal pathways as well as interhemispheric connections. Interestingly, rhythm-amusia was associated with additional deficits in left frontal connectivity. During listening to instrumental music, acquired amusics exhibited dysfunction of multiple frontal and temporal brain regions included in the large-scale music network. Interestingly, amusics showed less activation deficits during listening to vocal music, as compared to instrumental music, suggesting less defective processing of singing. Recovery from acquired amusia was related to increased activation in the right frontal and parietal areas as well as increased functional connectivity in the right and left frontoparietal networks.

Overall, the results provide a comprehensive neuroanatomical and functional picture of acquired amusia and highlight the neural structures crucial for normal music perception.

Keywords: Music, amusia, stroke, neuroimaging, neuroplasticity

TIIVISTELMÄ

Aleksi J. Sihvonen

AIVOINFARKTIN JA -VERENVUODON JÄLKEINEN MUSIIKIN KÄSITTELYN HÄIRIÖ JA SIITÄ KUNTOUTUMINEN

Turun yliopisto, Lääketieteellinen tiedekunta, kliininen laitos, neurologia, Turun kliininen tohtoriohjelma

Annales Universitatis Turkuensis, Medica-Odontologica, 2018, Turku, Finland
Suomen Yliopistopaino Oy - Juvenes Print – Turku, Finland, 2018

Hankinnaisessa amusiassa aivojen musiikinkäsittelyjärjestelmän normaali toiminta häiriintyy aivojen paikallisen vaurioitumisen takia. Tämä luo poikkeuksellisen mahdollisuuden tutkia musiikin käsittelylle tärkeitä aivorakenteita. Hankinnaisen amusian aivoperusta on kuitenkin suurelta osin vielä täysin tuntematonta.

Tässä aivoverenkiertohäiriön (AVH) sairastaneiden potilaiden 6 kuukauden seurantatutkimuksessa selvitimme magneettikuvantamisen avulla musiikin käsittelyn aivoperustaa tutkimalla, minkä aivoalueiden vauriot, mitkä harmaan ja valkean aineen rakenteelliset muutokset ja millaiset aivojen toiminnalliset muutokset liittyvät hankinnaiseen amusiaan ja siitä kuntoutumiseen.

Tuloksemme osoittivat, että AVH:n jälkeinen amusia syntyy oikean ohimolohkon yläosan, aivosaaren ja tyvitumakealueen vauriosta. Pysyvään amusiaan liittyi lisäksi harmaan aineen atrofiaa oikeassa ohimolohkossa. Rytmin havaitsemiseen liittyvässä amusiassa atrofia painottui ohimolohkon etuosaan ja äänenkorkeuden havaitsemiseen liittyvässä amusiassa ohimolohkon takaosaan. Lisäksi, pysyvään amusiaan liittyi laaja oikean aivopuoliskon ja aivopuoliskon välisten radastojen vaurio ja atrofia. Amusia aiheutti myös laajamittaisia aivojen toimintahäiriöitä musiikin kuuntelun aikana. Mielenkiintoista on, että toimintahäiriöt olivat suurempia kuunneltaessa instrumentaalimusiikkia kuin laulettua musiikkia. Amusiasta kuntoutuminen oli yhteydessä toiminnallisten yhteyksien vahvistumiseen oikean sekä vasemman aivopuoliskon otsa- ja päälakilohkojen välillä.

Tulokset antavat kattavan kuvan amusiaan johtavista aivovaurioista sekä siihen liittyvistä rakenteellisista ja toiminnallisista muutoksista. Lisäksi tulokset valottavat musiikin käsittelylle keskeisen tärkeitä aivorakenteita.

Avainsanat: Musiikki, amusia, aivoinfarkti, aivokuvantaminen, neuroplastisiteetti

TABLE OF CONTENTS

ABSTRACT.....	4
TIIVISTELMÄ	5
ABBREVIATIONS	9
LIST OF ORIGINAL PUBLICATIONS.....	11
1 INTRODUCTION	13
2 REVIEW OF THE LITERATURE	14
2.1 Stroke and its cognitive sequelae	14
2.2 Recovery after stroke: mechanisms and imaging.....	14
2.3 Music in the brain.....	17
2.3.1 Music processing in the healthy brain	17
2.3.2 Developmental and acquired deficits in music perception	20
2.3.2.1 Congenital amusia	20
2.3.2.2 Acquired amusia	22
3 AIMS.....	25
4 MATERIALS AND METHODS.....	26
4.1 Subjects	26
4.1.1 Helsinki cohort.....	26
4.2 Behavioural assessment.....	27
4.2.1 Assessment of music perception.....	27
4.2.2 Assessment of aphasia	28
4.3 Magnetic resonance imaging (MRI)	28
4.3.1 MRI data acquisition.....	28
4.3.2 MRI data processing	28
4.3.2.1 Preprocessing of diffusion data for Track-Based Spatial Statistics.....	29
4.3.2.2 Deterministic tractography	30
4.3.2.3 Functional MRIs	32
4.3.2.4 Independent component analysis and calculation of task-related networks	33
4.3.3 Voxel-based lesion-symptom mapping	33
4.3.4 Voxel-based morphometry.....	34
4.4 Statistical analyses.....	34
4.4.1 Study I: VLSM and VBM.....	35
4.4.2 Study II: TBSS and deterministic tractography	36
4.4.3 Study III: fMRI and ICA.....	37
5 RESULTS	39

5.1	Patient characteristics	39
5.1.1	Study I	39
5.1.2	Study II	39
5.1.3	Study III.....	39
5.2	Structural damage and volumetric changes associated with amusia and its recovery.....	42
5.2.1	Lesion patterns associated with amusia and aphasia.....	42
5.2.2	Grey and white matter changes associated with amusia recovery	45
5.3	White matter pathway damage in acquired amusia	46
5.3.1	Tract-based spatial statistics: amusia	46
5.3.2	Tract-based spatial statistics: pitch-amusia and rhythm-amusia	47
5.3.3	Deterministic tractography: amusia.....	49
5.3.4	Deterministic tractography: pitch-amusia	51
5.3.5	Deterministic tractography: rhythm-amusia.....	51
5.3.6	Deterministic tractography: regression analysis	51
5.4	Functional neural changes associated with acquired amusia and its recovery after stroke	54
5.4.1	fMRI activation patterns in amusic vs. non-music patients ..	54
5.4.2	fMRI activation patterns in amusia - the effect of aphasia	57
5.4.3	fMRI activation patterns in recovered vs. non-recovered amusic patients	59
5.4.4	Functional connectivity in amusic patients during music listening	61
6	DISCUSSION.....	63
6.1	Disrupted neural structures in acute acquired amusia	63
6.2	Recovery of post-stroke amusia.....	65
6.3	Dissociation of pitch and rhythm processing deficits in amusia	67
6.4	Neural model of acquired amusia	68
6.5	Limitations of the study	71
6.6	Clinical considerations.....	72
7	CONCLUSIONS	73
	ACKNOWLEDGEMENTS	74
	REFERENCES	77
	ORIGINAL PUBLICATIONS.....	99

ABBREVIATIONS

AC	Auditory cortex
ANOVA	Analysis of variance
ASRS	Aphasia Severity Rating Scale
BA	Brodmann area
BDAE	Boston Diagnostic Aphasia Examination
CC	Corpus callosum
CG	Cingulate gyrus
DT	Deterministic tractography
DTI	Diffusion tensor imaging
DW-MRI	Diffusion-weighted magnetic resonance imaging
EEG	Electroencephalography
FA	Fractional anisotropy
FC	Functional connectivity
FDR	False discovery rate
fMRI	Functional magnetic resonance imaging
FWE	Familywise error rate
GM	Grey matter
GMV	Grey matter volume
HG	Heschl's gyrus
ICA	Independent component analysis
IFG	Inferior frontal gyrus
IFOF	Inferior fronto-occipital fasciculus
ILF	Inferior longitudinal fasciculus
IPL	Inferior parietal lobule
ITG	Inferior temporal gyrus
LHD	Left hemisphere damage
MBEA	Montreal Battery of Evaluation of Amusia
MD	Mean diffusivity
MEG	Magnetoencephalography
MFG	Middle frontal gyrus
MMN	Mismatch negativity
MRI	Magnetic resonance imaging
MTG	Middle temporal gyrus
NA	Non-amusic
NRA	Non-recovered amusic
pNA	Non-pitch-amusic
pNRA	Non-recovered pitch-amusic

Abbreviations

pRA	Recovered pitch-amusic
Pre-SMA	Pre-supplementary motor area
RA	Recovered amusic
RHD	Right hemisphere damage
RD	Radial diffusivity
rNA	Non-rhythm-amusic
rNRA	Non-recovered rhythm-amusic
rRA	Recovered rhythm-amusic
SMA	Supplementary motor area
SOG	Superior occipital gyrus
SPL	Superior parietal lobule
STG	Superior temporal gyrus
STS	Superior temporal sulcus
TBSS	Tract-based spatial statistics
UF	Uncinate fasciculus
VBM	Voxel-based morphometry
VLSM	Voxel-based lesion-symptom mapping
WM	White matter
WMV	White matter volume

LIST OF ORIGINAL PUBLICATIONS

- I Sihvonen AJ, Ripollés P, Leo V, Rodríguez-Fornells A, Soinila S, Särkämö T. Neural Basis of Acquired Amusia and Its Recovery after Stroke. *J Neurosci* 2016; 36(34):8872–8881.

- II Sihvonen AJ, Ripollés P, Särkämö T, Leo V, Rodríguez-Fornells A, Saunavaara J, Parkkola R, Soinila S. Tracting the neural basis of music: deficient structural connectivity underlying acquired amusia. *Cortex* 2017; 97:253-271.

- III Sihvonen AJ, Särkämö T, Ripollés P, Leo V, Saunavaara J, Parkkola R, Rodríguez-Fornells A, Soinila S. Functional neural changes associated with acquired amusia across different stages of recovery after stroke. *Sci Rep* 2017; 7(1):11390.

The original communications have been reproduced with the permission of the copyright holders.

1 INTRODUCTION

H.C. Andersen (1805 – 1875) wrote: “*Where words fail, music speaks.*”¹. Similar to language, the ability to enjoy and produce music is unique to us humans. Music is ubiquitous, present in all societies and cultures, and a diverse form of art and expression of emotions.

Music virtually activates almost all brain lobes and involves a wide-range of demanding cognitive processes (e.g. memory, attention)²⁻⁷. While studies with healthy subjects have revealed the vast neural network activated by musical stimuli, they have been unable to pin down the most critical neural substrate of musical processing in the brain. For tracking down the crucial foundation for music processing in the brain, music, not words, needs to fail.

Amusia, caused by either abnormal brain development (congenital amusia) or brain damage (acquired amusia), is a neurological disorder characterized primarily by inability to perceive small-scale pitch changes. In addition, the processing of musical rhythm, timbre, memory, and emotions can also be affected.^{8,9} Congenital amusia is a life-long condition and therefore reflects not only impaired music perception, but also a developmental deficit in acquiring musical syntax and tonal representations¹⁰, whereas acquired amusia is characterized by a clear-cut transition from a normally functioning to deficient music processing system caused by brain damage. This creates a naturalistic opportunity to examine and pin down the brain areas that are crucial for music perception¹¹.

Although acquired amusia is relatively common after stroke, affecting 35 to 69 per cent of the patients¹²⁻¹⁴, the exploration of its neuroanatomical basis has previously been limited to symptom-led and lesion-led studies of individual cases or small patient groups. Acquired amusia has been associated with damage to various temporal, frontal, parietal, and subcortical regions⁸, but results regarding lesion location, even at hemispheric level, and type of musical deficit caused by the lesion have been variable: Some studies have reported spectral (e.g. pitch) or temporal (e.g., rhythm) deficits mainly after right hemisphere damage^{15, 16} or after both left and right hemisphere damage^{12, 13, 17-19}. Overall, the previous studies have been constrained by small sample sizes and low spatial accuracy, and thus they provide only coarse information about critical brain areas for perceiving the different elements of music.

To uncover the brain regions crucial for music perception, systematic and longitudinal research on the neural basis of acquired amusia and its recovery is still needed. Clinically, this information is also important for establishing a more accurate diagnosis and prognosis of amusia and for planning rehabilitation.

2 REVIEW OF THE LITERATURE

2.1 Stroke and its cognitive sequelae

Stroke is caused by interrupted or reduced blood supply to the brain, resulting from either a blocked artery (an ischaemic stroke) or a ruptured blood vessel (a haemorrhagic stroke). Stroke deprives the brain of oxygen and nutrients and leads to permanent neural damage. Of all strokes, approximately 80 per cent are ischemic strokes, 10 per cent are haemorrhagic strokes, and the remaining 10 per cent are due to subarachnoid haemorrhage or of undefined pathological type of stroke²⁰. Worldwide, approximately 80 out of 100,000 persons suffer from ischaemic stroke each year²⁰. In Finland, 16,000 ischaemic strokes occurred in the year 2014²¹. While the incidence of stroke is declining²², the overall prevalence of stroke remains high, and continues to increase, due to the rapid aging of the population²³.

Globally, stroke is a leading cause of acquired disability in adults and the second most common cause of death, surpassed in prevalence only by ischemic heart disease²⁴. Of the stroke survivors, two-thirds have been demonstrated to have some neurologic impairment and disability 5 years after the initial stroke²⁵. The most prevalent consequence of stroke is motor impairment (i.e. paresis) which affects approximately 80 per cent of the patients²⁶. In addition, more than half of the acute stroke patients demonstrate impairment in one or more cognitive domains²⁷, with a mean of three impaired domains per patient²⁸. Most frequently the patients show deficits in executive function (32-39%), visual perception and construction (32-38%), reasoning (24-26%), and language and verbal memory (22-26%)^{27, 28}. 6 to 10 months after the stroke onset, a substantial percentage of the patients still have impairments in executive function (13%), visual perception and construction (8%), reasoning (18%), and language and verbal memory (7-15%)²⁸. While the mean number of impaired cognitive domains per patient decreases over time, patients with a small number of cognitive impairments at the acute stage of stroke achieve complete cognitive recovery more often than patients with impairments in multiple cognitive domains²⁸.

2.2 Recovery after stroke: mechanisms and imaging

During an acute stroke, due to the halted supply of vital metabolic substrates, the normal function of neurons is disrupted within seconds and structural damage begins to occur after only two minutes²⁹. Continuing deprivation on oxygen and vital nutrients leads to cell death cascades^{30, 31} and, eventually, to impairment of motor, sensory, and cognitive functions^{31, 32}. Although neurons that have highly specific

functions are lost in stroke, spontaneous functional recovery takes place at least partially. Most of this recovery occurs within 3 months after stroke onset³³⁻³⁵, but recovery may take place even many years after the initial brain injury^{35,36}. As many as one third of stroke patients with cognitive impairment have been shown to improve their cognitive function beyond the first 3 months³⁷. The recovery of mild impairments is faster compared to more severe deficits. For example, in mild aphasia, the final level of language function is achieved after only 2 weeks post-stroke, while in severe aphasia it occurs by the 10-week post-stroke stage³⁸. However, the functional recovery can continue over years³⁶. In addition, patterns and rates of recovery can vary across different neurological domains³⁹.

Information derived from animal models of stroke has shown that repair-related molecular and cellular changes are pronounced in, but not limited to, the peri-infarct area (i.e. area surrounding the stroke zone)³⁵. Some changes occur also in homologous sites in the contralesional hemisphere as well as in remote regions functionally connected to the site of the lesion. Traditionally, functional MRI (fMRI) has been used to explore the neural changes associated with stroke recovery⁴⁰, and studies on humans have shown that the best spontaneous return of function (e.g. hand movement or language) is associated with return of brain activity in the primary lesion site³⁵. Furthermore, stroke patients with nearly normal task-related brain activity are more likely to recover⁴¹. Overall, the recovery of function is supported by reorganization observed in the neural network that survived the stroke. Three main elements of this reorganization are: 1) increased activity of the distant brain regions functionally connected to the primary lesion site, 2) increased activity in the contralesional hemisphere, and 3) somatotopic¹ shifts in the ipsilateral spared brain regions³⁵. In post-stroke aphasia, the recovery of language function has been observed to include three different phases: (i) initially reduced activation in the ipsilateral (left) frontotemporal language areas at acute stage, followed by (ii) upregulation or increase of activation in homologous contralesional (right) areas (especially right inferior frontal and supplementary motor areas) at subacute stage, and, finally, (iii) increased (normalized) activity in the ipsilateral (left) hemisphere at chronic stage³³. This suggests that the brain activity patterns associated with the recovery of post-stroke deficits are dynamic across time, including the recruitment of different brain regions during the acute and chronic phases of stroke, and overall, increased neural activity in remaining left language areas correlates with better language outcomes³³. The exact function of the contralesional increases in activity remains unclear, but they are thought to represent reduced interhemispheric inhibition (i.e. disinhibition) after stroke^{35,42}. In the motor domain, persisting disinhibition has been associated with poor recovery⁴². In

¹ Somatotopic refers to the specific relation between particular body regions and corresponding sensory and motor areas of the brain.

contrast, the increase in ipsilateral network-level activity and the reduction in laterality may compensate the reduced functional capacity caused by the stroke³⁵.

Post-stroke rehabilitation aims to reduce impairments and disabilities. At the brain level, rehabilitation-induced functional recovery is based on enhanced neuroplasticity, for example, axonal growth and sprouting, remyelination, and synaptogenesis⁴³ as well as reorganization of affected functional networks³⁵. Similar mechanisms are likely to underlie spontaneous recovery of stroke⁴³. These changes are not limited to the ischemic boundary zone, since stroke induces corresponding molecular and cellular changes in brain regions remote to the ischemic core, as well^{43, 44}. If the restitution of the lost function cannot be achieved, recovery may also take place through compensatory mechanisms: neural networks that did not subservise the lost function prior to stroke acquire the lost function during the recovery^{45, 46}. This compensatory neural recruitment leads to activation in alternative brain regions not normally observed in nondisabled individuals⁴⁵.

Diffusion-weighted magnetic resonance imaging (DW-MRI) is an advanced MRI method that uses the diffusion of water molecules to generate contrast in MR images. In biological tissues, such as brain, the molecular diffusion movement is not free, but reflects interactions with anatomical structures such as fibres and membranes. One of the extensions of DW-MRI is diffusion tensor imaging (DTI) which can be used to evaluate connectivity of white matter (WM) pathways and pathological tract disruption associated with stroke deficits and their recovery. Various indices of WM structure can be extracted by calculating tensors from the acquired diffusion images. Fractional anisotropy (FA) is a scalar value between zero and one that describes diffusion in different directions (anisotropy)⁴⁷. A value of zero reflects isotropic diffusion, whereas a value of one means that diffusion occurs only along one axis. FA is highly sensitive to microstructural changes. Mean diffusivity (MD) is a directionally averaged measure of the total diffusion within a voxel⁴⁷. MD is an inverse measure of the membrane density, and it is sensitive to cellularity, edema, and necrosis⁴⁷. Radial diffusivity (RD) describes the diffusivity perpendicular to the main axis, and it is influenced by changes in axonal density⁴⁷. Comparison of different DTI indices in the same WM pathway gives more specific information about the type of change. For example, aphasics have lower FA values and higher MD and RD values in language-related white matter tracts than patients without post-stroke aphasia⁴⁸. Also in post-stroke motor deficits, axonal damage and poor outcome have been linked to decreased FA and increased MD and RD in motor pathways⁴⁹. Increased RD⁵⁰⁻⁵² and decreased FA⁵² have also been linked to dys- and demyelination.

Neuroimaging analysis techniques such as voxel-based lesion-symptom mapping (VLSM) and voxel-based morphometry (VBM) are not in clinical use but are widely applied in studies with stroke patients. Using similar voxel-based procedures used to analyse functional neuroimaging data, VLSM is used to analyse the

relationship between focal brain damage and behaviour⁵³ whereas VBM can be used to compare local grey matter volume (GMV) and white matter volume (WMV) differences between two groups of subjects or across time⁵⁴. For example, in stroke, VLSM and VBM have been used to map crucial brain regions in aphasia and its recovery^{53, 55-61} as well as to identify critical areas for motor function recovery⁶²⁻⁶⁵ and post-stroke cognitive deficits^{66, 67}. Combining modern MRI analysis methods with multimodal stroke imaging techniques can potentially provide a more comprehensive conception of the neural changes associated with the post-stroke deficit under inspection as well as the various mechanisms underlying the functional recovery.

2.3 Music in the brain

The ability to perceive, enjoy, and produce music is a core element of human mental function. Since birth, infants show functional specializations for processing musical structures, such as tonality and chord categories, in the brain^{68, 69}, and at the age of 6 months, prelinguistic infants enjoy moving rhythmically to music⁷⁰. Although music is a source of one of the most powerful stimulation for the human brain^{71, 72}, its evolutionary origins are still largely unknown. Archaeological findings have provided evidence that musical instruments have existed in human culture at least for the last 35,000 years⁷³. Furthermore, it has been suggested that the ability to sing could even have pre-dated the development of speech, which manifested as early as 200,000 years ago⁷⁴. Indisputably, music has a vital role in both history of human evolution and in modern human life. Given our long history with music, it is likely that our brains have evolved to process music in a specific way.

2.3.1 Music processing in the healthy brain

Attempts to unravel the neural structures underlying music processing in the brain have been active during the past two decades. Advanced neuroimaging methods evaluating both brain structure and function in healthy subjects have provided evidence of the large-scale music network comprising bilateral temporal, frontal, parietal, and subcortical regions^{2, 4-6, 75, 76}. Studies in healthy subjects have indicated that superior temporal areas, especially in the right hemisphere, are crucial for processing pitch and melodies⁷⁷⁻⁸¹. Interestingly, the processing of spectral and temporal auditory information has been observed to be lateralised in the brain: the right auditory cortex (AC) is more specialized in fine-grained spectral processing whereas the left AC is active in rapid temporal processing of sounds^{82, 83}. Moreover, the superior temporal gyrus (STG), and region around the superior temporal

sulcus (STS), seem to be functionally segregated in anterior-posterior direction for temporal and spectral auditory information processing in both animals⁸⁴ and humans^{75, 83, 85}: anterior regions show greater sensitivity to changes in the temporal domain and posterior regions to changes in the spectral domain. However, no clear lateralisation effects for rhythm processing in music have been observed in healthy subjects^{4, 75}.

Music is much more than the sum of its acoustic components. Mere music listening engages various cognitive, emotional, and motor responses and involves multiple spatially distributed brain regions via the wide-spread musical network (Figure 1). The processing of higher order musical features (e.g. chords, harmony) requires simultaneous and sequential analysis of pitch structures. This involves the STG, the inferior frontal gyrus (IFG), the medial prefrontal cortex, the inferior parietal lobule (IPL), and the premotor cortex⁸⁶⁻⁹¹. In contrast to pitch, the perception of rhythm involves a motor network comprising the cerebellum, the basal ganglia, and the primary motor cortex⁹²⁻⁹⁵. When musical features such as melodies are followed in time, a frontoparietal network, including the IFG, the prefrontal cortex, the anterior cingulate gyrus (CG), and the IPL, is engaged to serve focused attention and working memory⁹⁶⁻⁹⁸. Partly overlapping brain regions are involved in recognising familiar music and recalling associated musical memories. Both engage the episodic memory network comprising the prefrontal cortex, the IFG, the middle temporal gyrus (MTG), the angular gyrus, the precuneus, and the hippocampus⁹⁹⁻¹⁰¹. Finally, emotionally engaging music activates the dopaminergic reward and emotion network, including the nucleus accumbens, the amygdala, the ventral tegmental area, the hippocampus, the striatum, the anterior CG, and the orbitofrontal cortex¹⁰²⁻¹⁰⁷.

One core facet of music is singing which combines characteristics of both language (e.g. linguistic syntax, semantics) and music (e.g. melody, harmony, rhythm). Neuroimaging studies on healthy subjects have shown that the processing of music and speech share resources in the brain, but preferentially engage distinct cortical networks: listening to music activates the insula and superior temporal regions bilaterally as well as the right IFG more than listening to speech¹⁰⁸. Similarly, both shared and distinct neural networks facilitate singing and speaking. Both functions engage a large network including sensorimotor areas and inferior frontal regions, but compared to speaking, singing induces greater activations in the right STG and Heschl's gyrus (HG) as well as in the right pre- (PreCG) and postcentral gyri (PCG) and the right IFG^{109, 110}. An interesting lateralisation pattern is also present in music containing sung lyrics (i.e. vocal music): it activates, in addition to the right STG and HG activations induced by music in general, also language-related left hemisphere structures such as the left STG and IFG, as well as the putamen, cuneus, PCG, and the cerebellum². However, the degree to which the processing of lyrics and tunes in a song is integrated in the brain is under debate,

as lyrics and tunes have been shown to have separate¹¹¹⁻¹¹³ and associated^{114, 115} processes.

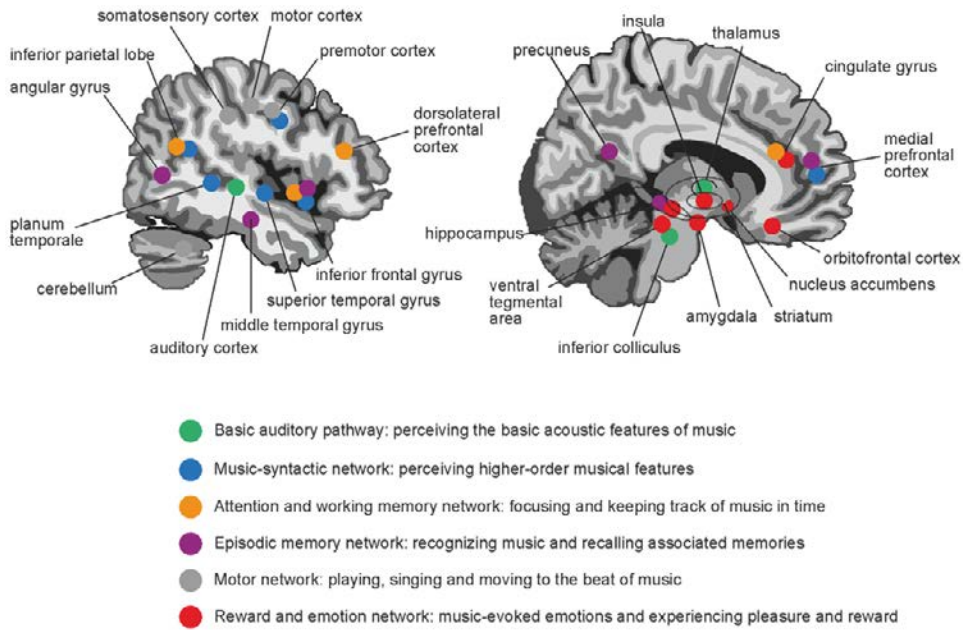


Figure 1 Schematic illustration of the key brain areas associated with music processing. While the figure displays the lateral and medial parts of the right hemisphere, musical subfunctions are largely bilateral, with the exception of pitch and melody processing which are dominantly right-lateralised. Modified from Särkämö et al. 2013¹¹⁶.

Cortically processed information is distributed by WM pathways which form neural networks interconnecting spatially distributed brain regions. As music processing involves a large-scale network comprising bilateral temporal, frontal, parietal, and subcortical regions^{2, 4, 76}, it is most likely mediated by various WM pathways interconnecting these brain areas. For example, temporal regions crucial for music are connected to frontal and occipital regions by the inferior fronto-occipital fasciculus (IFOF)¹¹⁷⁻¹²¹ and to inferior frontal areas by the uncinate fasciculus (UF)¹¹⁸. Interestingly, these structures differ in individuals with exceptional musical capabilities as compared to average healthy subjects. Persons with absolute pitch have increased WM integrity in both of these tracts in the right hemisphere¹²² as well as in the inferior longitudinal fasciculus (ILF), which connects temporal and occipital cortices¹¹⁷. Moreover, increased WM integrity in the right IFOF has been associated with musical synesthesia¹²³.

Studies of long-term musical training have provided another line of evidence to support the involvement of particular WM pathways in music processing. Compared to non-musicians, musicians have been reported to show neuroplastic changes of WM (e.g. changes in tract volume and FA) in the IFOF¹²⁴, the arcuate fasciculus (AF)/superior longitudinal fasciculus (SLF)¹²⁵⁻¹²⁷, the corpus callosum (CC)^{124, 125, 128}, the pyramidal tracts^{124, 125, 129, 130}, and in the cerebellar tracts^{124, 131}. Musical training also induces grey matter (GM) structural changes. For example, compared to non-musicians, musicians have been shown to have larger volume of the motor cortex^{132, 133}, as well as different temporal auditory^{132, 134, 135}, inferior frontal^{135, 136}, and subcortical regions¹³⁴. Moreover, the GM plastic changes seem to be correlated with the age of onset of musical training^{134, 137}. However, given the complexity and diverse nature of long-term musical training, these neuroplastic changes reflect not only the improved auditory-perceptual functions, but also the interaction of multiple auditory, motor, tactile, and cognitive functions.

2.3.2 Developmental and acquired deficits in music perception

2.3.2.1 Congenital amusia

The ability to perceive music can be impaired by either abnormal brain development (congenital amusia) or brain damage (acquired amusia). While the deficit in processing fine-grained pitch changes is the hallmark symptom of amusia – arguably due to an impairment of pitch perception and/or pitch-specific short-term or working memory – other domains of music, such as rhythm, timbre, memory, and emotions, can also be affected^{8, 9, 138-140}.

The majority of the neuroimaging studies examining defective music processing in the brain have been carried out in congenital amusia which affects around 2 per cent of the population¹⁴¹⁻¹⁴³. Morphological studies on the brain utilizing VBM⁵⁴ have provided evidence of reduced white matter concentration in the right IFG^{144, 145} and STG¹⁴⁵ in congenital amusics. In the same brain regions, congenital amusics have been observed to have thicker cortex than healthy controls which has been proposed to be related to a malformation in cortical development¹⁴⁶. However, in congenital amusia, the reported results regarding the laterality of the observed differences have been contradictory. Mandell et al. (2007) reported that congenital amusics had decreased GMV in the left IFG and STG while the homologous areas of the right hemisphere showed no differences¹⁴⁷.

These findings suggest that congenital amusia is most likely a heterogeneous condition¹⁴⁸. On the other hand, variable VBM methodology has been used in the studies cited. One of the most critical preprocessing steps in VBM is modulation

which multiplies the voxel intensity by the Jacobian determinant from the normalization process to allow testing for regional differences in the absolute amount (volume) of GM^{54, 149}. Out of the three VBM studies published in congenital amusia, only that by Mandell et al. (2007) has incorporated modulation in the processing of MRI data. In contrast, the two other studies^{144, 145} analysed unmodulated data and therefore looked at differences in concentration of GM (per unit volume in native space)^{54, 149}. Results derived from modulated and unmodulated data do not represent the same phenomena and, therefore, need to be interpreted differently. Incorporation of modulation step in the preprocessing is preferable to ensure that intersubject alignment preserves intergroup differences in morphology¹⁵⁰.

In addition to the findings on cortical anomaly, studies have provided information on structural connectivity deficits in congenital amusia. However, the direct evidence for structural WM abnormalities in congenital amusia is scarce and insufficient: there are only two previous tractography studies which both investigated only one tract, the AF^{151, 152}. Moreover, these two studies yielded conflicting findings: while Loui et al. (2009) compared 10 congenital amusics to 10 healthy controls and found that congenital amusics had decreased volume of the right AF, Chen et al. (2015) compared 26 congenital amusics to 26 healthy subjects and found no significant differences between the groups. In addition to these two tractography studies evaluating a specific neural tract, a recent study suggests that congenital amusics have reduced whole brain global connectivity in WM structure as well as alterations in the nodal strength of the right IPL compared to controls¹⁵³.

To date, only three published fMRI studies have investigated brain processing deficits in congenital amusia. Passive listening tasks with simple melodic sequence¹⁵⁴ and harmonic tone¹⁵⁵ stimuli have revealed normal activity patterns in the pitch-responsive brain regions in the AC in congenital amusics. However, the function of the right IFG as well as the connectivity between the right IFG and AC have been reported to be abnormal during a melody listening task¹⁵⁴. Furthermore, using resting-state fMRI (i.e. functional imaging without any stimulus), frontotemporal functional connectivity (FC) has been found to be reduced in congenital amusia¹⁵⁶. Electrophysiological recordings using electroencephalography (EEG) have provided additional information on the functional deficits in congenital amusia. Unlike controls, congenital amusics have been reported to elicit abnormal right-lateralised brain responses to pitch deviants in melody¹⁵⁷⁻¹⁵⁹ and abnormal frontal responses to timbre deviants in melody¹⁶⁰. Furthermore, congenital amusics have shown aberrant EEG responses while detecting the direction of pitch change¹⁶¹.

Although the previous fMRI studies have revealed brain structures involved in the processing of individual musical features in congenital amusia, they have utilized artificially manipulated and controlled auditory paradigms instead of naturalistic music. As music is much more than the sum of its acoustic components, studying natural music listening could provide more thorough and accurate outlook

on how the processing of musical elements is affected in the amusic brain⁴. Logically, if the processing of musical components is affected in amusia, it should also induce deficits in the action of the large-scale music network when using natural music as stimuli.

Recent studies have begun to explore potential ways to train musical skills in congenital amusia. A singing intervention has been found to improve song production in congenital amusics^{162, 163} as well as improve their performance in the Scale¹⁶² and Meter¹⁶³ subtests of the Montreal Battery of Evaluation of Amusia (MBEA). Interestingly, congenital amusics can apparently sing pitch intervals in correct directions while being unable to consciously perceive their differences¹⁶⁴, suggesting a dissociation of music perception and production in amusia. Moreover, congenital amusics have been suggested to be able to recognize the lyrics of familiar songs while they are unable to recognize the corresponding melodies¹⁶⁵. Taken together, these findings suggest that in spite of impaired pitch processing, the processing of vocal music may be partially spared in amusia, although the neural basis for this effect has never been studied.

2.3.2.2 *Acquired amusia*

The two types of amusia, congenital and acquired, may have partly different neural basis: congenital amusia is a life-long condition and reflects both impaired music perception and a developmental deficit in acquiring musical syntax and tonal representations¹⁰, which may hamper the early development of the music processing network in the brain¹⁰. Contrary to developmental deficit of music perception, acquired amusia is characterized by a transition from previously normal to deficient function of the music processing system caused by a brain lesion (e.g. stroke). This transition creates a unique opportunity to examine and pin down the neural structures that are crucial for music perception^{11, 166}.

In contrast to congenital amusia, the prevalence of acquired amusia after stroke in the middle cerebral artery (MCA) territory is substantially higher, ranging between 35 per cent and 69 per cent¹²⁻¹⁴. However, the exploration of its neuroanatomical foundation has been mostly limited to symptom-led and lesion-led studies of individual cases or small ($N \leq 20$) patient groups. Moreover, the results regarding the lesion site, lesion lateralisation (left, right), and the type of musical deficit (e.g. spectral, temporal) have not been consistent⁸. Studies have reported spectral (e.g. pitch) deficits mainly after right hemisphere damage^{16, 167-178}, but also after left hemisphere damage^{13, 169, 170, 172, 175, 179}. Temporal (e.g. rhythm) deficits in acquired amusia have also been reported after both left^{13, 169, 170, 175, 180, 181} and right hemisphere damage^{13, 16, 168-170, 174, 175, 182, 183}. Särkämö et al. (2010) reported that

amusia caused by right hemisphere damage, especially to temporal and frontal regions, was more severe than that caused by left hemisphere damage¹⁸⁴. Furthermore, in a 6-month follow-up, the acquired amusics who had damage in the right AC showed worse recovery than the non-amusic patients or the amusic patients without AC damage¹⁸⁴. A more recent study reported that acquired amusics who had right hemisphere damage were more impaired in recognizing basic emotions of music than patients with left hemisphere damage¹⁸.

While fMRI studies on acquired amusia have not been published, functional deficits in acquired amusia have been studied using EEG and magnetoencephalography (MEG). Johannes et al. (1998) have showed that post-stroke acquired amusia was associated with right-lateralised functional deficits¹⁷⁴. Still, the impairments in processing music in acquired amusia might be due to more generic rather than music-specific cognitive processes. In an auditory classification task, acquired amusics exhibited abolished P3a responses¹⁶⁹, indicative of impaired attentional orienting, compared to non-amusic patients and healthy controls. Moreover, in a passive listening task with frequent standard and infrequent pitch deviants, acquired amusics showed grossly reduced mismatch negativity (MMN) responses to the pitch deviants¹⁷⁰. Using MEG, Särkämö et al. (2010) also reported that acquired amusics had functional deficits in both basic auditory encoding (MMN) and in higher domain-general cognitive processing¹⁸⁴, but their relative contribution to acquired amusia depended on whether the lesion included the right AC or not¹⁸⁴.

In spite of the reasonable amount of published literature on acquired amusia, the previous studies have been mainly constrained by small sample sizes and low spatial accuracy, and therefore they provide only coarse information about the brain areas crucial for perceiving the different elements of music. Studies utilizing modern MRI analysis methods in acquired amusia are lacking: VBM, DTI, and fMRI studies have not been published. Only one recent study has utilized modern lesion-mapping methods to investigate the relationship between the brain damage site and occurrence of acquired amusia¹⁸⁵. Using VLSM, Hirel et al. (2017) reported that insular stroke lesions were associated with musical deficits¹⁸⁵. However, their exploratory analysis was carried out in a small sample of patients (N = 20) and by using a liberal statistical thresholding. Moreover, the lesion analyses were carried out with combined data from both hemispheres (i.e. lesions in the right hemisphere were flipped to the left hemisphere), and therefore the information on lateralisation was lost.

In the healthy brain, both music-related ventral (i.e. extreme capsule) and dorsal streams in the right hemisphere have been suggested to act in parallel in transferring musical auditory information between the temporal, inferior parietal, and inferior frontal regions¹⁸⁶⁻¹⁹⁰. However, roles of the ventral and dorsal streams in music perception and production are not clear. Similarly to aphasia, where damage to language-related dorsal stream is associated with productive impairments and

damage to language-related ventral stream with comprehension deficits¹⁹¹, music perception and production could rely on different streams^{164, 188, 189}. To disclose the WM pathways as well as the brain areas that are crucial for music perception, systematic research on the neural basis of acquired amusia and its recovery is still needed.

3 AIMS

Altogether, the precise neural basis of amusia still remains systematically unmapped and poorly understood. The utilization of modern MRI analysis techniques has been limited: only one study utilizing VBM with modulated data to evaluate GM volumetric differences in congenitally amusic and non-amusic subjects has been published¹⁴⁷. Moreover, only two DTI studies on congenital amusia have been published: both investigated only one WM tract and yielded conflicting findings^{151, 152}. Functional brain imaging has been used in three studies on congenital amusia¹⁵⁴⁻¹⁵⁶, but the processing of natural music in the amusic brain has not been studied. Studies utilizing VBM, DTI, or fMRI in acquired amusia are lacking. Furthermore, the structural changes associated with the recovery of acquired amusia have not been studied.

Systematic and longitudinal study of acquired amusia with modern multimodal MRI techniques is expected to uncover the accurate neural basis of amusia. Clinically, this information would improve the diagnostics of amusia, provide better information on prediction of amusia recovery, and facilitate the targeting of music-based rehabilitation methods. Furthermore, studying acquired amusia specifies neural architectures crucial and necessary for normal music perception.

The aims of the study were set as follows:

1. To determine the specific stroke lesion patterns giving rise to acquired amusia (Study I).
2. To evaluate longitudinal volumetric grey and white matter changes related to acquired amusia and its recovery (Study I).
3. To systematically examine quantitative changes in white matter pathways in acquired amusia and to evaluate the changes in the tracts associated with the recovery of amusia (Study II).
4. To evaluate deficits and changes in brain activation and functional connectivity in acquired amusia during natural music listening (Study III).
5. To assess changes in brain activation and functional connectivity associated with the recovery of amusia (Study III).

4 MATERIALS AND METHODS

4.1 Subjects

The subjects (N = 50) were acute stroke patients recruited during 2013-2015 from the Division of Clinical Neurosciences, Turku University Hospital (Tyks) for a music intervention study. All subjects gave written informed consent in accordance with the Declaration of Helsinki, and the study was approved by the Ethics Committee of the Hospital District of Southwest Finland. All patients had an acute ischemic stroke (N = 36) or intracerebral haemorrhage (N = 14) in the left (N = 24) or right (N = 26) hemisphere and subsequent minor cognitive impairment and motor deficits, and they were all right-handed. The following inclusion criteria were used: (1) no prior neurological or psychiatric disease, (2) no drug or alcohol abuse, (3) no hearing defect, (4) ≤ 80 years old, (5) Finnish-speaking, and (6) able to co-operate to carry out the study protocol. All patients received standard medical treatment and rehabilitation of stroke. Patients underwent an MRI and behavioural assessment at the acute (< 3 weeks post-stroke), 3-month post-stroke, and 6-month post-stroke stages. During each MRI session, structural, DTI, and fMRI scans were acquired.

Of the 50 patients originally recruited for the study, five dropped out before the 3-month follow-up and one before the 6-month follow-up due to refusal. One patient did not undergo MRI at the 3-month post-stroke stage due to medical operation, and one patient's fMRI scans could not be obtained at the 6-month post-stroke stage due to MRI scanner malfunction. In addition, one aphasic patient was unable to perform MBEA used to diagnose amusia at the acute stage. As a result, from the Turku cohort, data from 27 patients (first 27 patients who had completed the follow-up at the end of 2014) were used in the analyses of Study I, data from 42 patients (42 patients with complete three time-point DTI scans) were used in the analyses of Study II, and data from 41 patients (41 patients with complete three time-point fMRI scans) were used in the analyses of Study III.

4.1.1 Helsinki cohort

In addition to the primary cohort, patients recruited to a previous music intervention study¹⁹² were used in the Study I. Subjects (N = 50) were stroke patients recruited during 2004-2006 from the Department of Neurology, Helsinki University Central Hospital (HUCH). All patients had an MRI-verified acute ischemic stroke in the left or right hemisphere, primarily in MCA territory, presented cognitive or motor deficits, and were right-handed. All patients had normal hearing. Patients

with prior neurological or psychiatric disease or substance abuse were excluded. The study was approved by the Ethics Committee of the Hospital District of Helsinki and Uusimaa and carried out conforming with the Declaration of Helsinki. All patients signed an informed consent, and received standard stroke treatment and rehabilitation. All participants underwent a behavioural assessment and an MRI within 3 weeks of the stroke. Behavioural assessment was repeated during the follow-up at 3 months and MRI was repeated at 6 months post-stroke. Out of the 50 patients who completed acute stage assessment, 47 completed the follow-up. Therefore, 50 patients were included in the VLSM analyses and 47 patients in the VBM analyses in the Study I.

4.2 Behavioural assessment

4.2.1 Assessment of music perception

The music perception ability of the patients was evaluated with a shortened version¹⁷⁵ of the MBEA¹⁹³. Evaluation was carried out in the acute stage (< 3 weeks post-stroke) and at the 3-month and 6-month post-stroke stage. The original MBEA consists of six subtests, three of which evaluate spectral organization (scale, contour, and interval subtest), two evaluate temporal organization (rhythm and meter subtest), and one evaluates spectral memory (memory subtest), based on the music processing model¹⁹⁴. Due to the fact that music perception was evaluated as a part of larger neuropsychological testing battery, we utilized only the Scale and Rhythm subtests as indices of musical pitch and rhythm perception, respectively, and their average score as an overall index of music perception¹⁷⁵ (hereafter referred to as MBEA total score). Both subtests comprise 14 pairs (originally 30 pairs) of short piano melodies, half of which are identical and half of which contain a musically altered tone in the latter melody. The patient is asked to judge on each trial whether the two melodies sound the same or not (same-different classification). In the Scale subtest, the altered tones had a pitch change which was out-of-scale, but still retained the original melodic contour. In the Rhythm subtest, the alteration was a change in the duration values of two adjacent tones (rhythmic grouping) in the melody, while retaining its original meter and tone pitch. The stimuli were presented using a laptop computer and head-arch headphones. Before testing, sound volume was adjusted individually for each patient and the subtests were practiced with two training trials. Following a previous study¹⁴ and the established cut-off values of the original MBEA¹⁹³, patients with the MBEA total score < 75% were classified as amusic.

4.2.2 Assessment of aphasia

To control the specificity of the findings for amusia, aphasia was also assessed using the Aphasia Severity Rating Scale (ASRS) from Boston Diagnostic Aphasia Examination (BDAE)¹⁹⁵. Additionally, the performance of the patients in Verbal Fluency Test [listing words from a semantic category (animals)]¹⁹⁶, shortened Token Test¹⁹⁷ and shortened Boston Naming test¹⁹⁸ was used to determine the clinical ASRS estimate.

4.3 Magnetic resonance imaging (MRI)

4.3.1 MRI data acquisition

Patients were scanned with a 3T Siemens Verio scanner using a 12-channel Head Matrix coil (Siemens Medical Solutions, Erlangen, Germany) at the Medical Imaging Centre of Southwest Finland. T1-weighted 3D magnetization-prepared rapid gradient-echo (MPRAGE) scans [flip angle = 9°, repetition time (TR) = 2300 ms, echo time (TE) = 2.98 ms, voxel size = 1.0 x 1.0 x 1.0 mm], diffusion MRI scans (TR = 11700 ms, TE = 88 ms, acquisition matrix = 112 x 112, 66 axial slices, voxel size = 2.0 x 2.0 x 2.0 mm) with one non-diffusion weighted volume and 64 diffusion weighted volumes (b-values of 1000 s/mm²), and functional images using a single-shot T2*-weighted gradient-echo planar imaging (EPI) sequence (slice thickness 3.5 mm; number of slices = 32; TR = 2010 ms; TE = 30 ms; flip angle = 80°; voxel size = 2.8 x 2.8 x 3.5 mm³) were acquired.

Patients from the Helsinki cohort used in the Study I were scanned with a 1.5T Siemens Vision scanner (Siemens Medical Solutions, Erlangen, Germany) of the HUCH Department of Radiology to obtain high-resolution T1 images (flip angle = 15°, TR = 1900 ms, TE = 3.68 ms, voxel size = 1.0 x 1.0 x 1.0 mm³).

4.3.2 MRI data processing

Normalization of MRI images to a standard template is a necessity for accurate comparison of subjects or groups. This is especially important when dealing with aberrant brain tissue, such as that of stroke patients. To accomplish optimal normalization of the MRI images with no post-registration lesion shrinkage or out-of-brain distortion, cost function masking (CFM) was implemented¹⁹⁹. The cost function masks were created by the author by manually depicting the lesioned areas, on a slice-by-slice basis, by drawing the precise boundaries of the lesion directly

into the T1 image²⁰⁰. The lesion tracking was carried out using The MRICron software package (<http://people.cas.sc.edu/rorden/mricron/index.html>)²⁰¹.

T1 images and binary lesion masks were then processed using the Statistical Parametric Mapping software (SPM8, Wellcome Department of Cognitive Neurology, UCL) under MATLAB 8.0.0 (The MathWorks Inc., Natick, MA, USA, version R2012b). Unified Segmentation²⁰² with medium regularization and CFM was applied to T1 images segmenting them precisely into GM, WM, and cerebrospinal fluid probability maps before normalizing them into the MNI space (Montreal Neurological Institution). This technique has been commonly used in studies of stroke patients^{200, 203, 204}. The GM and WM segmented images were then modulated to preserve the original signal strength during the normalization, and to reduce residual inter-individual variability, and smoothed using an isotropic spatial filter (FWHM = 6 mm). Using the normalization parameters obtained during the segmentation process, the lesion masks defined in native space were also registered to MNI space.

4.3.2.1 Preprocessing of diffusion data for Tract-Based Spatial Statistics

Tract-Based Spatial Statistics (TBSS) is a recently developed method allowing voxel-wise statistical analysis of the DTI data to evaluate and compare changes in WM structures. Using non-linear registration and alignment-invariant tract representation, TBSS overcomes several issues of group analysis, such as image alignment and the amount of spatial smoothing used²⁰⁵.

In this study, voxel-wise statistical analysis of the FA, MD, and RD data was carried out using TBSS²⁰⁵, part of FMRIB Software Library (University of Oxford, FSL v5.0.8, www.fmrib.ox.ac.uk/fsl)²⁰⁶. First, eddy current distortions and head motion were corrected. Second, the gradient matrix was rotated using FSL's `fdt rotate bvecs` to provide more accurate estimate of diffusion tensor orientations²⁰⁷. After these steps, the Brain Extraction Tool was used to perform the brain extraction²⁰⁸ and diffusion tensors were reconstructed using the linear least-squares algorithm included in Diffusion Toolkit 0.6.2.2 (Ruopeng Wang, Van J. Wedeen, trackvis.org/dtk, Martinos Center for Biomedical Imaging, Massachusetts General Hospital). Finally, FA, MD and RD maps for each subject and session were calculated using the eigenvalues extracted from the diffusion tensors. Then all subjects' FA data were aligned into a common space using the nonlinear registration tool FNIRT, which uses a b-spline representation of the registration warp field²⁰⁹ CFM was used to improve the normalization. Next, the mean FA image was created and thinned to create a mean FA skeleton which represents the centres of all tracts common to the group. Each patient's aligned FA data was then projected onto this

skeleton and the resulting data fed into voxel-wise cross-subject statistics. Eventually, the transformations calculated with the FA maps were then applied for the MD and RD maps.

4.3.2.2 Deterministic tractography

The diffusion images can be used to delineate and compare WM tracts in vivo^{210, 211}. One of the most common algorithms used for tractography is deterministic tractography (DT), where voxels are interconnected through their preferred diffusion directions to form a projection to represent a WM tract²¹⁰. The statistical information of these tracts dissected in vivo can then be analysed. Based on the previous information and the lack of comprehensive evidence on tract deficits in amusia, we chose to systematically evaluate all WM pathways in both hemispheres interconnecting/connecting to the superior and medial temporal gyri (AF, IFOF, ILF, UF, CC, tapetum) and inferior and medial frontal gyri [AF, IFOF UF, frontal aslant tract (FAT); see Figure 2]. Tract-specific dissections are described below. Dissections of individual WM tracts were performed using TrackVis (version 0.6.0.1, Build 2015.04.07) and following commonly used published guidelines for the number and positioning of the regions of interest (ROIs) in both healthy and clinical populations.

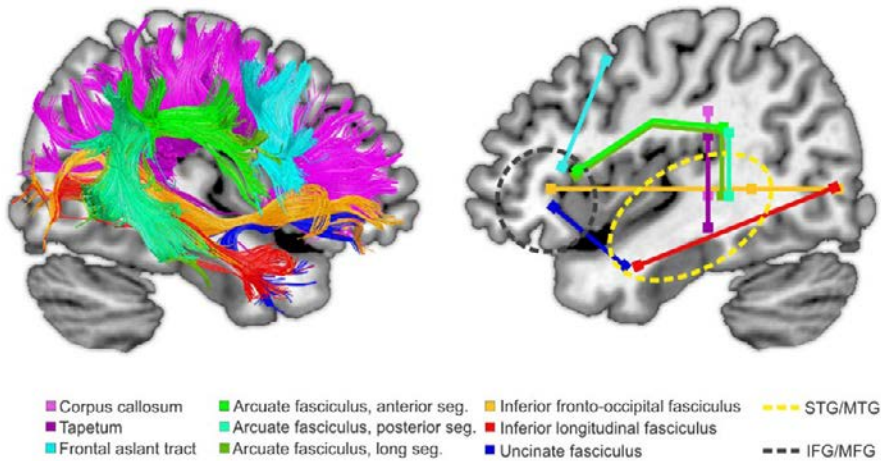


Figure 2 Schematic representation of the white matter pathways included in the tractography analyses in Study II.

The AF consists of three pathways: (i) long direct segment connecting the temporal and frontal lobe, (ii) anterior indirect segment connecting the frontal lobe to IPL, and (iii) posterior indirect segment connecting temporal lobe and IPL²¹². To

dissect the three segments of AF, we used a three-ROI approach²¹²⁻²¹⁶: using a DTI FA colour map, the first ROI was drawn on a coronal plane to capture fibres running in the anterior-posterior direction, the second ROI on an axial plane near the temporoparietal junction to capture all the fibres running to the temporal lobe, and finally, the third ROI on a sagittal plane to capture fibres connecting to the IPL.

The IFOF interconnects occipital, inferior parietal, posterior temporal, and orbitofrontal areas^{117-121, 217}. The IFOF was dissected using a two-ROI approach^{215, 218, 219}: defined on coronal plane, the first ROI was placed between occipital and temporal lobes and the second ROI to the anterior floor of the external capsule.

The ILF runs from the occipital cortex to the temporal pole¹¹⁷. The ILF was dissected with a two-ROI approach: drawn on coronal plane, the first ROI was placed in the anterior temporal lobe and the second subcortically in the occipital lobe^{215, 218}.

The UF is a tract connecting the temporal pole and parts of limbic system, such as hippocampus and amygdala, with the superior, middle, and inferior frontal gyri¹¹⁸. The UF was dissected with two ROIs defined in coronal plane: the first ROI was placed in the anterior floor of the external capsule and the second in the anterior temporal lobe^{215, 218}.

The CC connects homologous areas in left and right hemispheres facilitating interhemispheric communication. The CC was dissected using a single ROI defined in sagittal plane²¹⁸. We also defined two additional ROIs in axial plane in the temporal projections of the CC to capture its temporal projections (tapetum). Tapetum was analysed separately from CC²²⁰.

The FAT connects the IFG and pre-supplementary (pre-SMA) and supplementary (SMA) motor areas^{221, 222}. The FAT was dissected with two-ROI approach, the first ROI placed in axial plane to pre-SMA and SMA and the second ROI in sagittal plane to IFG^{221, 222}.

In all subjects and all the WM tracts included, the individual-level ROIs were first defined in the left and right hemispheres using the 6-month post-stroke images. Then, to avoid varying ROI sizes affecting the results, the ROIs were copied to the acute and 3-month images. The ROIs placed in the acute and 3-month images were manually spatially adjusted to achieve as accurate tracking as possible. When necessary, exclusion ROIs were used. To ensure that no fibres were missed, all ROIs were defined large enough to have at least one empty ROI voxel between the edge of the ROI and the tracked fibres²¹³. All dissections were performed by one person, blinded to the patients' music perception performance.

In the acute stage, the CC, tapetum, left AF (posterior segment), left UF, and left ILF were successfully traced in all subjects. The tracing was unsuccessful in the left AF (anterior segment, N = 2; long segment, N = 1), left FAT (N = 5), left IFOF (N = 1), right AF (anterior segment, N = 8; long segment N = 8; posterior

segment N = 7), right FAT (N = 5), right IFOF (N = 4), right UF (N = 2), and right ILF (N = 1).

4.3.2.3 Functional MRIs

Functional magnetic resonance imaging (fMRI) measures brain activity by detecting blood-oxygen-level dependent (BOLD) contrast changes or fluctuations in the brain. It can be used to uncover brain areas involved in specific functional domains, such as music processing. Furthermore, fMRI can be utilized to unravel how the reorganization of the music network in acquired amusia takes place over time.

A single fMRI session was acquired in acute, 3-month, and 6-month post-stroke stages. Using the Presentation software (Neurobehavioral Systems, Inc., Version 16.3 Build 12.20.12), the patients were presented auditory stimuli consisting of six well-known Finnish songs which were presented in both versions with sung lyrics (vocal music) and in instrumental versions without vocals (instrumental music). A block design with total of 12 blocks of music (six vocal music and six instrumental music blocks) and 12 blocks of rest (no-stimuli) in between the music blocks was used. The duration of each block was 15 seconds. The instrumental music pieces used were instrumental versions of the vocal music pieces. The main melody was sung in the vocal music pieces, whereas it was played with various instrumentation (guitar, saxophone, violin) in the instrumental music pieces. To overcome the issue of familiarizing to the music during the follow-up sessions, six different versions of auditory stimuli with randomized order of the blocks were created. The versions were randomly ordered for each subject. Auditory stimuli were presented through MR-compatible headphones to the patients while they were instructed to lay still with eyes fixed at a fixation point.

Data were preprocessed using SPM8. First, the fMRI images were realigned and a mean image was created. Images were reoriented according to the anterior commissure. To improve normalization, CFM was applied when images were normalized to MNI space using Unified Segmentation²⁰² and re-sampled into $2 \times 2 \times 2$ mm³ voxel size. Finally, the preprocessed images were smoothed using an isotropic spatial filter (FWHM = 8 mm).

4.3.2.4 Independent component analysis and calculation of task-related networks

Functional MRI can also be utilized to assess the integrated activity of spatially distributed brain regions by evaluating FC. One data-driven approach for FC assessment is independent component analysis (ICA)²²³, which explores temporally consistent brain areas (i.e. functional networks)²²⁴ without a priori assumptions²²⁵.

Group Spatial ICA was used to extract the networks present in the fMRI task experiment in the three time points using the GIFT software (<http://icatb.sourceforge.net/>). Following previous studies, the number of possible independent components was set to 20²²⁶⁻²²⁸. To begin with, the intensity of the acquired images was normalized. Secondly, the data were concatenated and reduced to the 20 temporal dimensions using principal component analysis. The data were analysed using the infomax algorithm²²⁹. No scaling was applied as the intensities of the acquired spatial maps are in percentages of signal change. To detect deficits and artefacts (e.g. noise), the acquired components were inspected visually. Previous studies have implicated defective right frontotemporal connectivity in congenital amusia and that music containing lyrics activates frontal and temporal areas bilaterally². Therefore, all components comprising temporal and frontoparietal regions were included in the final ICA to evaluate the FC changes associated with acquired amusia. These networks were: (i) auditory, (ii) auditory-motor, and (iii) left and (iv) right frontoparietal (attentional) network.

A multiple regression model was calculated with GIFT to evaluate which of the four networks were associated with the auditory fMRI tasks (i.e. listening to vocal music or instrumental music). First, this procedure fitted the time course of each retrieved network in each participant to the fMRI model previously defined. Then, beta values of each component (network) were obtained from each condition regressor (vocal music, instrumental music). These beta values represented the level of engagement of each network during a particular condition.

4.3.3 Voxel-based lesion-symptom mapping

Lesion studies are essential in revealing causal link between brain regions and a given behaviour or skill¹¹. VLSM is a state-of-the-art lesion analysis method which allows analysing the relationship between local brain damage and behavioural data in a voxel-by-voxel basis⁵³. Compared to the traditional lesion analysis (lesion-led or a symptom-led) approaches, VLSM is more sophisticated and provides a detailed functional map of lesioned brain regions affecting in a given task. In lesion-led approach, patients are grouped based on the lesion location and then tested for

behavioural differences on a given domain compared to a control group²³⁰. Although this provides information about the functional roles of the lesioned brain region, the spatial resolution of this method is far from optimal. Additionally, in lesion-led approach, the areas outside the specific injury site are not considered affecting the behavioural performance and valuable information may be lost. In symptom-led studies, the brain region contributing to the cognitive deficit is deduced from lesion overlap images of patients sharing the same behavioural impairment²³¹. However, this method requires specific cut-off values on behavioural tasks to categorize patients. Therefore, parametric analysis is not possible and information of varying performance across a broad spectrum is lost. In contrast to the previous, VLSM does not require patient grouping by lesion location or behavioural data cut-off, although VLSM allows binary variables as well. Using the three-dimensional lesion maps, each voxel is analysed and the presence, or absence, of lesion is correlated with the behavioural data. Finally, statistical results and maps of areas associated with the behavioural deficits are constructed.

In this study, VLSM was carried out with non-parametric mapping software (Chris Rorden's NPM, version 6 June 2013) using the normalized acute phase lesion maps for all patients.

4.3.4 Voxel-based morphometry

VBM is an MRI analysis technique that allows estimation of anatomical differences in specific brain regions between groups⁵⁴. These local distinctions in GM and WM can be evaluated after spatial normalization, smoothing and segmentation of MRI images (described in the 4.3.2). VBM can also be used to analyse within-subject changes across time. In this study, VBM analysis was carried out using SPM8.

4.4 Statistical analyses

As described earlier, patients recruited for this study as well as the additional cohort from Helsinki¹⁹² were enrolled in two larger music intervention studies. First, it was verified that the individual music intervention arms did not effect on amusia recovery. To evaluate the effect of the received music intervention on amusia recovery in the primary cohort, a mixed-model analysis of variance (ANOVA) with Time (acute / 3-month / 6-month) and Group (3 intervention arms) was calculated. No significant Time x Group interactions were found in the MBEA total score ($p = 0.825$), the MBEA Scale subtest score ($p = 0.839$), or the MBEA Rhythm subtest score ($p = 0.791$). Similarly, in the Helsinki cohort, no significant Time x Group

interactions were found in the MBEA total score ($p = 0.898$), the MBEA Scale subtest score ($p = 0.889$), or the MBEA Rhythm subtest score ($p = 0.791$). These results suggest that the music listening intervention did not have any effect on amusia recovery and, therefore, does not impact the results of the studies.

A chi-square test was performed to examine the relation between the type of stroke and amusia recovery. In the primary cohort, the relation between these variables was nonsignificant, $\chi^2 = 0.531$, $p = 0.767$. In the Helsinki cohort, all patients had an ischemic stroke.

4.4.1 Study I: VLSM and VBM

Parametric VLSM analyses were carried out using the MBEA total (Scale and Rhythm average) score, Rhythm score, Scale score, and the BDAE-ASRS score. In addition, following binary analyses were performed: amusic vs. non-amusic; amusic (no aphasia) vs. aphasic (no amusia); amusic vs. non-amusic (all aphasics excluded); aphasic vs. non-aphasic (all amusics excluded); and amusic vs. amusic and aphasic. As the Rhythm and Scale subtest scores correlated strongly ($r = 0.71$) at the acute stage, binary analyses were not performed and only parametric VLSM analyses were carried out. All voxels damaged at least in 10% of the patients were included in the statistical analysis^{59, 232, 233}. Correction for multiple comparisons was achieved by using a False Discovery Rate (FDR) corrected $p < 0.05$ threshold.

As VBM uses voxel intensities and different MRI acquisition parameters may have an effect on the results, we used only patients from the Helsinki study with acute and 6 month images ($N = 47$) for the longitudinal VBM analyses. Amusic patients were divided into those who showed and those who did not show recovery on the MBEA total scores from the acute to the 3-month stage. Amusic patients with $> 20\%$ increase in MBEA total score were classified as recovered amusics (RA, $N = 13$, mean 42%, range 21–85%), amusic patients with a $\leq 20\%$ increase in MBEA score were classified as non-recovered amusics (NRA, $N = 16$, mean 5%, range -21–19%), and patients above the acute stage cut-off were classified as non-amusics (NA, $N = 18$). Individual preprocessed GM and WM images were entered into a second-level analysis using a Group (RA / NRA / NA) x Time (Acute / 6 months) mixed between-within subjects ANOVA. Six different Group (RA $>$ NRA, RA $>$ NA, NRA $>$ NA) x Time (Acute $>$ 6 months, 6 months $>$ Acute) contrasts were calculated. Unless otherwise noted, results were thresholded at a whole-brain uncorrected $p < 0.001$ threshold at the voxel level and a familywise error rate (FWE) corrected $p < 0.05$ at the cluster level with a cluster extent of more than 50 contiguous voxels. Anatomical areas were identified using the Automated Anatomical Labelling Atlas²³⁴ included in the xjView toolbox (<http://www.alivelearn.net/xjview/>).

4.4.2 Study II: TBSS and deterministic tractography

Based on the acute stage MBEA total score, 25 patients were defined as amusic and 17 as NA. Amusic patients were further subdivided to RA (N = 10), who were tested as non-amusic at the 6-month stage according to the initial cut-off values, and to NRA (N = 15). To evaluate pitch and rhythm amusia separately, similar approach was applied to the Scale and Rhythm subtest scores using the established cut-off values¹⁹³. Subjects with Scale subtest score < 73% in the acute stage were defined as pitch-amusic [N = 20, non-pitch-amusic (pNA) N = 22]. At the 6-month post-stroke stage, seven patients were classified as recovered pitch-amusics (pRA) and 13 as non-recovered pitch-amusics (pNRA). When Rhythm subtest was evaluated with cut-off score < 77%, the figures were: 10 non-rhythm-amusics (rNA), 21 non-recovered rhythm-amusics (rNRA), and 11 recovered rhythm-amusics (rRA).

Differences in TBSS results in the NA, RA, and NRA subjects were compared using independent samples t-tests at each time point. Six different Group (NRA > NA, NRA > RA, NA > NRA, NA > RA, RA > NRA, RA > NA) x Time contrasts were calculated at each time point (Acute / 3 months / 6 months). In addition, to evaluate longitudinal changes, 12 different interactions [Group (NRA > NA, NRA > RA, NA > NRA, NA > RA, RA > NRA, RA > NA) x Time (3 months > Acute, 6 months > Acute)] were calculated. Rhythm-amusia and pitch-amusia were evaluated using the same preceding contrasts/interactions but with previously described pNRA, pRA and pNA, and rNRA, rRA and rNA groups. Unless otherwise noted, TBSS results are reported with an FWE-corrected $p < 0.05$ threshold using threshold-free cluster enhancement and a non-parametric²³⁵ permutation test with 5000 permutations²³⁶.

In tractography analysis, statistical information (tract volume, FA, MD and RD values) of each WM tract in each time point was gathered using a MATLAB toolbox “along-tract statistics”²³⁷. Statistical information was then further analysed with SPSS (IBM Corp. Released 2012. IBM SPSS Statistics for Windows, Version 21.0. Armonk, NY: IBM Corp.). Second-level analysis was performed using a mixed between-within repeated-measures ANOVA [Group (RA / NRA / NA) x Time (Acute, 3 months, 6 months)]. Similarly, pNRA, pRA, and pNA as well as rNRA, rRA, and rNA were compared to evaluate tractography results in pitch and rhythm amusia. Correction for multiple comparisons in post hoc analyses was achieved using the Bonferroni adjustment.

4.4.3 Study III: fMRI and ICA

Statistical analyses were carried out using SPM8. The statistical evaluation in each time point (acute, 3 months, 6 months) was based on a least-square estimation using the general linear model. The lesion zones were included in the fMRI analysis. The different conditions were modelled with a box-car regressor waveform convolved with a canonical hemodynamic response function. Data were high-pass filtered (to a maximum of 1/128 Hz) and serial autocorrelations were estimated using an autoregressive model [AR(1) model]. Confounding factors from head movement were also included in the model. A block-related design matrix was created including the conditions of interest (Vocal, Instrumental). After model estimation, main effects for both conditions against rest (no-stimuli) were calculated. In order to detect brain activation patterns specific to the processing of lyrics, a contrast between the vocal and instrumental conditions (Vocal>Instrumental) was also calculated.

To evaluate longitudinal changes, a flexible factorial ANOVA with Group (NA, RA, NRA) and Time (Acute, 3 months, 6 months) as factors was calculated. To compare RA and NRA groups, six different Group (RA > NRA, NRA > RA) x (3 months > Acute, 6 months > Acute, 6 months > 3 months) interactions were calculated. In addition, to evaluate the longitudinal changes between the NAs and amusics, the RA and NRA groups were combined and labelled as amusics, and six different Group (NA > amusics, Amusics > NA) x (3 months > Acute, 6 months > Acute, 6 months > 3 months) interactions were calculated. Longitudinal analyses were performed separately for each condition of interest (Vocal, Instrumental, Vocal>Instrumental).

Furthermore, as the functional recovery in post-stroke aphasia has been shown to take place in three different phases³³ and since the reorganization includes various elements³⁵, cross-sectional comparisons between the NA vs. amusics and RA vs. NRA groups were also performed. First level contrasts were entered into second-level analyses and two-sample t-tests comparing NA vs. Amusic or RA vs. NRA were calculated in each of the three time points separately for each condition of interest (Vocal, Instrumental, Vocal>Instrumental). Additionally, Group (NA/Amusics or RA/NRA) x Time (Acute / 3 months / 6 months) ANOVA was calculated for each condition. To evaluate the effects of concurrent aphasia on music-induced brain activations in amusia, a subgroup analysis of 23 patients [only aphasic (N = 10), only amusic (N = 8), amusic and aphasic (N = 15)] was carried out using the acute stage data. Due to the small number of patients in this subgroup analysis, recovery was not assessed. A one-way ANOVA with Group as a factor (Only aphasic / Only amusic / Amusic and aphasic) was used for each contrast of interest. For any significant effect, independent t-tests among all groups were calculated.

Unless otherwise indicated, all results were thresholded at a whole-brain uncorrected $p < 0.005$ at the voxel level. Only clusters surviving a FWE-corrected $p < 0.05$ at the cluster level with a minimal cluster size set to 50 voxels are reported. Anatomical brain areas were identified using the Automated Anatomical Labelling Atlas²³⁴. In addition, Pearson correlations (two-tailed) of the mean activation in individual significant clusters and the MBEA total percentage of the corresponding point of time were calculated. To control for multiple comparisons in cross-sectional correlational analyses, FDR approach was used ($N = 18$), and only significant results are reported. Similar approach was applied for the longitudinal analysis comparisons ($N = 1$).

For the ICA of the fMRI music listening task, the engagement of four selected networks during vocal and instrumental listening conditions was evaluated using the extracted beta values. The second level analysis was carried out with SPSS. Results were analysed using two mixed-model ANOVAs: [Group (NA / Amusics) x Time (Acute, 3 months, 6 months)] and [Group (RA / NRA) x Time (Acute, 3 months, 6 months)]. Additionally, Pearson correlations (two-tailed) of the mean engagement of a significant component and the MBEA total percentage of the corresponding point of time were calculated. FDR approach was used to control for multiple comparisons ($N = 6$).

5 RESULTS

5.1 Patient characteristics

5.1.1 *Study I*

The demographic and clinical characteristics of the patients are presented in Table 1. The groups were relatively well-matched demographically and clinically. However, in VLSM analysis, the amusic group had less education, larger overall lesion volume, and higher incidence of neglect. Importantly, there was no significant difference in the pre-stroke musical background of the patients. In the longitudinal VBM analyses, the three groups differed with respect to education, lesion volume, and neglect, but there were not differences between the RA and NRA patients. Again, the pre-stroke musical background of the groups was comparable. Across patients, changes in the Rhythm and Scale subtest scores from acute stage to 3 months post-stroke did not correlate significantly ($r = 0.25$, $p = 0.085$).

The stroke of the patients in the amusic groups was significantly more often in the right hemisphere. However, as the acquired amusia is thought to stem from right hemisphere damage, lesion laterality was not used as a covariate. Furthermore, as the coincidence of neglect and amusia is expected due their similar lesion locations²³⁸, neglect was not included as a covariate in the analyses.

5.1.2 *Study II*

The demographic and clinical characteristics of the patients are presented in Table 2. Three covariates were used in the tractography analyses: educational years, acute lesion size, and a composite (average) score of acute stage verbal memory performance (derived from a word-list learning and the story recall tasks of the Rivermead Behavioural Memory Test)¹⁹², which were available for all patients. Similarly to the Study I, lesion laterality or neglect were not included as a covariate in the analyses.

5.1.3 *Study III*

The demographic and clinical characteristics of the patients are presented in Table 3. As the NA and amusic groups differed significantly in the number of educational

years, it was added as a covariate for the NA vs. amusic analyses and for the longitudinal analyses. The RAs and NRAs did not differ in any demographic parameters and thus no covariates were used in the amusia recovery analyses. Similarly to the Study I, lesion laterality or neglect were not included as a covariate in the analyses.

Table 1 Demographic and clinical characteristics of the patients in Study I.

	VLSM analysis (N = 77) Helsinki and Turku patients			VBM analysis (N = 47) Helsinki patients			
	Amusic (N = 49)	Non-amusic (N = 28)	p-value	NRA (N = 16)	RA (N = 13)	NA (N = 18)	p-value
Demographic							
Gender (male/female)	26/23	17/11	0.515 (χ^2)	6/10	7/6	12/6	0.247 (χ^2)
Age (years)	59.9 (10.6)	55.8 (10.3)	0.096 (<i>t</i>)	62.2 (7.7)	58.5 (5.4)	56.6 (9.9)	0.139 (<i>F</i>)
Education (years)	10.6 (3.7)	13.6 (3.1)	0.000 (<i>t</i>)	9.6 (2.6)	9.8 (4.2)	13.2 (3.1)	0.003 (<i>F</i>)
Music background (pre-stroke)							
Formal music training ^a	0.04 (0.29)	0.11 (0.58)	0.653 (<i>U</i>)	0.00 (0.00)	0.00 (0.00)	0.19 (0.68)	0.191 (<i>K</i>)
Instrument playing ^a	1.10 (1.70)	1.96 (2.25)	0.117 (<i>U</i>)	1.46 (1.86)	1.26 (1.94)	1.30 (1.81)	0.904 (<i>K</i>)
Music listening prior to stroke ^b	4.8 (2.0)	3.8 (1.8)	0.961 (<i>U</i>)	3.3 (1.8)	3.4 (1.4)	3.9 (1.1)	0.616 (<i>K</i>)
Clinical							
Aphasia (no/yes) ^c	29/20	17/11	0.895 (χ^2)	10/6	10/3	11/7	0.616 (χ^2)
BDAE-ASRS	4.3 (1.1)	4.4 (0.9)	0.511 (<i>U</i>)	4.3 (1.1)	4.5 (1.1)	4.3 (1.1)	0.891 (<i>K</i>)
MBEA total score %	58.0 (8.6)	84.3 (6.2)	0.000 (<i>t</i>)	57.8 (10.5)	55.2 (8.8)	84.9 (7.1)	0.000 (<i>F</i>)
MBEA Rhythm score %	58.1 (12.0)	82.0 (8.9)	0.000 (<i>t</i>)	60.3 (13.8)	56.0 (12.3)	84.1 (9.7)	0.000 (<i>F</i>)
MBEA Scale score %	57.8 (12.3)	86.6 (8.4)	0.000 (<i>t</i>)	55.5 (12.6)	54.4 (8.5)	85.7 (9.2)	0.000 (<i>F</i>)
Other cognitive dysfunction (no/yes) ^e	2/47	4/24	0.110 (χ^2)	0/16	1/12	2/16	0.410 (χ^2)
Hemiparesis (no/yes)	11/38	8/20	0.550 (χ^2)	4/12	2/11	4/14	0.810 (χ^2)
Visual neglect (no/yes) ^d	26/18	28/0	0.000 (χ^2)	9/7	7/6	18/0	0.004 (χ^2)
Lesion laterality (left/right)	18/31	16/12	0.083 (χ^2)	8/8	3/10	10/8	0.174 (χ^2)
Lesion volume in cm ³	55.8 (43.7)	25.5 (27.8)	0.001 (<i>t</i>)	57.6 (46.4)	49.2 (35.9)	25.3 (31.7)	0.049 (<i>F</i>)

Data are mean (SD) unless otherwise stated. χ^2 = chi-squared test, *F* = one-way ANOVA, *K* = Kruskal–Wallis test, *t* = *t* test, *U* = Mann–Whitney *U* test.

^aNumbers denote values on a Likert scale: 0, no; 1, <1 year; 2, 1–3 years; 3, 4–6 years; 4, 7–10 years; 5, >10 years of training/playing.

^bNumbers denote values on a Likert scale: range, 0 (never does) to 5 (does daily).

^cClassification based on BDAE ASRS: scores 0–4, aphasia; score 5, no aphasia.

^dClassification based on the Lateralized Inattention Index of the Balloons Test.

^eOther cognitive dysfunction (attention/executive function or memory deficit).

Table 2 Demographic and clinical characteristics of the patients in Study II.

	Amusia overall				Pitch-amusia				Rhythm-amusia			
	NRA (N=15)	RA (N=10)	NA (N=17)	p-value	pNRA (N=13)	pRA (N=7)	pNA (N=22)	p-value	rNRA (N=21)	rRA (N=11)	rNA (N=10)	p-value
Demographic												
Gender (male/female)	8/7	8/2	8/9	0.231 (χ^2)	9/4	4/3	11/11	0.540 (χ^2)	13/8	6/5	5/5	0.805 (χ^2)
Age (years)	56.9 (14.3)	58.0 (15.6)	55.4 (14.7)	0.909 (K)	57.8 (14.5)	64.9 (10.6)	53.1 (14.8)	0.167 (K)	60.1 (14.0)	56.2 (15.1)	49.5 (13.3)	0.193 (K)
Education (years)	12.0 (3.3)	13.2 (4.1)	15.7 (3.8)	0.026 (K)	11.8 (3.5)	12.9 (4.4)	15.2 (3.7)	0.042 (K)	12.8 (4.0)	15.0 (1.7)	15.0 (1.7)	0.074 (K)
Music background (pre-stroke)												
Formal music training ^a	0.0 (0.0)	0.7 (1.4)	0.7 (1.7)	0.197 (K)	0.0 (0.0)	0.0 (0.0)	0.8 (1.7)	0.092 (K)	0.4 (1.2)	0.5 (1.3)	0.5 (1.6)	0.823 (K)
Other music training ^a	0.5 (1.5)	1.9 (2.4)	2.1 (2.2)	0.075 (K)	0.6 (1.6)	1.7 (2.6)	1.9 (2.2)	0.164 (K)	1.4 (2.2)	1.8 (2.3)	1.2 (1.8)	0.788 (K)
Active music listening ^b	4.5 (2.2)	4.6 (2.0)	4.8 (2.1)	0.908 (K)	4.5 (2.1)	3.4 (2.1)	5.1 (1.9)	0.216 (K)	4.8 (1.9)	4.6 (2.4)	4.5 (2.3)	0.966 (K)
Passive music listening ^b	6.4 (1.5)	5.9 (1.5)	6.3 (1.7)	0.552 (K)	6.2 (1.6)	6.0 (1.7)	6.3 (1.6)	0.882 (K)	5.9 (1.7)	6.2 (1.8)	7.0 (0.0)	0.075 (K)
Musical reward ^c	79.4 (10.0)	77.8 (10.5)	73.4 (14.0)	0.449 (K)	78.2 (10.0)	77.7 (12.7)	75.4 (13.0)	0.847 (K)	78.1 (12.3)	74.0 (11.3)	76.9 (12.0)	0.542 (K)
Clinical												
Aphasia (no/yes) ^d	7/8	1/9	8/9	0.111 (χ^2)	6/7	2/5	8/14	0.721 (χ^2)	6/15	4/7	6/4	0.240 (χ^2)
MBEA total score %	55.7 (9.3)	63.5 (7.0)	83.7 (4.5)	0.000 (K)	52.8 (5.2)	61.7 (8.4)	80.7 (7.3)	0.000 (K)	60.5 (12.8)	71.8 (10.2)	83.3 (8.6)	0.000 (K)
MBEA Rhythm score %	57.1 (10.5)	57.3 (11.7)	77.8 (6.4)	0.000 (K)	54.6 (8.9)	64.3 (10.5)	72.4 (13.0)	0.000 (K)	57.8 (11.0)	65.2 (10.8)	82.3 (3.2)	0.000 (K)
MBEA Scale score %	54.2 (11.1)	69.7 (16.1)	89.6 (6.5)	0.000 (K)	51.0 (6.1)	59.0 (7.9)	89.0 (6.0)	0.000 (K)	63.2 (17.6)	78.5 (17.2)	84.3 (15.0)	0.000 (K)
Visual neglect (no/yes) ^e	7/6	7/3	15/2	0.110 (χ^2)	5/6	4/3	20/2	0.014 (χ^2)	11/8	9/2	9/1	0.132 (χ^2)
Lesion laterality (left/right)	2/13	6/4	13/4	0.001 (χ^2)	1/12	3/4	17/5	0.000 (χ^2)	7/14	5/6	9/1	0.012 (χ^2)
Lesion volume in cm ³	73.7 (58.4)	52.6 (44.9)	40.4 (47.2)	0.166 (K)	80.1 (57.9)	65.9 (48.9)	37.1 (43.6)	0.031 (K)	67.1 (52.3)	55.1 (63.1)	30.3 (27.6)	0.179 (K)

Data are mean (SD) unless otherwise stated. χ^2 = chi-square test, K = Kruskal-Wallis test.

^aNumbers denote values on a Likert scale where 0 = no, 1 = less than 1 year, 2 = 1–3 years, 3 = 4–6 years, 4 = 7–10 years, and 5 = more than 10 years of training/playing.

^bNumbers denote values on a Likert scale with a range 0 (does never) to 7 (does daily).

^cClassification based on Barcelona Music Reward Questionnaire to reflect pre-stroke musical reward.

^dClassification based on the Boston Diagnostic Aphasia Examination - Aphasia Severity Rating Scale.

^eClassification based on the Lateralized Inattention Index of the Balloons Test.

Table 3 Demographic and clinical characteristics of the patients in Study III.

	Amusia analysis			Recovery analysis		
	Amusic (N = 24)	Non-amusic (N = 17)	p-value	NRA (N = 15)	RA (N = 9)	p-value
Demographic						
Gender (male/female)	16/8	8/9	0.335 (χ^2)	8/7	8/1	0.178 (χ^2)
Age (years)	58.7 (13.1)	55.4 (14.7)	0.615 (K)	56.9 (14.3)	61.8 (10.6)	0.411 (K)
Education (years)	12.3 (3.6)	15.7 (3.8)	0.006 (<i>t</i>)	12.0 (3.3)	12.9 (4.2)	0.555 (<i>t</i>)
Music background (pre-stroke)						
Formal music training ^a	0.2 (0.8)	0.7 (1.7)	0.481 (K)	0.0 (0.0)	0.5 (1.4)	0.636 (K)
Other music training ^a	1.0 (2.0)	2.1 (2.2)	0.141 (K)	0.5 (1.5)	1.9 (2.6)	0.325 (K)
Active music listening ^b	4.5 (2.1)	4.8 (2.1)	0.633 (K)	4.5 (2.2)	4.4 (2.0)	1.000 (K)
Passive music listening ^b	6.2 (1.5)	6.3 (1.7)	0.817 (K)	6.4 (1.5)	5.8 (1.6)	0.347 (K)
Musical reward ^c	78.9 (10.2)	73.4 (14.0)	0.233 (K)	79.4 (10.0)	78.0 (11.1)	0.726 (K)
Clinical						
Aphasia (no/yes) ^d	8/16	8/9	0.518 (χ^2)	7/8	1/8	0.178 (χ^2)
MBEA total score% A	58.3 (9.0)	83.7 (4.5)	0.000 (K)	55.7 (9.3)	62.6 (6.8)	0.030 (K)
MBEA total score% 3M	66.8 (11.9)	88.0 (6.1)	0.000 (K)	61.1 (8.9)	76.3 (10.2)	0.001 (K)
MBEA total score% 6M	68.3 (13.2)	88.1 (7.3)	0.000 (K)	61.0 (9.3)	80.4 (9.4)	0.000 (K)
Lesion laterality (left/right)	7/17	13/4	0.004 (χ^2)	2/13	5/4	0.061 (χ^2)
Lesion volume in cm ³	67.5 (53.5)	40.4 (47.2)	0.064 (K)	73.7 (58.4)	57.0 (45.2)	0.599 (K)

Data are mean (SD) unless otherwise stated. χ^2 = chi-squared test, 3M = 3-month stage, 6M = 6-month stage, A = Acute stage, K = Kruskal-Wallis test, *t* = *t* test.

^aNumbers denote values on a Likert scale where 0 = no, 1 = less than 1 year, 2 = 1–3 years, 3 = 4–6 years, 4 = 7–10 years, and 5 = more than 10 years of training/playing.

^bNumbers denote values on a Likert scale with a range 0 (does never) to 7 (does daily).

^cClassification based on Barcelona Music Reward Questionnaire to reflect pre-stroke musical reward.

^dClassification based on the Boston Diagnostic Aphasia Examination - Aphasia Severity Rating Scale.

5.2 Structural damage and volumetric changes associated with amusia and its recovery

5.2.1 Lesion patterns associated with amusia and aphasia

Parametric VLSM analyses showed that lower MBEA total scores were associated with lesions in the right STG, MTG, HG, putamen, and insula (Figure 3A). In contrast, lower BDAE-ASRS scores were associated with lesions comprising the left STG and left insula (Figure 3B). Binary VLSM analyses directly comparing amusic vs. NA patients and aphasic vs. non-aphasic patients resulted in largely similar

results: amusia was associated with lesions in the right STG, HG, putamen, and insula (Figure 3C), and aphasia with lesions in the left STG and insula (Figure 3D).

As 41% of amusics had concurrent aphasia and 65% of aphasics had concurrent amusia, binary analyses first excluding aphasic patients and then comparing pure amusic vs. NA patients were performed to control for the comorbidity of amusia and aphasia. Likewise, amusic patients were excluded and pure aphasic patients were compared with non-aphasic patients. These analyses yielded essentially the same results as the first binary analyses: amusia was associated with lesions in the right STG, MTG, HG, putamen, and insula (Figure 3E), and aphasia with lesions in the left HG and insula (Figure 3F). Furthermore, when amusic patients were compared to patients with both amusia and aphasia, lesion pattern comprising the right STG, MTG, putamen, and insula was again significant (Figure 3G). Additional comparison between purely amusic patients (no aphasia) and purely aphasic (no amusia) patients was carried out. In these analyses, amusia was again linked to lesion in the right STG, putamen, and insula, and aphasia was associated with a lesion pattern localized in the left HG and insula (Figure 3H).

To determine whether the lesion patterns were similar for pitch and rhythm perception deficits, separate parametric VLSM analyses for the MBEA Scale and Rhythm subtest scores were performed. Lower scores on both Scale and Rhythm subtests were associated with lesions in the right STG, MTG, HG, insula, and basal ganglia (BG; putamen, caudate, pallidum; Figure 3I-J). Differences in the amount of voxels damaged in separate anatomical areas are presented in Table 4. While the same brain regions were affected in both Scale and Rhythm, the lesions associated with lower Rhythm subtest scores covered a larger proportion of the areas. When the lesion pattern associated with poor performance in the Rhythm subtest was limited only to the most significant areas (t -value > 4.5), the right basal ganglia (putamen and caudate) remained as the most significant components.

Table 4 Anatomical correlates of VLSM results for MBEA Scale and Rhythm scores.

Anatomical region	Scale	Rhythm
Right Caudate	90.02%	94.86%
Right HG**	40.58%	90.53%
Right Insula*	38.56%	59.23%
Right Pallidum	86.82%	89.81%
Right Putamen	90.02%	94.86%
Right MTG**	1.97%	18.55%
Right STG**	11.25%	57.04%
Right Middle Temporal Pole	0.70%	1.98%
Right Superior Temporal Pole	2.70%	6.33%

* $p < 0.05$, ** $p < 0.005$. Comparison (χ^2) between the percentages of damaged voxels in Rhythm vs. Scale (i.e. if the damaged area within the structure is larger in Rhythm than in Scale).

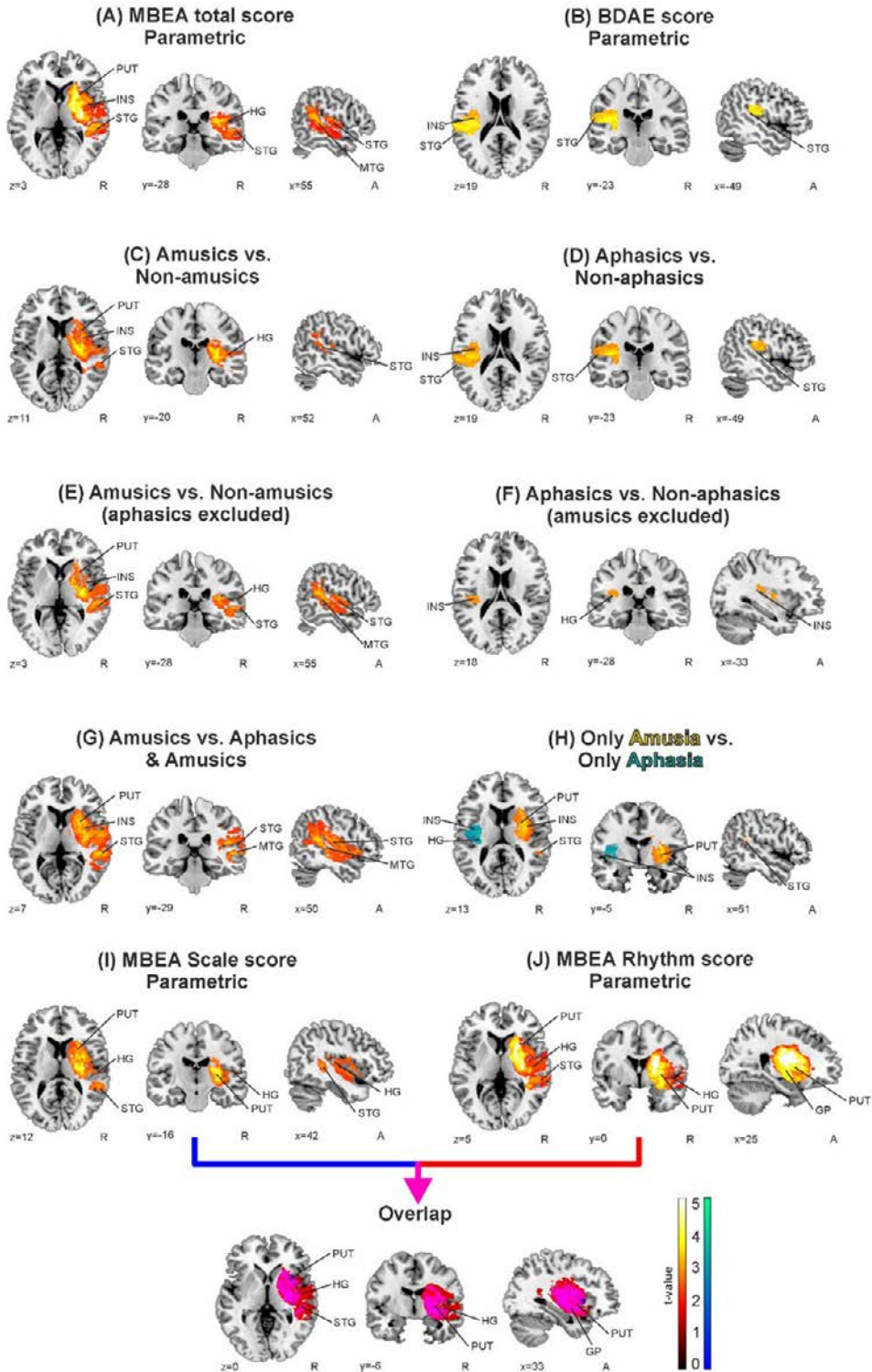


Figure 3 VLSM results. Modified from Sihvonon et al. 2016²³⁹.

5.2.2 Grey and white matter changes associated with amusia recovery

A longitudinal VBM analysis of GMV changes showed a significant Time (Acute > 6 months) x Group (NRA > NA) interaction. The NRAs had more GMV decrease in the right STG and MTG than the NAs (Figure 4A). Other comparisons (NRA > RA, RA > NA) did not yield any statistically significant results. Significant WMV changes were not found.

Separate analyses of the Rhythm and Scale subtests showed that, in the Rhythm subtest, the NRAs had greater GMV decrease in anterior temporal areas than the NAs (Figure 4B). Furthermore, the NRA group had also greater WMV decrease in inferior temporal areas compared to the NAs (Figure 4B). In the Scale subtest, the NRA group showed greater GMV decrease in the posterior STG / temporoparietal junction than the NA [interaction: Time (Acute > 6 months) x Group (NRA, Scale > NA, Scale; $p < 0.01$ uncorrected)] (Figure 4C). All significant GMV and WMV decreases are shown in Table 5.

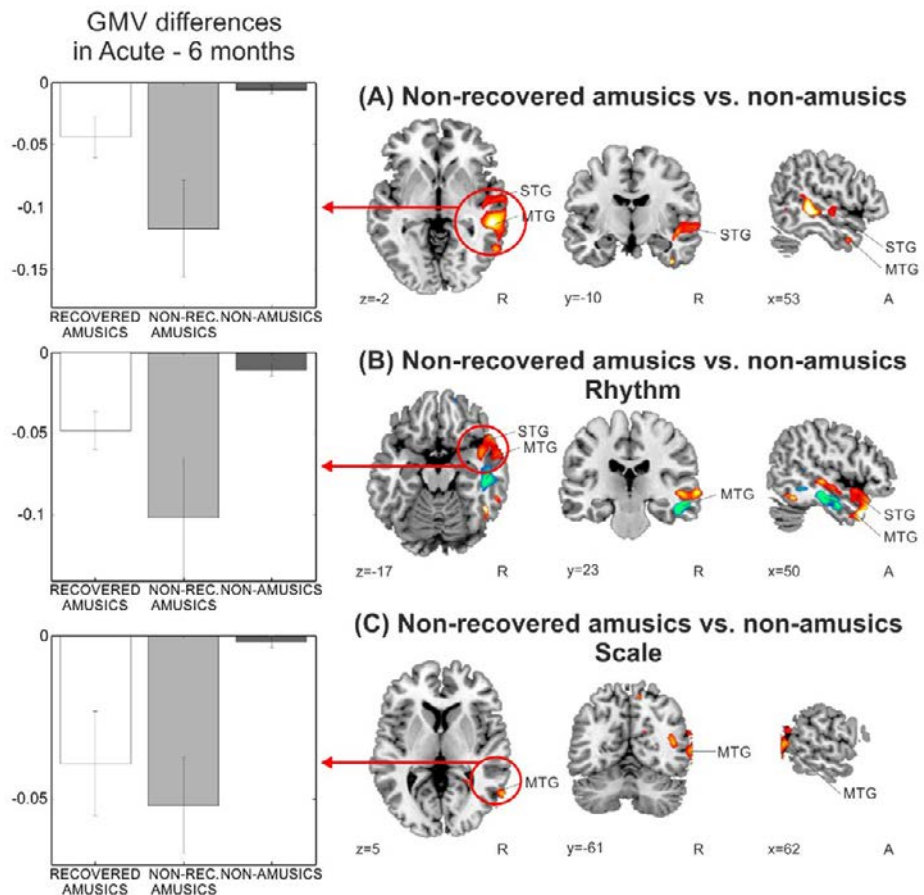


Figure 4 VBM results. Modified from Sihvonen et al. 2016²³⁹.

Table 5 GMV and WMV decreases in acquired amusia (6-month – acute).

Contrast	Probability map	Area name	Coordinates	Cluster size	t-value
NRA vs. NA	GM	Right MTG (BA 21)	54 -33 -3	8443	4.20*
		Right STG (BA 22)	53 -35 -4		
		Right ITG (BA 37)	58 -62 -6		
rNRA vs. rNA	GM	Right STG (BA 38)	47 17 -41	15866	4.85*
		Right Middle Temporal Pole	53 17 -32		
rNRA vs. rNA	WM	Right MTG	50 -24 -14	3931	4.66*
		Right ITG	49 -8 -26		
pNRA vs. pNA	GM	Right MTG (BA 19, 21)	63 -62 6	790	3.76**

*p < 0.05 FWE-corrected at the cluster level

**p < 0.01 uncorrected at the cluster level

5.3 White matter pathway damage in acquired amusia

In longitudinal analyses, Time (3 months > acute, 6 months > acute) x Group interactions showed largely similar results and therefore only significant interactions from acute to 6-month stage are reported.

5.3.1 Tract-based spatial statistics: amusia

Cross-sectional TBSS analyses of Group (NRA / RA / NA) effects consistently showed that the NRAs had significantly lower FA in the right IFOF, AF, UF, internal capsule (IC), and CC compared to the NA group at all three time points (Table 6 and Figure 5). At the 3-month and 6-month post-stroke stages, the NRAs additionally showed lower FA in the tapetum as well as greater MD and RD in the right IFOF, AF, UF, CC, and tapetum compared to the NAs. Although there were no differences at the acute and 3-month stages, at the 6-month stage the NRAs had lower FA and greater MD and RD in the right IFOF, AF, and UF compared to the RA groups. No other contrasts were significant at the acute, 3-month, and 6-month stages.

The MD of the right IFOF, AF, UF, IC, CC, and tapetum increased more in the NRAs compared to the NAs. Furthermore, the NRAs also showed a greater RD increase in the right IFOF, AF, UF, IC, CC, and tapetum than the NAs from the acute to 6-month stage. Compared to the NAs, RAs showed a greater MD increase in the left IFOF, AF, UF, and CC from the acute to 6-month stage. No other significant interactions were observed.

In summary, NRAs showed consistent signs of WM damage in the right IFOF, AF, UF, CC, and tapetum compared to the NAs. In addition, the RAs showed signs of longitudinal WM degeneration in the left IFOF, AF, UF, and CC.

Table 6 TBSS results of cross-sectional analyses for persistent amusia, pitch-amusia, and rhythm-amusia.

AMUSIA									
Tract	FA			MD			RD		
	A	3	6	A	3	6	A	3	6
R IFOF	↓	↓	↓/-		↑	↑/+		↑	↑/+
R UF	↓	↓	↓/-		↑	↑/+		↑	↑/+
R AF	↓	↓	↓/-		↑	↑/+		↑	↑/+
R IC	↓	↓	↓						↑
CC	↓	↓	↓					↑	
Tapetum		↓	↓			↑		↑	↑
PITCH-AMUSIA									
Tract	FA			MD			RD		
	A	3	6	A	3	6	A	3	6
R IFOF	↓	↓	↓		↑	↑		↑	↑
R UF	↓	↓	↓		↑	↑		↑	↑
R ILF	↓	↓	↓		↑			↑	↑
R AF	↓	↓	↓		↑	↑		↑	↑
R IC	↓	↓	↓					↑	↑
CC	↓	↓	↓		↑	↑		↑	↑
Tapetum		↓	↓						
RHYTHM-AMUSIA									
Tract	FA			MD			RD		
	A	3	6	A	3	6	A	3	6
R IFOF	↓	↓	↓		↑	↑		↑	↑
R UF	↓	↓	↓		↑	↑		↑	↑
R ILF	↓	↓	↓			↑			↑
R AF	↓	↓	↓		↑	↑		↑	↑
R IC	↓	↓	↓						
L AF									↑
CC	↓	↓	↓		↑	↑		↑	↑
Tapetum						↑			↑

NRA vs. NA/pNRA vs. pNA/rNRA vs. rNA (arrow up or down), and NRA vs. RA (+ or -). Arrow up or + indicates greater value and arrow down or - a lower value for the contrast in question. 3 = 3 months stage, 6 = 6 months stage, A = Acute.

5.3.2 Tract-based spatial statistics: pitch-amusia and rhythm-amusia

Separate TBSS analyses for pitch-amusia (pNRA / pRA / pNA) and rhythm-amusia (rNRA / rRA / rNA) were also performed. Cross-sectionally, these analyses yielded essentially the same results as in amusia (overall): both pNRAs and rNRAs showed lower FA and greater MD and/or RD in the right IFOF, AF, UF, CC, and tapetum than the pNAs and rNAs, at all three time points (Table 6 and Figure 5). Similar effects on FA and MD/RD were seen also in the right ILF for both pNRAs and rNRAs compared to the pNAs and rNAs, respectively. Furthermore, at all stages studied, the pNRAs showed decreased FA and increased RD in the right IC compared to the pNAs.

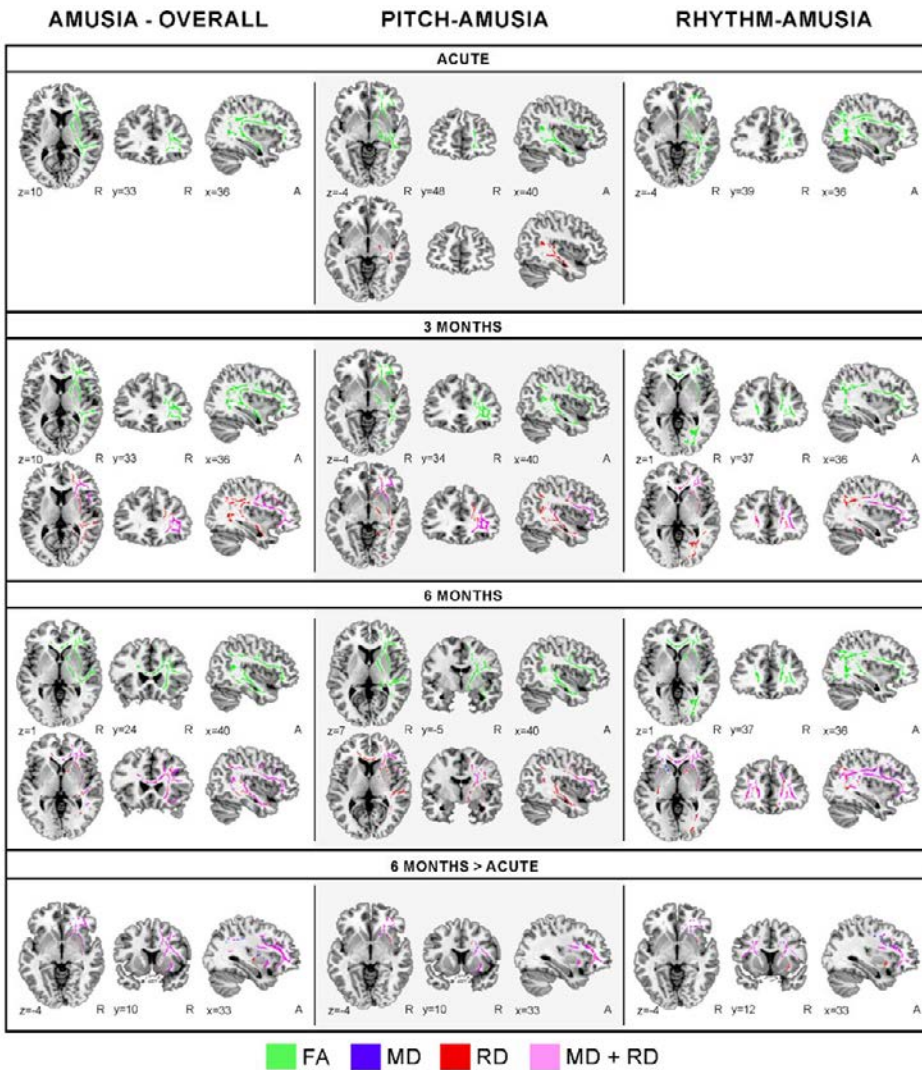


Figure 5 TBSS results for persistent acquired amusia. Lower FA and increased MD and RD values are presented for persistent amusia, pitch-amusia, and rhythm-amusia cross-sectionally in all three time points and Group (NRA vs. NA/pNRA vs. pNA/rNRA vs. rNA) x Time (6 months>Acute) interaction. Neurological convention is used with MNI coordinates at the middle each section. Modified from Sihvonen et al. 2017²⁴⁰.

Longitudinal analyses showed that the MD and RD of the right IFOF, AF, and UF increased more in the pNRAs than in pNAs and also more in the rNRAs than in the rNAs. There was an additional increase in the RD of the left AF in the rNRAs compared to the rNAs.

In summary, in both pitch-amusia and rhythm-amusia, signs of consistent WM damage were observed in the right IFOF, AF, UF. Damage to the left AF was observed in rhythm-amusia, but not in pitch-amusia.

5.3.3 Deterministic tractography: amusia

A mixed-model ANOVA with Time (acute / 3-month / 6-month) and Group (NRA / RA / NA) revealed significant between-subjects effects in the volume of the right IFOF, AF long segment, and FAT, and the left AF posterior segment as well as in the FA of the right IFOF (Table 7 and Figure 6). Post hoc testing showed that, compared to the NRAs, both the RAs and the NAs had greater right IFOF volume ($p = 0.002$ and $p = 0.036$, respectively) and FA ($p = 0.002$; $p = 0.027$) as well as greater right AF long segment volume ($p = 0.019$; $p = 0.016$). The NRAs also showed lower right FAT volume ($p = 0.049$) than the NAs. In contrast, the RAs had lower volume of the left AF posterior segment than the NAs ($p = 0.017$).

In addition, the NRAs showed greater increase in MD and RD in the tapetum than the NAs (6 months > acute). No other significant interactions were observed.

Table 7 Significant group and group x time interactions of tractography analyses.

GROUP EFFECTS						GROUP X TIME INTERACTIONS						
Tract	Variable	df	F	P	η^2	Tract	Variable	df	F	P	η^2	
AMUSIA						AMUSIA						
R IFOF	VOL	2, 36	3.9	0.030	0.177	Tapetum	MD	4, 72	4.3	0.003	0.194	
	FA	2, 36	4.5	0.018	0.200		RD	4, 72	3.9	0.006	0.178	
R FAT	VOL	2, 36	4.6	0.017	0.202	PITCH-AMUSIA						
R AF Long seg.	VOL	2, 36	3.5	0.041	0.163	R AF Ant. seg.	MD	4, 72	4.5	0.003	0.201	
L AF Post. seg.	VOL	2, 36	4.1	0.025	0.184		RD	4, 72	4.4	0.003	0.198	
PITCH-AMUSIA						R UF	MD	4, 72	4.0	0.005	0.183	
R IFOF	VOL	2, 36	3.6	0.038	0.167		RD	4, 72	4.0	0.005	0.182	
	FA	2, 36	4.3	0.022	0.191	Tapetum	MD	4, 72	3.3	0.015	0.156	
RHYTHM-AMUSIA							RD	4, 72	3.3	0.015	0.155	
R IFOF	VOL	2, 36	4.5	0.018	0.201	RHYTHM-AMUSIA						
	VOL	2, 36	3.3	0.048	0.155	L UF	RD	4, 72	2.7	0.035	0.132	
R UF	FA	2, 36	4.1	0.025	0.185							
	MD	2, 36	4.9	0.013	0.214							
CC	RD	2, 36	4.2	0.023	0.188							

Statistical information presented: df = degrees of freedom, F = f value, P = p-value, η^2 = partial eta squared. L = left, R = right, VOL = volume.

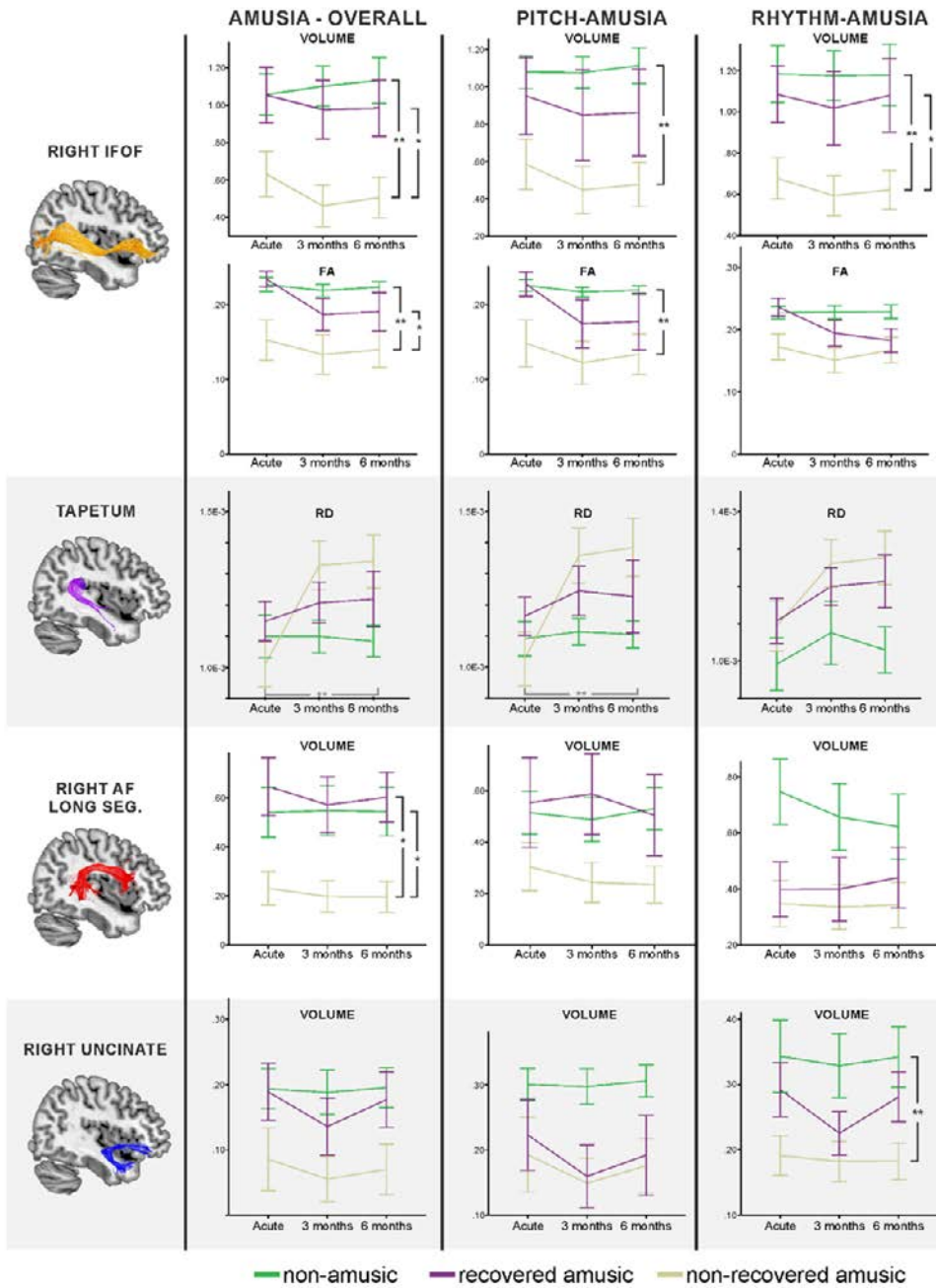


Figure 6 Main tractography results. Group x Time (Acute, 3 months, 6 months) repeated measured results. Significant Group effect (black bar), significant Group x Time interaction (grey bar). Error-bar = standard error of the mean. *p < 0.05, **p < 0.01. Modified from Sihvonen et al. 2017²⁴⁰.

5.3.4 *Deterministic tractography: pitch-amusia*

DT analyses were also performed separately for pitch-amusia (pNRA / pRA / pNA; Table 7 and Figure 6). Significant between-subject (Group) effects were observed in the volume and FA of the right IFOF with post hoc tests revealing lower volume and FA in the pNRAs than pNAs ($p = 0.001$; $p < 0.001$). Significant Time x Group interactions were found in MD and RD of the tapetum and in MD and RD of the right AF anterior segment as well as in MD and RD of the right UF. Concerning the change from acute stage to 6-month, post hoc tests indicated a greater increase in the tapetum MD ($p = 0.002$) and RD ($p = 0.002$) and the right AF anterior segment MD ($p = 0.001$) and RD ($p = 0.001$) in pNRAs compared to pNAs. In addition, the pNRAs showed a greater increase in the right UF MD ($p = 0.030$) and RD ($p = 0.030$) than the pNAs and the pRAs showed a greater decrease in the right AF anterior segment MD ($p = 0.004$) and RD ($p = 0.004$) than the pNAs. No other significant interactions were observed.

5.3.5 *Deterministic tractography: rhythm-amusia*

In rhythm-amusia, significant Group effects were found in the volume of the right IFOF (Table 7 and Figure 6). Post hoc tests revealed that the rNRAs had lower volume ($p = 0.008$) than the rNAs. The right IFOF volume was also lower in the rNRAs than in the rRAs ($p = 0.040$). Rhythm-amusia also showed additional between-subject effects in the right UF volume. Post hoc tests indicated lower volume in the rNRAs than in the rNAs ($p = 0.009$). Additional group effects were observed in the FA, MD, and RD of the CC. Post hoc tests showed, that the rNRAs had greater CC MD ($p = 0.026$) and RD ($p = 0.025$) than the rNAs. The rRAs had lower CC FA than the rNAs ($p = 0.010$).

The longitudinal tractography results (Table 7) revealed a somewhat different pattern of effects for the rhythm-amusia than for the pitch-amusia. In rhythm-amusia, significant Time x Group interaction was found in the RD of the left UF. Post hoc tests revealed that the left UF RD increased more in the rNAs than in the rNRAs from acute to 6-month stage ($p = 0.014$). No other significant interactions were observed.

5.3.6 *Deterministic tractography: regression analysis*

A step-wise linear regression analysis including only the significant tractography results was performed to further determine which of the tractography results were the strongest predictors of MBEA performance. Based on the regression analysis,

a Pearson correlation between the MBEA performance and the most significant predictor in all three time points was carried out. Correction for multiple comparisons in the Pearson correlations was made with the Bonferroni adjustment ($N = 3$). Three different models (MBEA total score, Scale subtest score, and Rhythm subtest score) were formed for each time point (acute / 3 months / 6 months) and all tracts and their parameters that showed significant effects (see 5.3.3 and 5.3.4) were entered as independent variables.

Across all time points, volume of the right IFOF was the most significant predictor of the MBEA total score and Scale, and Rhythm scores (Table 8 and Table 9). Volume of the left AF posterior segment and the MD and RD of the tapetum emerged as additional predictors of the MBEA total score at the acute and 3-month/6-month post-stroke stages, respectively. Rhythm scores were predicted only by the right IFOF volume across all time points, while the Scale scores were predicted also by the tapetum RD and the right UF MD at the 6-month stage.

Correlations between the strongest predictor (volume of the right IFOF) and the MBEA total score and Scale and Rhythm subtests scores were also calculated. The volume of the right IFOF correlated significantly with the MBEA total performance ($r = 0.595$, $p < 0.001$) as well as with the subtests (Scale $r = 0.580$, $p < 0.001$; Rhythm $r = 0.498$, $p = 0.001$) at 6 months post-stroke stage.

Table 8 Regression analysis of the amusia tractography results.

ACUTE						
Model	Variable	Beta	T	F(df)	R ²	R ² change
1				$F_{(1,40)} = 14.162$	0.261	0.261
2	R IFOF volume	0.511	3.763**			
				$F_{(1,39)} = 4.163$	0.333	0.071
	R IFOF volume	0.484	3.684**			
	L AF post. volume	0.268	2.040*			
3 MONTHS						
Model	Variable	Beta	T	F(df)	R ²	R ² change
1				$F_{(1,40)} = 24.905$	0.384	0.384
2	R IFOF volume	0.619	4.990**			
				$F_{(1,39)} = 15.677$	0.446	0.062
	R IFOF volume	0.535	4.248**			
	Tapetum RD	-0.263	-2.088*			
6 MONTHS						
Model	Variable	Beta	T	F(df)	R ²	R ² change
1				$F_{(1,40)} = 21.874$	0.354	0.354
2	R IFOF volume	0.595	4.677**			
				$F_{(1,39)} = 14.640$	0.429	0.075
	R IFOF volume	0.479	3.642**			
	Tapetum MD	-0.298	-2.267*			

For MBEA total score, seven variables were entered: volume of the right IFOF, AF (long segment), FAT and the left AF (posterior segment) as well as FA of the right IFOF and MD and RD of the tapetum. Statistical information presented: Beta = standardized regression coefficient, T = t value, F(df) = F value (degrees of freedom), R² = R Square, R² change = R Square change. L = Left, R = Right. * $p < 0.05$, ** $p < 0.005$

Table 9 Regression analysis of the pitch-amusia and rhythm-amusia tractography results.

ACUTE						
MBEA Scale subtest						
Model	Variable	Beta	T	F(df)	R ²	R ² change
1	R IFOF volume	0.469	3.355**	F _(1,40) = 11.259	0.220	0.220
MBEA Rhythm subtest						
Model	Variable	Beta	T	F(df)	R ²	R ² change
1	R IFOF volume	0.432	3.031**	F _(1,40) = 9.186	0.187	0.187
3 MONTHS						
MBEA Scale subtest						
Model	Variable	Beta	T	F(df)	R ²	R ² change
1	R IFOF volume	0.551	4.171**	F _(1,40) = 17.396	0.303	0.303
MBEA Rhythm subtest						
Model	Variable	Beta	T	F(df)	R ²	R ² change
1	R IFOF volume	0.617	4.959**	F _(1,40) = 24.593	0.381	0.381
6 MONTHS						
MBEA Scale subtest						
Model	Variable	Beta	T	F(df)	R ²	R ² change
1	R IFOF volume	0.580	4.502**	F _(1,40) = 20.268	0.336	0.336
2	R IFOF volume	0.453	3.464**	F _(1,39) = 14.791	0.431	0.095
	Tapetum RD	-0.334	-2.553*			
3	R IFOF volume	0.521	4.095**	F _(1,38) = 12.777	0.502	0.071
	Tapetum RD	-0.397	-3.128**			
	R UF MD	-0.288	-2.325*			
MBEA Rhythm subtest						
Model	Variable	Beta	T	F(df)	R ²	R ² change
1	R IFOF volume	0.498	3.632**	F _(1,40) = 13.189	0.248	0.248

For MBEA Scale subtest score, eight variables were entered: volume and FA of the right IFOF as well as MD and RD of the right AF (anterior segment), UF, and tapetum. For MBEA Rhythm subtest, five variables were entered: volume of the right IFOF and UF, FAs of the right IFOF and CC as well as RD of the left UF. Statistical information presented: Beta = standardized regression coefficient, T = t value, F(df) = F value (degrees of freedom), R² = R Square, R² change = R Square change. L = Left, R = Right. *p < 0.05, **p < 0.005

5.4 Functional neural changes associated with acquired amusia and its recovery after stroke

5.4.1 *fMRI activation patterns in amusic vs. non-amusic patients*

Longitudinal analyses of the Instrumental condition revealed a significant Group (NA > Amusic) x Time (3 months > Acute) interaction, with the NAs showing increased activation in the right PreCG, PCG, and IFG compared to the amusic patients (Table 10 and Figure 7). No other significant interaction effects were observed.

In the cross-sectional analyses of the Instrumental condition, the amusic patients showed significantly reduced activations in the right STG and MTG compared to the NAs at the acute stage (Table 11 and Figure 8). The mean activation in this cluster also correlated with the acute stage MBEA scores ($R = 0.629$, $P < 0.001$). At the 3-month post-stroke stage, the defective activation pattern during the Instrumental condition was more wide-spread: the amusics had less activity bilaterally in the IFG, PreCG, STG, SMA, and in the right insula and cerebellum as well as in the left PCG and HG. The MBEA total score at 3-month stage correlated significantly with the mean activity observed in the clusters in the right IFG ($r = 0.55$, $p < 0.001$) and in the left PCG ($r = 0.497$, $p = 0.001$) and the STG ($r = 0.508$, $p = 0.001$).

In the Vocal condition, the amusic patients showed significantly increased activation bilaterally in the cuneus at the 3-month stage compared to the NAs. In the Vocal>Instrumental condition, the amusics showed more activation in the right superior occipital gyrus (SOG), precuneus, IFG, middle frontal gyrus (MFG), HG, IPL, and PCG as well as bilaterally in the cuneus, CG and in the left SMA at the 3-month stage, compared to the NA patients. No other significant Group or Group x Time interactions were observed.

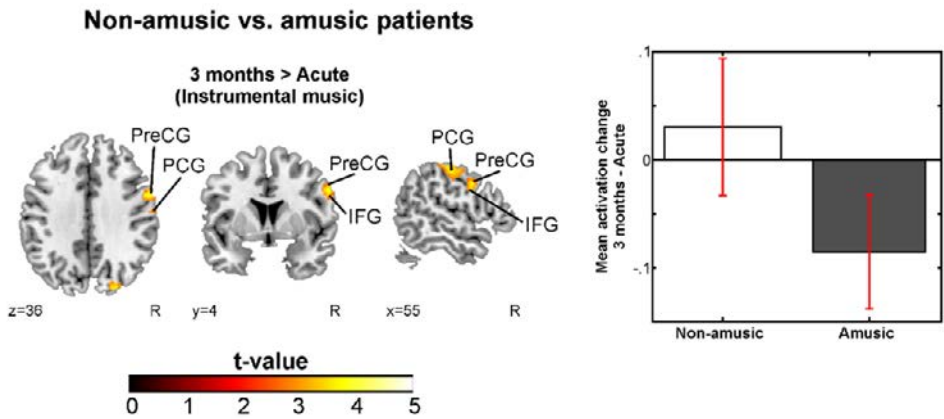


Figure 7 Longitudinal activation pattern changes of NA vs. amusic patients in 3 months > acute (Instrumental); $N = 41$. Results are shown at $p < 0.005$ (uncorrected) with ≥ 50 voxels of spatial extent and overlaid over a canonical template with MNI coordinates at the bottom right of each slice (see also Table 10). Only clusters surviving a FWE-corrected $p < 0.05$ threshold are labelled. Bar plot for mean cluster activation change in 3 months - Acute in significant cluster is shown: bar = mean, error-bar = standard error of the mean. Modified from Sihvonen et al. 2017²⁴¹.

Table 10 Longitudinal fMRI activation decreases during music listening in acquired amusia.

3 MONTHS > ACUTE						
Contrast	Condition	Area name	Coordinates	Cluster size	t-value	R
NA > Amusic	Instrumental	Right PCG (BA 2, 3)	48 -18 55	776	4.78*	n.s.
		Right PreCG (BA 4, 6)	56 2 33			
		Right IFG (BA 9)	54 5 29			

* $p < 0.05$ FWE-corrected at the cluster level

R = Pearson correlation (2-tailed p-value, FDR-corrected). The mean activation change in the cluster is correlated to the MBEA total score % change over the corresponding time change. BA = Brodmann area, n.s. = not significant.

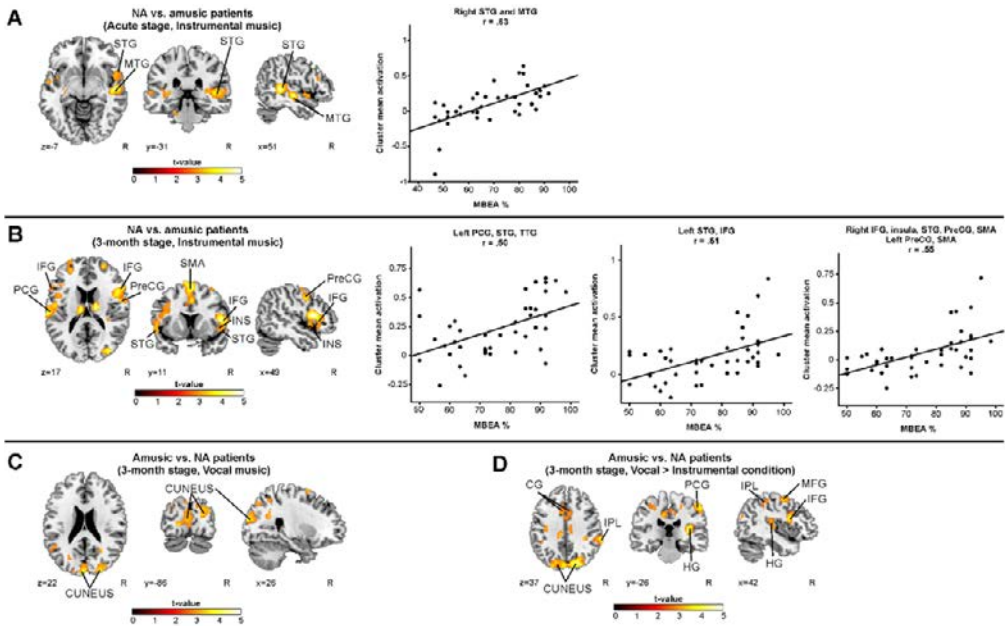


Figure 8 fMRI activation patterns during music listening – a comparison between the NA and amusic patients; $N = 41$. (A) NA vs. amusic patients (Acute, Instrumental); (B) NA vs. amusic patients (3-month stage, Instrumental); (C) Amusic vs. NA patients (3-month stage, Vocal); (D) Amusic vs. NA patients (3-month stage, Vocal vs. Instrumental). Results are shown at $p < 0.005$ (uncorrected) with ≥ 50 voxels of spatial extent and overlaid over a canonical template with MNI coordinates at the bottom right of each slice. Only clusters surviving a FWE-corrected $p < 0.05$ threshold are labelled (see also Table 11). The scatter plots display the correlation between the mean cluster activation and the MBEA total score across the whole sample. INS = insula. Modified from Sihvonen et al. 2017²⁴¹.

Table 11 fMRI results during music listening – a comparison between the NAs and amusic patients.

ACUTE STAGE								
Contrast	Condition	Area name	Coordinates	Cluster size	t-value	R		
NA > Amusic	Instrumental	Right STG (BA 22)	46 -40 5	1422	5.09*	0.629 (<0.001)		
		Right MTG (BA 21)	54 -16 -5					
3-MONTH STAGE								
Contrast	Condition	Area name	Coordinates	Cluster size	t-value	R		
NA > Amusic	Instrumental	Right IFG (BA 44)	50 16 13	5926	5.22**	0.547 (<0.001)		
		Right Insula (BA 22)	48 8 -3					
		Right STG (BA 38)	54 -16 -7					
		Right PreCG (BA 4)	56 -4 17	596	4.27*	n.s.		
		Left PreCG (BA 6)	-48 -6 53					
		Right SMA (BA 6)	2 12 65					
		Left SMA (BA 6)	-5 -4 69	587	4.18*	0.497 (0.001)		
		Right Cerebellum	22 -56 -25					
		Left PCG (BA 40, 43)	-64 -22 17					
		Amusic > NA	Vocal	Left STG (BA 41)	-44 -34 11	868	4.13*	0.508 (0.001)
				Left HG (BA 42)	-61 -21 12			
				Left STG (BA 22)	-52 2 3			
				Left IFG (BA 44)	-56 16 17	2232	4.39**	n.s.
Left Cuneus (BA 17)	-16 -82 3							
Right Cuneus (BA 18)	22 -90 21			9053	5.32**	n.s.		
Right SOG (BA 19)	34 -86 23							
Right Cuneus (BA 18)	10 -80 25							
Right Precuneus (BA 5)	4 -42 49							
Right CG (BA 24)	2 2 41							
Left Cuneus (BA 19)	-6 -92 27							
Amusic > NA	Vocal > Instrumental	Left SMA (BA 6)	-4 -6 55				662	4.64*
		Left CG (BA 32)	-8 12 33					
		Right IFG (BA 44)	50 10 13					
		Right HG (BA 41)	34 -26 11	1734	4.62**	n.s.		
		Right IPL (BA 40)	52 -40 51					
		Right PCG (BA 1)	54 -24 55					
		Right MFG (6)	36 -4 55	955	3.96*	n.s.		

*p < 0.05 FWE-corrected at the cluster level, **p < 0.001 FWE-corrected at the cluster level

R = Pearson correlation (2-tailed p-value, FDR-corrected). The mean activation in the cluster is correlated to the MBEA total score % of the corresponding point of time. BA = Brodmann area, n.s. = not significant.

5.4.2 fMRI activation patterns in amusia - the effect of aphasia

In the Instrumental condition, aphasic patients without amusia showed greater activations in the right STG and MTG compared to the patients with both aphasia and amusia (Table 12 and Figure 9). These activations also correlated with the acute stage MBEA total scores ($r = 0.689$, $P < 0.001$). In contrast, in the Vocal condition, amusic patients without aphasia showed greater activation of the left MTG compared to the patients with both aphasia and amusia. Furthermore, in the

Vocal condition, aphasic patients without amusia showed increased activations in the right STG, MTG, and insula compared to the amusic patients. These results were not significant at the corrected cluster level threshold, and therefore should be considered tentative.

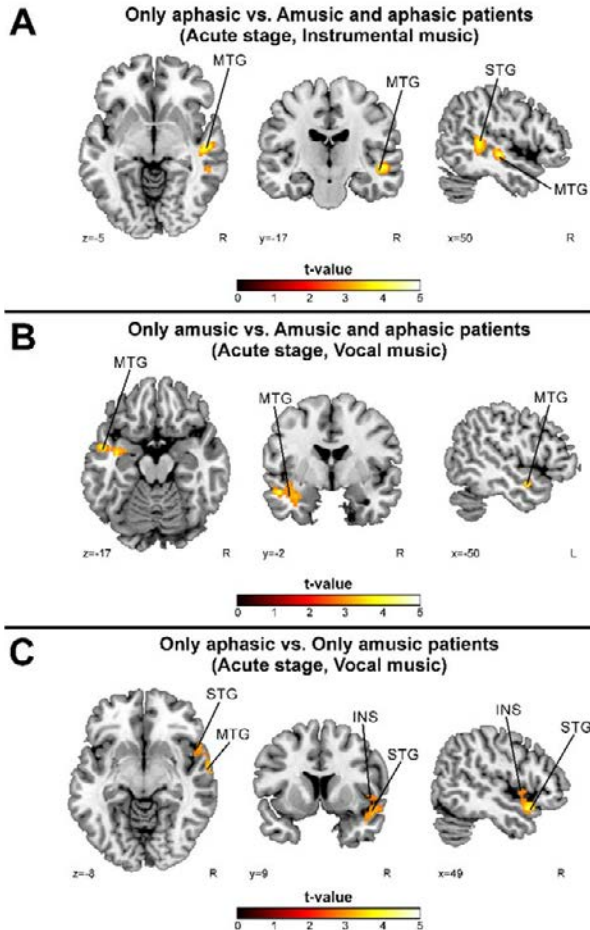


Figure 9 fMRI activation pattern differences between only aphasic, only amusic, and patients with both amusia and aphasia in the acute stage; $N = 23$. (A) Only aphasic vs. Amusic and aphasic patients (Instrumental; $p < 0.01$ uncorrected at the cluster level); (B) Only amusic vs. Amusic and aphasic patients (Vocal; $p < 0.05$ uncorrected at the cluster level); (C) Only aphasic vs. Only amusic patients (Vocal; $p < 0.05$ uncorrected at the cluster level). Results are shown at $p < 0.005$ (uncorrected) with ≥ 50 voxels of spatial extent and overlaid over a canonical template with MNI coordinates at the bottom right of each slice. See also Table 12. INS = insula. Modified from Sihvonen et al. 2017²⁴¹.

Table 12 fMRI activation pattern differences between only aphasic, only amusic, and patients with both amusia and aphasia in the acute stage.

ACUTE STAGE						
Contrast	Condition	Area name	Coordinates	Cluster size	t-value	R
Aphasic > Amusic&Aphasic	Instrumental	Right STG (BA 21)	44 -38 7	632	4.71**	0.634 (< 0.001)
		Right MTG (BA 48)	50 -18 -5			
Amusic > Amusic&Aphasic	Vocal	Left MTG (BA 21)	-50 -2 -17	299	4.07*	0.419 (0.006)
		Right STG (BA 38)	50 12 -17	310	4.32*	0.426 (0.006)
Aphasic > Amusic	Vocal	Right MTG (BA 21)	64 -4 -11			
		Right Insula (BA 48)	50 6 -3			

* $p < 0.05$ uncorrected at the cluster level, ** $p < 0.01$ uncorrected at the cluster level

R = Pearson correlation (2-tailed p-value, FDR-corrected). The mean activation in the cluster is correlated to the MBEA total score % of the corresponding point of time. BA = Brodmann area, n.s. = not significant.

5.4.3 fMRI activation patterns in recovered vs. non-recovered amusic patients

Longitudinal analyses of the Instrumental and the Vocal condition did not yield any significant interactions. In the cross-sectional analysis of the Instrumental condition at the 3-month stage, the RAs showed significantly increased activations bilaterally in the MFG and IPL as well as in the left SPL and the right PCG compared to the NRAs (Table 13 and Figure 10). The MBEA total correlated significantly with the mean activity observed in the clusters comprising the right IPL ($r = 0.430$, $p = 0.005$), the right PreCG and MFG ($r = 0.481$, $p = 0.001$) and the left SPL, IPL, and MFG ($r = 0.436$, $p = 0.004$). At the 6-month stage, the RAs showed greater activations in the right IFG and MFG compared to the NRAs. In the Vocal condition, the NRAs showed greater activation bilaterally in the cerebellum at the 6-month stage. No other significant Group or Group x Time interactions were observed. None of the correlations between the MBEA performance and cluster mean activity at 6-month stage survived the FDR adjustment.

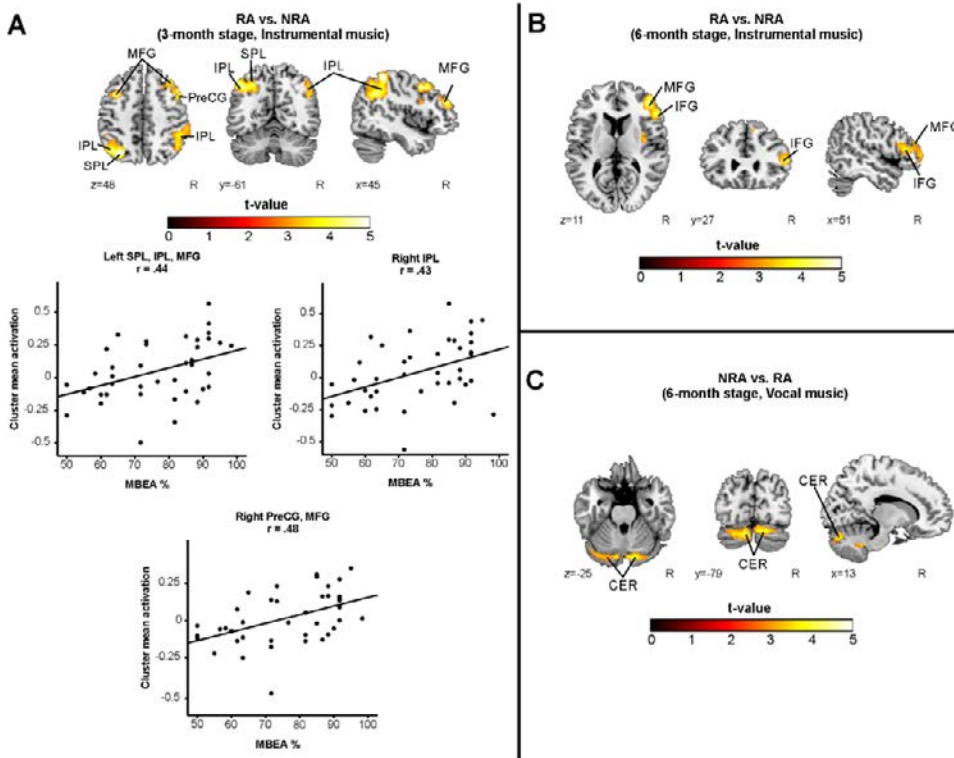


Figure 10 fMRI activation patterns during music listening – a comparison between the recovered and non-recovered amusics; $N = 24$. (A) RA vs. NRA (3-month stage, Instrumental); (B) RA vs. NRA (6-month stage, Instrumental); (C) NRA vs. RA (6-month stage, Vocal). $N = 24$. Results are shown at $p < 0.005$ (uncorrected) with ≥ 50 voxels of spatial extent and overlaid over a canonical template with MNI coordinates at the bottom right of each slice. Only clusters surviving a FWE-corrected $p < 0.05$ threshold are labelled (see also Table 13). The scatter plots display the correlation between the mean cluster activation and the MBEA total score across the whole sample. CER = cerebellum. Modified from Sihvonen et al. 2017²⁴¹.

Table 13 fMRI results during music listening – comparison between the RA and NRA groups.

3 MONTHS STAGE							
Contrast	Condition	Area name	Coordinates	Cluster size	t-value	R	
RA > NRA	Instrumental	Right IPL (BA 40)	46 -44 57	1480	5.96**	0.430 (0.005)	
		Left SPL (BA 7)	-30 -68 49	1085	5.86**	0.436 (0.004)	
		Left IPL (BA 7)	-36 -66 43				
		Left MFG (BA 9)	-44 -62 49				
		Right PreCG (BA 8)	46 8 43	857	5.30*	0.481 (0.001)	
		Right MFG (BA 10)	42 42 23				
6 MONTHS STAGE							
Contrast	Condition	Area name	Coordinates	Cluster size	t-value	R	
RA > NRA	Instrumental	Right MFG (BA 10)	42 42 13	1304	4.94**	n.s.	
		Right IFG (BA 46)	54 28 11				
NRA > RA	Vocal	Left Cerebellum	-12 -70 -37	1101	4.64*	n.s.	
		Right Cerebellum	16 -48 -37				

*p < 0.05 FWE-corrected at the cluster level, **p < 0.001 FWE-corrected at the cluster level

R = Pearson correlation (2-tailed p-value, FDR-corrected). The mean activation in the cluster is correlated to the MBEA total score % of the corresponding point of time. BA = Brodmann area, n.s. = not significant.

5.4.4 Functional connectivity in amusic patients during music listening

The engagement of the four chosen ICA networks (auditory, auditory-motor, left and right frontoparietal) was analysed in the Instrumental and Vocal conditions using two different mixed-model ANOVAs: Time (Acute / 3 months / 6 months) and Group (NA / Amusic) and Time (Acute / 3 months / 6 months) and Group (RA / NRA). The first ANOVA (NA / Amusic) yielded no significant effects. However, the second ANOVAs (RA / NRA) showed a Group effect for the right frontoparietal network [$F(1,22) = 28.20$, $p < 0.001$] and a Time x Group interaction for the left frontoparietal network [$F(1.5, 33.39) = 3.93$, $p = 0.040$] in the Instrumental condition (Figure 11). The RAs showed greater right frontoparietal network FC already at the acute stage as well as increasing left frontoparietal engagement from the acute to the 6-month stage compared to the NRAs. The engagement of the right frontoparietal network correlated significantly with the MBEA score at the 3-month stage ($r = 0.456$, $p = 0.025$).

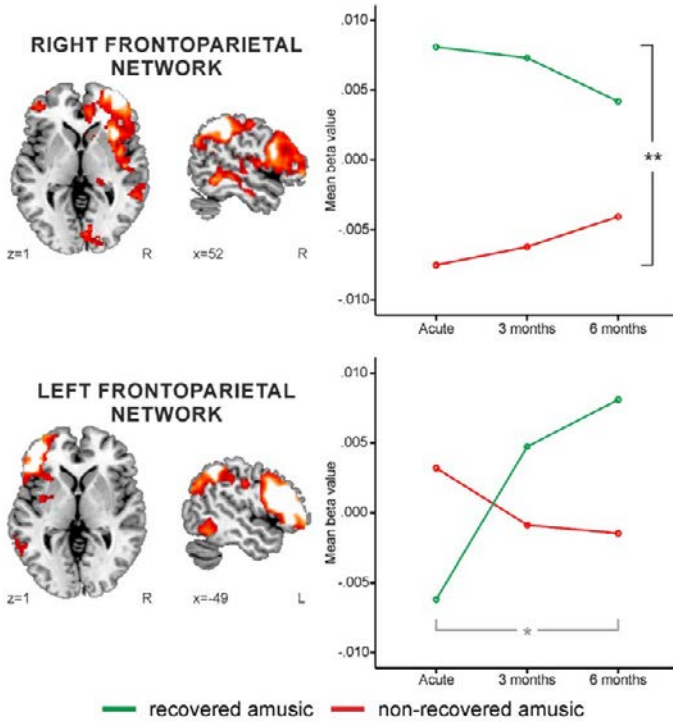


Figure 11 Functional connectivity differences between the RA and NRA groups during instrumental music listening. Group (RA/NRA) \times Time (Acute, 3 months, 6 months) repeated measures ANOVA results. A representation of the ICA network is shown overlaid over a canonical template with MNI coordinates at the bottom right of each slice. Significant Group effect (black bar), significant Group \times Time interaction (grey bar). * $p < 0.05$, ** $p < 0.001$. Modified from Sihvonen et al. 2017²⁴¹.

6 DISCUSSION

Using multiple advanced MRI methods, the three studies discussed here aimed to determine the specific stroke lesion patterns giving rise to acquired amusia and to reveal which GM changes and WM changes (volumetric and tract-level) are related to persistent acquired amusia and its recovery. In addition, the effect of amusia on brain activity patterns and functional connectivity changes during natural music listening was evaluated. In this longitudinal study with 6-month follow-up, the MBEA, gold standard assessment for amusia, and MRI were repeatedly performed on a large sample of stroke patients to achieve the pre-set aims. The main findings were that stroke lesions comprising the right temporal areas, insula, and putamen form the critical neural substrate for acquired amusia (Study I). Persistent amusia was associated with GM atrophy in the right STG and MTG, locating more anteriorly for rhythm-amusia and more posteriorly for pitch-amusia (Study I). The evaluation of WM tracts (Study II) revealed that persistent amusia is associated with damage and subsequent degeneration of multiple WM pathways in the right hemisphere, including the right IFOF, AF, and UF as well as the interhemispheric tracts CC and tapetum. While the specific right hemispheric lesion pattern leading to the observed GM and WM damage gave rise to amusia, the brain activation deficits in amusia during instrumental music listening were wide-spread initiating from the right temporal areas and, over time, proceeding to bilateral frontal, temporal, and parietal regions (Study III). Interestingly, amusics showed clearly less activation deficits when listening to vocal music, suggesting preserved processing of singing in the amusic brain. Amusia recovery was related to increased activation in the right frontal and parietal areas coupled with increased functional connectivity in right and left frontoparietal attention networks. In the following sections, six topics pertinent to the studies will be discussed in more detail: (1) disrupted neural structures in acute acquired amusia, (2) recovery of post-stroke amusia, (3) dissociation of pitch and rhythm processing deficits in amusia, (4) neural model of acquired amusia, (5) limitations of the study, and (6) clinical considerations.

6.1 Disrupted neural structures in acute acquired amusia

Stroke lesions associated with amusia and lower MBEA total scores were localised in the right MCA territory comprising the right STG, MTG, insula, and putamen. This is in line with the previous small-scale group and case studies that have linked the right MCA territory^{12, 13, 16, 167-178, 182-184} and especially the right temporal lobe lesions^{12, 167, 168, 171-173, 175-178, 183, 184} to acquired amusia. The lesion pattern associated with amusia was clearly distinct from the one associated with aphasia: the

lesion pattern giving rise to aphasia comprised the left STG and insula, in accordance to previous studies^{56, 57, 60}. Our finding supports the dissociation of language and music processing in the brain, suggesting, at least partly, recruitment of different neural networks for either cognitive domain¹⁹⁴. However, in the patient sample in Study I, 41% of the amusic patients had at least minor aphasia. This is similar to the percentages (43-55%) reported in previous studies^{8, 13} and indicates that music and language impairments can occur together. While the sample size did not allow full 2 x 2 analysis [amusia (no/yes) × aphasia (no/yes)] or separate analyses within left hemisphere damage (LHD) and right hemisphere damage (RHD) subgroups, binary analyses on amusics (no aphasia) versus aphasics (no amusia), amusics versus NAs with all aphasics excluded, aphasics versus non-aphasics with all amusics excluded, and amusics versus amusics and aphasics were performed to control for the comorbidity of these disorders. These analyses yielded essentially the same results as the analyses of primary amusia and aphasia analyses, thereby supporting the dissociation of the neuroanatomical correlates of amusia and aphasia. The present results are important given the longstanding discrepancy between the findings of lesion studies and functional neuroimaging studies of healthy subjects, the former reporting cases of selective post-stroke impairment of music and language^{194, 242-244} and the latter frequently reporting anatomical overlap in responses to music and speech^{108, 245-247}.

In line with the previous lesion studies^{12, 17, 173, 176}, the present results showed that amusia is associated with lesions comprising the right superior temporal cortex. Acquired amusics also exhibited decreased activations during instrumental music listening in the right STG and MTG compared to non-amusics at the acute stage. The activation in this region also strongly correlated with the acute stage MBEA total score. Neuroimaging studies on healthy subjects have indicated that the right STG is one of the key brain areas in the large-scale network for music processing^{2, 4, 76} and that it plays a crucial role in processing of pitch and melody⁷⁷⁻⁸¹, music syntax⁹⁶, and in singing^{109, 110}. A very recent study utilising direct electrical stimulation showed that stimulation of the right STG induced errors in pitch processing during melody repetition task²⁴⁸. Moreover, the volume of the right STG correlates with the amount of musical practice²⁴⁹ and is greater in individuals with absolute pitch²⁵⁰. Based on our findings, the pitch processing deficit in acquired amusia seems to stem from damage to the right temporal region leading to the observed activation deficits. This is in line with previous MEG results showing that severe acquired amusia is associated with damage to the right AC and consequently decreased function during pitch processing and duration discrimination¹⁸⁴.

Right insular lesions were associated with amusia in all of the present results. While lesions in the insula have previously been linked to pitch-amusia after stroke^{173, 176}, the present results might also reflect damage to WM tracts locating

near insula. Previously, the AF has been considered as the primary WM tract involved in congenital amusia¹⁵¹, although the evidence is conflicting. In Study II, our novel finding was that acquired amusia was linked to clear damage of the right IFOF at the acute stage. Moreover, the volume of the right IFOF was the most significant predictor of MBEA performance. The IFOF is a ventral tract that originates from posterior occipital region, runs through posterior temporal lobe, and then medially to the insula (i.e. in the extreme capsule) to connect to the orbito-frontal and inferior frontal areas^{117-121, 251}. Although the exact auditory function of IFOF remains unknown, it has been linked to absolute pitch¹²², musical synaesthesia¹²³, and hearing loss²⁵². In addition to the right IFOF, amusia was also associated with acute stage damage to the right AF. Conversely, increased volume of the left AF (posterior segment) was associated to higher MBEA overall scores at the acute stage. Previous studies have concluded that the right AF is implicated in congenital amusia¹⁵¹, the left AF in musicians' absolute pitch^{126, 253}, and bilateral/right AF more generally in musical training^{125, 127}.

Amusia was also associated with damage to the interhemispheric WM connectivity (i.e. CC) at the acute stage, reflecting reduced structural connectivity between the right and left superior temporal regions. Reduced lateral connectivity between the ACs has been reported in a recent MEG study on congenital amusics during a memory-based processing of tone changes²⁵⁴. Coupled with the fact that the amusics had more extensive stroke lesions and further atrophy in the right STG and MTG than NAs (see 6.2), the present findings are consistent with recent studies reporting that inhibiting the right AC with transcranial magnetic stimulation reduces connectivity between the ACs²⁵⁵ and that the strength of the callosal auditory tracts correlates with performance in an auditory-speech perception task²⁵⁶. Musicians have been shown to have larger volume and increased FA in the anterior^{125, 128} and posterior^{124, 125} CC, as compared to non-musicians. In addition, musicians exhibit activity patterns during music listening that are hemispherically more symmetrical than those of non-musicians²⁵⁷.

6.2 Recovery of post-stroke amusia

Lack of amusia recovery was associated with negative plastic changes in core auditory areas of the right hemisphere: the NRAs showed longitudinal GMV decrease in the right STG and MTG. Structural abnormalities in the right STG have also been observed in congenital amusics^{145, 146} and the GM anomalies have been associated with decreased connectivity between the right frontal and temporal regions^{144, 145}. Correspondingly, in Study I, non-recoverable acquired amusia was associated with WMV decrease in the right MTG, a region within the right fronto-temporal pathway. In Study II, the RA patients showed clearly less acute damage

and less delayed degeneration in two right frontotemporal pathways, the IFOF and AF, compared to the NRAs. While the right AF has been implicated in congenital amusia¹⁵¹, although with conflicting evidence¹⁵², the IFOF has not been previously linked to amusia. The dorsal pathway AF was also implicated in recovery of pitch-amusia as the pRAs showed longitudinal decrease in MD/RD in the right anterior AF. This suggests that recovery from pitch-amusia may be associated with preservation of this WM tract connecting the IFG and IPL. This may be related to spared tonal working memory in recovery from pitch-amusia since the right IPL has been associated with maintenance of tonal pitch structure in working memory during pitch discrimination⁸⁷. The NRAs had also increased axonal damage (i.e. higher MD and RD) in the callosal auditory fibres (i.e. the tapetum), indicating that Wallerian degeneration of these pathways is linked to persistent amusia⁴⁸⁻⁵². As the axonal degeneration progresses, the cortical axon terminals become affected, leading to the GM atrophy observed in Study I.

Both the right IFOF and the AF have right inferior frontal and inferior parietal terminations^{212, 217, 251}. Reasonably, the cross-sectional results in Study III showed that RAs had significantly increased activations in the right MFG/IFG during instrumental music listening at 3-month and 6-month post-stroke stages compared to the NRAs. At 3-month stage, the activation correlated significantly with the MBEA performance. Previously, congenital amusics have been shown to have dysfunction in the right IFG^{144-146, 148} and its reduced connectivity to the right AC¹⁵⁴. The IFG is implicated in sequencing of auditory information as well as analysing the structural relationships in music⁹⁶. Moreover, the IFG is involved in musical priming²⁵⁸, recognition of music²⁵⁹, perceiving musical emotions²⁶⁰, analysing musical syntax²⁶¹, and performing structural integration of harmonic information⁹⁸. On the grounds of this information, the increased activation observed in the right IFG in the RAs compared to the NRAs might represent preserved processing of music and its components as well as functioning analysis of structural and harmonic information in music. Furthermore, the NRAs showed activation deficits in the right PreCG and bilaterally in the IPL. Precentral areas are involved in rhythm processing and structural analysis^{93, 96, 262}, which further suggests defective higher-order computations in amusia during natural music listening. This could also clarify the observed bilateral IPL activation deficits in the NRAs compared to the RAs, since the IPL is involved in evaluation of pitch information in tonal structures⁸⁷ as well as in recognition of melodies²⁶³ and detection of melodic deviance²⁶⁴, and in rhythm perception^{264, 265}.

Parietal regions, along with frontal areas, are also activated during attentive listening to music²⁶⁶. Therefore, the observed spared activity in these areas in RAs might reflect the ability of the patient to focus attention towards natural music and thus enable its neural processing. This rationale is supported by the observed increase in the network connectivity in the RAs compared to the NRAs. The RAs

had greater right frontotemporal network FC already at the acute stage, indicating that amusia recovery is based on preserved function and connectivity in this network. The FC in the right frontoparietal network also correlated significantly with the MBEA total score in the 3-month post-stroke stage. Moreover, the RAs showed longitudinally increasing FC in the left frontoparietal network, reflecting changes in network connectivity in the left hemisphere associated with amusia recovery. The observed differences in task activity in frontoparietal regions and in FC in the frontoparietal attentional networks between the RAs and the NRAs cannot be due to deficits in general attentional orientation, since no differences were observed during vocal music listening. The longitudinal left frontoparietal FC increase might echo that the RAs regain the access to utilize cross-hemispheric local and global music networks¹³. While the resting-state/intrinsic frontotemporal connectivity has been shown to be reduced in congenital amusia^{145, 156}, no previous task-ICA analyses exist nor are there studies on acquired amusics concerning this issue. The present results provide evidence that while damage to the right ventral pathway leads to acquired amusia, preserved dorsal connectivity promotes amusia recovery and is linked to compensatory network remodelling. Moreover, the observed functional differences between the RAs and NRAs most likely reflect similar longitudinal network reorganization associated with spontaneous recovery of function after stroke^{33, 35}.

6.3 Dissociation of pitch and rhythm processing deficits in amusia

Separate VLSM analyses of the parametric MBEA Scale and Rhythm scores revealed a predominantly overlapping lesion pattern in the aforementioned right hemisphere regions. Naturally, stroke lesions follow the vascular territories and thus are not restricted to a single functional brain region. To probe the most critical brain areas illustrated by VLSM results, the t-value cut-off can be adjusted to only view the most significant results (i.e. brain areas) in a particular lesion pattern. When this approach was applied to the VLSM results on MBEA Rhythm subtest, the right basal ganglia remained as the most significant element. Previously, studies on healthy subjects have linked basal ganglia closely to rhythm processing^{4, 262, 267, 268}. Moreover, professional pianists have skill-related GMV changes in the basal ganglia¹³⁴. However, to our best knowledge, the present study is the first lesion study providing direct evidence of the role of the right basal ganglia in rhythm perception deficits¹¹.

Interestingly, longitudinal GMV decrease was observed in the right anterior temporal areas in rhythm-amusia and in posterior temporal areas in pitch-amusia. Similar functional distribution of the superior temporal region has been reported in both animals⁸⁴ and in humans^{75, 83, 85}; anterior superior temporal region showing

greater sensitivity to changes in the temporal domain and posterior regions showing greater sensitivity to changes in the spectral domain. Moreover, anterior temporal lesions have been linked to rhythm (i.e. meter, tempo) perception deficits in temporal lobectomy patients^{15, 17}.

In addition to the longitudinal GMV differences observed in pitch and rhythm-amusia, Study II provided dissociative DTI results on pitch-amusia and rhythm-amusia. Longitudinal MD and RD increase in the right anterior AF, UF, and tapetum was observed in the pNRA group but not in the rNRA groups. As the increases in MD and RD have been shown to be markers of Wallerian degeneration⁴⁹⁻⁵², the findings especially in the AF and tapetum are well in line with the posterior temporal GMV decrease observed in pitch-amusia in Study I. Moreover, the MD/RD of the tapetum and right UF were the most significant predictors of MBEA Scale performance, but not MBEA Rhythm performance, at the 6-month post-stroke stage. Overall, the results of the present study converge with previous neuroimaging studies^{78, 81} and lesions studies^{12, 17} showing that right superior temporal areas are crucial for pitch and melody processing. Present results further suggest that the interhemispheric connectivity of superior temporal areas as well as right frontal pathways have an important role in pitch-amusia.

Contrary to pitch-amusia, rhythm-amusia was associated with axonal damage in the left AF, marked by longitudinal increase in RD. Moreover, lower volume in the right UF and higher MD and RD in the CC were observed in the rNRAs but not in the pNRAs. The rNRAs also showed lower volume of the right IFOF than rRAs, and right IFOF volume also came out as the only significant predictor of MBEA Rhythm performance in the regression analyses across all three time points. Coupled with the findings of Study I, these results suggest that rhythm-amusia is associated with more extensive and bilateral damage of frontal and frontotemporal pathways than pitch-amusia. This finding is supported by the lack of clear lateralisation effects for musical rhythm processing in healthy subjects^{4, 75} and lesion studies^{12, 13, 15-17}.

6.4 Neural model of acquired amusia

Functional neuroimaging studies on healthy subjects have shown that music perception involves a wide-spread network comprising bilateral temporal, frontal, parietal, and subcortical brain regions^{2, 4, 76}. Studies on stroke patients have provided similar evidence of cross-hemispheric network underlying music perception. However, as suggested first by Peretz (1990) and later by Schuppert and colleagues (2000), music perception relies on initial recognition of global musical structures in the right hemisphere, supported by the left hemisphere subsystems that are subordinate to the right hemisphere^{13, 269}. In general, spatially distributed brain areas

subserving a cognitive function are connected through WM tracts which form a network to maximize the processing, storage, and manipulation of information²⁷⁰. Disruption of the neural network and its connections can lead to a disconnection syndrome and a cognitive-behavioural deficit^{271, 272}. Based on the present study, and in contrast with the bilateral large-scale music network observed in healthy subjects, the critical connections for music perception seem to be located in the right hemisphere. The initial acute stage lesion pattern associated with acquired amusia was located in the right hemisphere and comprised the striatum, insula, STG, and MTG. This lesion pattern compromised crucial WM pathways, especially the IFOF, linking the right temporal and inferior frontal regions, thus leading to acquired amusia. From ontogenetic and phylogenetic standpoints, our results linking the right IFOF to music perception is particularly interesting since in humans, the IFOF is known to be present already at birth²⁷³, but it is clearly less developed in monkeys²⁷⁴. While the prime neural architectures in acquired amusia were right-lateralised, amusia was also associated with damage to interhemispheric connectivity (i.e. the CC and tapetum), more pronouncedly in rhythm-amusia. This supports the rationale of additional left hemispheric subsystems needed in music perception and processing, although with right hemisphere dominance.

The mechanisms of amusia recovery might be related to spared WM tracts interconnecting crucial regions underlying music processing. In language research, two processing streams, dorsal and ventral, are broadly accepted to underlie the perception and production of language^{187, 275, 276}. A similar dual-stream model has been proposed to act in parallel in music processing, transferring crucial musical auditory information between the temporal, inferior parietal, and inferior frontal regions in the right hemisphere¹⁸⁶⁻¹⁹⁰. Of the two streams, the dorsal stream (“where” or “how”) connecting temporal and inferior parietal regions with frontal areas is hypothesized to be important for evaluation of audio-motor movement and spatial information, whereas the ventral stream (“what”) is involved in categorizing sound to auditory objects^{187, 188, 275, 277}. In aphasia, damage to the dorsal stream (SLF and AF) is associated with productive impairments, while comprehension deficits are associated with injury of the ventral stream (extreme capsule, or rather the IFOF)¹⁹¹. In the musical domain, it is likewise possible that damage to individual pathways (dorsal or ventral) would manifest in different musical impairments (production versus perception)^{164, 188, 189}. If both the ventral and dorsal streams are damaged, it is unlikely that acquired amusia recovers. Instead, acquired amusics with at least one preserved right hemispheric music-related pathway interconnecting frontoparietal regions could engage recovery as the two streams have been found to share functionalities and mediate compensatory mechanisms in the language domain²⁷⁸. This rationale is supported by the present study.

Interestingly, acquired amusics showed less activation deficits during vocal music listening than instrumental music listening, and as there were no significant

differences between the groups in the occurrence of post-stroke language deficit (i.e. aphasia), the observed results are unlikely explained by dissimilarities in language processing in the amusic and non-amusic patients. Indeed, the subgroup analysis comparing patients with amusia without aphasia to patients with aphasia without amusia, or patients with amusia and aphasia, further supports the conclusion that areas important for music processing are located in the right temporal and insular areas. In contrast, aphasia does affect the processing of vocal music, and is observed as activation deficits in the left temporal region. These findings support the idea that the disruption of neuronal activity shown by amusic patients during music listening might be more related to music rather than to language processing deficit. Overall, the preserved vocal music processing in amusic brain might reflect that the amusic brain processes the musical components using the left-lateralised brain regions responsive to vocal stimuli². Fascinatingly, congenital amusics can vocalize pitch intervals in correct directions¹⁶⁴ and improve in MBEA subtest performance and song production after singing intervention^{162, 163}. These findings suggest that the processing of vocal music is, at least partially, spared and active in amusic patients. Moreover, while the congenitally amusic persons recognize familiar song lyrics, but are unable to recognize the corresponding melodies¹⁶⁵, amusic patients might be able to access the episodic memory through the vocal content of the music rather than by melody.

While the structural findings in acquired amusia were largely right-lateralised, functional anomalies were observed in both hemispheres during instrumental music listening. In addition to the global (right-lateralised) versus local (left-lateralised) dissociation of auditory information processing discussed previously^{13, 269}, an additional explanation is that the critical hubs in the bilateral music network are located in the right hemisphere^{2, 4, 76} and damage to these neural structures manifests in wide-spread processing deficits during music perception. In this vein, as acquired amusia can occur also after LHD¹³, lesions affecting the crucial WM tracts interconnecting music processing areas in the left hemisphere to the crucial right hemispheric music-related brain regions (i.e. critical hubs) might lead to acquired amusia. Moreover, intact right hemisphere has been suggested to compensate for the music perception deficits after LHD¹³ which underlines the importance of the right hemisphere in music processing. One other possible explanation is that during naturalistic music listening (used in Study III), more global auditory information processing is needed, in contrast to local processing^{13, 269}. Moreover, the disparity between the lateralisation of lesion and functional anomalies could arise from stimulus complexity. In language domain, the lateralisation of prosodic emotion processing is dependent on the verbal complexity: As the complexity increases, the brain activity observed shifts from predominantly right-lateralized to bilateral activity²⁷⁹. Similarly, music contains complex acoustic components as well as a language component, and therefore it is reasonable to expect bilateral

wide-spread brain activations during music listening. Taken together, RHD leading to acquired amusia might manifest in wide-spread global music processing deficits whereas LHD might affect only local processing and thus lead to small-scale activation deficits.

Overall, the present findings converge on the proposal of recent dual-stream studies on processing of music syntax¹⁹⁰ and prosody¹⁸⁸ in the healthy brain concluding that both ventral and dorsal streams are implicated in these functions. Acting in conjunction, the two streams transform complex acoustic feature combinations into abstract representations and analyse sensorimotor information to be integrated with these representations²⁷⁷. The present study suggests that normal music perception relies on this dual route especially in the right hemisphere.

6.5 Limitations of the study

The groups showed differences in some demographical (education) and clinical (lesion volume, spatial neglect) factors. Lower education level²⁸⁰ and larger lesion size²⁸¹ are associated with higher severity of stroke, which in turn may lead to a higher likelihood of acquired amusia. The coincidence of neglect and acquired amusia is expected given their similar lesion locations²³⁸, and therefore neglect was not included as a covariate in the analyses. In Study II and III, educational years and acute lesion size were entered as covariates, but in Study I, no covariates were used as the RA and NRA groups did not show any significant differences in demographic data. However, this may influence the results of the VLSM binary analyses. The groups did not show significant differences in the pre-stroke musical background factors. Evaluation of the potential facilitating effect of musical training on recovery from acquired amusia would call for a larger sample of patients with different levels of musical background. Furthermore, the possible protective effect of higher education in acquired amusia needs further investigation.

While the study showed that acquired amusia is strongly associated with RHD, there were also LHD patients with persistent acquired amusia. Therefore, studies with larger samples of LHD are still needed to determine how different left hemisphere regions are associated with amusia. One key area associated with rhythm processing is the cerebellum^{94, 267}. However, due to our inclusion criteria, cerebellar involvement in the rhythm-amusia could not be evaluated in the present material.

6.6 Clinical considerations

Several studies have shown that acquired amusia is common after stroke. However, in clinical practice, acquired amusia is not systematically evaluated and information on its recovery is lacking. Therefore, acquired amusia is probably underdiagnosed in clinical populations. The present results have important implications in enabling accurate identification of acquired amusia as well as offering tools for predicting recovery. Diagnosing amusia is especially important in patients who are vocationally engaged to music, such as musicians, and music teachers, but also patients with pre-stroke musical hobbies. Amusic persons most likely have concurrent deficits also in perceiving affective prosody (emotional content and connotations of speech expressed through subtle pitch, timbre, and intensity variations), as has been shown in^{282, 283} congenital and acquired amusia¹⁸, leading to difficulties in perceiving and expressing emotions in everyday communication. The presence of acquired amusia should also be taken into consideration when designing and targeting music-based intervention strategies in neurological rehabilitation²⁸⁴.

7 CONCLUSIONS

1. Damage to the right STG, MTG, insula, and putamen form the crucial neural substrate for acquired amusia after stroke. This lesion pattern is distinct from the stroke lesion pattern giving rise to aphasia.
2. Persistent acquired amusia is associated with atrophy in the right STG and MTG, locating more anteriorly in rhythm-amusia and more posteriorly in pitch-amusia.
3. Persistent acquired amusia is associated with damage and later degeneration in multiple right frontotemporal tracts as well as in interhemispheric pathways. Damage to the right ventral pathway (i.e. IFOF) is the strongest predictor of acquired amusia. In addition to impaired right frontotemporal connectivity, pitch-amusia is additionally linked to deficits in right frontoparietal and temporal interhemispheric connectivity, whereas rhythm-amusia is additionally linked to deficits in left frontal connectivity.
4. Acquired amusia causes wide-spread dynamic brain activation deficits during instrumental music listening. The activation deficits initiate in right temporal areas at the acute stage and progress bilaterally to frontal, temporal, and parietal areas over time.
5. The recovery of acquired amusia is associated with increased brain activity in right superior and inferior parietal regions and in right inferior frontal areas during instrumental music listening. Moreover, amusia recovery is mediated by increased FC during instrumental music listening in frontoparietal (i.e. dorsal) networks.

ACKNOWLEDGEMENTS

This work was carried out at the University of Turku, Faculty of Medicine, Department of Clinical Medicine, Neurology and the Department of Clinical Neurosciences, Turku University Hospital during the years 2011-2018.

This study was financially supported by Finnish Brain Research and Rehabilitation Foundation, Finnish Medical Foundation, Finnish Brain Foundation, Miina Sillanpää Foundation, Maire Taponen Foundation, Signe and Ane Gyllenberg Foundation, and Foundation of Municipal Doctor Uulo Arhio.

Firstly, I would like to express my sincere gratitude to my supervisors, professor Seppo Soinila and docent Teppo Särkämö for their guidance, advice, and continuous strong support for this study and related research. I thank professor Soinila for providing me the opportunity to grow scientifically under the supervision of such a brilliant and intelligent person. His example is not only inspiring me as a researcher, but drives me to be a better clinician, now and in the future. I thank docent Särkämö for guiding me and for sharing his vast knowledge in cognitive neuroscience. I greatly appreciate all the knowledge and skills he has imparted to me, and I thank for the support, friendship and advice that helped shape my professional career. I could not have imagined having better supervisors and mentors to support the beginning of my academic path, working with you has been a privilege.

Besides my supervisors, I warmly thank professor Mari Tervaniemi for giving me the opportunity to become a part of the wonderful Cognitive Brain Research Unit (CBRU) family at University of Helsinki as well as a part of this wonderful project, for support, encouragement, and trust over the years. My heartfelt thanks to professor Antoni Rodríguez Fornells for his warm support. Antoni provided excellent facilities and work environment for me to learn advanced MRI analysis methods in the IDIBELL Cognition and Brain Plasticity lab at the University of Barcelona and Bellvitge University Hospital. I am truly grateful for making me feel welcomed to be a part of the lab and sharing me your knowledge of neuroscience. I would also like to thank professor Riitta Parkkola, professor Matti Laine, and Ph.D. Jani Saunavaara for their encouragement and support during this study. In addition, I would like to express my gratitude to the fantastic radiographers Ulla Anttalainen (†), Riku Luoto and Tuija Vahtera, and the music therapists Terhi Lehtovaara, Pekka Rajanaro, and Aki Ylönen.

This study would have not been possible without my MRI mentor Ph.D. Pablo Ripollés. My humblest thanks for teaching me everything I know about MRI, for teaching it with passion and patience, and for the encouragement and support during all these years. I thank for the opportunity to work with the most gifted young researcher I have met, and most importantly for friendship. I would also like to thank all the gifted people from the IDIBELL Cognition and Brain Plasticity lab at the University of Barcelona: Lucia, Jenni, Claudia, Asia, Noelia, Helena, Clem,

Cucu, Joan, and Ernest. Thank you for your friendship and for welcoming me to your scientific family. Gracias por todo!

I would like to express my sincere gratitude to my Ph.D. student colleague M.A. Vera Leo. I thank Vera for the support, friendship, encouragement, and the journey we have shared over the years. I would also like to thank the amazing people at CBRU at University of Helsinki: Tommi, Peter, Paula, Sanna, Sini, Eino, Iina, Anja, Emma, Linda, Tanja, Emmi, Anni, Miika, Anastasia, Tuomas, Teemu, Sini-Tuuli, and Irina. Special thanks go to professor Teija Kujala for sharing the same passion for music as well as for all the interesting discussions we have had over the years.

I was extremely fortunate to receive reviews of my thesis from two esteemed experts, professor David Copland and Ph.D. Daniela Sammler. I am humbled and grateful for their positive evaluations. I would also like to thank my Thesis Committee members professors Lauri Soinne, Sakari Suominen and Marja Hietanen for their support, comments and encouragement during these years.

I would like to express my great appreciation to my medical school class' super group "Takikset" for being a big part of my life and making me feel at home in Turku during our studies. I wish you all the very best in life and as medical doctors. I would like to offer my special thanks to Marko Ristola, who quickly became one of my closest friends and whom I hold in high esteem.

In addition to my later studies in life, one earlier school class group is extremely close to my heart. I express my deepest gratitude to Arto, Kalle, Tommi, Tuomas, and Ezra, the amazing guys whom I met back in the days at the Kruununhaka middle school. I think meeting you has been a life-changing moment for me and I truly admire you all and I appreciate our long-lasting friendship. Furthermore, I would like to express my heartfelt thanks to my important friends Timi, Roni and Iiro: thank you for your support, encouragement, and warm friendship.

Music has always been extremely important for me and provided me a way to express something I cannot put into words. While making, playing, and performing music is a powerful experience for me, it is even greater when shared with amazing friends. I have been very fortunate to have made, played, and performed music with guys from my bands: Imperanon, Norther, and Medicated. Jaska, Eki, Lauri, Aleksi, Teemu, Aki, Jukkis, Heikki, Kride, Dane, Tuomas, Tomi, Samuli, Dani, Jani, and Pertti, thank you all from the bottom of my heart.

I express my special gratitude to my parents Irma and Ari as well as my brother Antti and his family for their love, encouragement, and help. Finally, I owe my profound gratitude to my family: my wife Jenni for all her love, support, and understanding, and to our little sons Anton and Joonatan for bringing me endless joy and making me laugh every day. Thank you for teaching me what is truly important in life, and I hope that daddy can make you proud.

REFERENCES

1. Andersen, H. C. in *Bilderbuch ohne Bilder* (Verlag von Carl B. Lorck., Leipzig, 1847).
2. Brattico, E. *et al.* A Functional MRI Study of Happy and Sad Emotions in Music with and without Lyrics. *Front. Psychol.* **2**, 308 (2011).
3. Toiviainen, P., Alluri, V., Brattico, E., Wallentin, M. & Vuust, P. Capturing the musical brain with Lasso: Dynamic decoding of musical features from fMRI data. *Neuroimage* **88**, 170-180 (2014).
4. Alluri, V. *et al.* Large-scale brain networks emerge from dynamic processing of musical timbre, key and rhythm. *Neuroimage* **59**, 3677-3689 (2012).
5. Zatorre, R. J. & Salimpoor, V. N. From perception to pleasure: music and its neural substrates. *Proc. Natl. Acad. Sci. U. S. A.* **110 Suppl 2**, 10430-10437 (2013).
6. Koelsch, S. Brain correlates of music-evoked emotions. *Nat. Rev. Neurosci.* **15**, 170-180 (2014).
7. Koelsch, S. Toward a neural basis of music perception - a review and updated model. *Front. Psychol.* **2**, 110 (2011).
8. Stewart, L., von Kriegstein, K., Warren, J. D. & Griffiths, T. D. Music and the brain: disorders of musical listening. *Brain* **129**, 2533-2553 (2006).
9. Marin, M. M., Gingras, B. & Stewart, L. Perception of musical timbre in congenital amusia: categorization, discrimination and short-term memory. *Neuropsychologia* **50**, 367-378 (2012).
10. Stewart, L. Fractionating the musical mind: insights from congenital amusia. *Curr. Opin. Neurobiol.* **18**, 127-130 (2008).
11. Rorden, C. & Karnath, H. O. Using human brain lesions to infer function: a relic from a past era in the fMRI age? *Nat. Rev. Neurosci.* **5**, 813-819 (2004).
12. Ayotte, J., Peretz, I., Rousseau, I., Bard, C. & Bojanowski, M. Patterns of music agnosia associated with middle cerebral artery infarcts. *Brain* **123**, 1926-1938 (2000).
13. Schuppert, M., Münte, T. F., Wieringa, B. M. & Altenmüller, E. Receptive amusia: evidence for cross-hemispheric neural networks underlying music processing strategies. *Brain* **123 Pt 3**, 546-559 (2000).
14. Särkämö, T. *et al.* Amusia and cognitive deficits after stroke: is

- there a relationship? *Ann. N. Y. Acad. Sci.* **1169**, 441-445 (2009).
15. Kester, D. B. *et al.* Acute effect of anterior temporal lobectomy on musical processing. *Neuropsychologia* **29**, 703-708 (1991).
16. Rosslau, K. *et al.* Clinical investigations of receptive and expressive musical functions after stroke. *Front. Psychol.* **6**, 768 (2015).
17. Liegeois-Chauvel, C., Peretz, I., Babai, M., Laguitton, V. & Chauvel, P. Contribution of different cortical areas in the temporal lobes to music processing. *Brain* **121 (Pt 10)**, 1853-1867 (1998).
18. Jafari, Z., Esmaili, M., Delbari, A., Mehrpour, M. & Mohajerani, M. H. Post-stroke acquired amusia: A comparison between right- and left-brain hemispheric damages. *NeuroRehabilitation* **40**, 233-241 (2017).
19. Uetsuki, S. *et al.* A case of expressive-vocal amusia in a right-handed patient with left hemispheric cerebral infarction. *Brain Cogn.* **103**, 23-29 (2016).
20. Feigin, V. L., Lawes, C. M., Bennett, D. A., Barker-Collo, S. L. & Parag, V. Worldwide stroke incidence and early case fatality reported in 56 population-based studies: a systematic review. *Lancet Neurol.* **8**, 355-369 (2009).
21. https://sampon.thl.fi/pivot/prod/fi/cvdr/first/fact_str_015.
22. Benjamin, E. J. *et al.* Heart Disease and Stroke Statistics-2017 Update: A Report From the American Heart Association. *Circulation* **135**, e146-e603 (2017).
23. http://apps.who.int/iris/bitstream/10665/186463/1/9789240694811_eng.pdf?ua=1.
24. GBD 2013 Mortality and Causes of Death Collaborators. Global, regional, and national age-sex specific all-cause and cause-specific mortality for 240 causes of death, 1990-2013: a systematic analysis for the Global Burden of Disease Study 2013. *Lancet* **385**, 117-171 (2015).
25. Feigin, V. L. *et al.* Auckland Stroke Outcomes Study. Part 1: Gender, stroke types, ethnicity, and functional outcomes 5 years post-stroke. *Neurology* **75**, 1597-1607 (2010).
26. Rathore, S. S., Hinn, A. R., Cooper, L. S., Tyroler, H. A. & Rosamond, W. D. Characterization of incident stroke signs and symptoms: findings from the atherosclerosis risk in communities study. *Stroke* **33**, 2718-2721 (2002).
27. Nys, G. M. *et al.* Cognitive disorders in acute stroke: prevalence and clinical determinants. *Cerebrovasc. Dis.* **23**, 408-416 (2007).

28. Nys, G. M. *et al.* Domain-specific cognitive recovery after first-ever stroke: a follow-up study of 111 cases. *J. Int. Neuropsychol. Soc.* **11**, 795-806 (2005).
29. Murphy, T. H., Li, P., Betts, K. & Liu, R. Two-photon imaging of stroke onset in vivo reveals that NMDA-receptor independent ischemic depolarization is the major cause of rapid reversible damage to dendrites and spines. *J. Neurosci.* **28**, 1756-1772 (2008).
30. Besancon, E., Guo, S., Lok, J., Tymianski, M. & Lo, E. H. Beyond NMDA and AMPA glutamate receptors: emerging mechanisms for ionic imbalance and cell death in stroke. *Trends Pharmacol. Sci.* **29**, 268-275 (2008).
31. Hossmann, K. A. Pathophysiology and therapy of experimental stroke. *Cell. Mol. Neurobiol.* **26**, 1057-1083 (2006).
32. Zhang, S. & Murphy, T. H. Imaging the impact of cortical microcirculation on synaptic structure and sensory-evoked hemodynamic responses in vivo. *PLoS Biol.* **5**, e119 (2007).
33. Saur, D. *et al.* Dynamics of language reorganization after stroke. *Brain* **129**, 1371-1384 (2006).
34. Kertesz, A. & McCabe, P. Recovery patterns and prognosis in aphasia. *Brain* **100 Pt 1**, 1-18 (1977).
35. Cramer, S. C. Repairing the human brain after stroke: I. Mechanisms of spontaneous recovery. *Ann. Neurol.* **63**, 272-287 (2008).
36. Hope, T. M. H. *et al.* Right hemisphere structural adaptation and changing language skills years after left hemisphere stroke. *Brain* **140**, 1718-1728 (2017).
37. Desmond, D. W., Moroney, J. T., Sano, M. & Stern, Y. Recovery of cognitive function after stroke. *Stroke* **27**, 1798-1803 (1996).
38. Pedersen, P. M., Jorgensen, H. S., Nakayama, H., Raaschou, H. O. & Olsen, T. S. Aphasia in acute stroke: incidence, determinants, and recovery. *Ann. Neurol.* **38**, 659-666 (1995).
39. Hier, D. B., Mondlock, J. & Caplan, L. R. Recovery of behavioral abnormalities after right hemisphere stroke. *Neurology* **33**, 345-350 (1983).
40. Johansen-Berg, H. Functional imaging of stroke recovery: what have we learnt and where do we go from here? *Int. J. Stroke* **2**, 7-16 (2007).
41. Ward, N. S., Brown, M. M., Thompson, A. J. & Frackowiak, R. S. Neural correlates of outcome after stroke: a cross-sectional fMRI study. *Brain* **126**, 1430-1448 (2003).
42. Manganotti, P., Acler, M., Zanette, G. P., Smania, N. & Fiaschi, A. Motor cortical disinhibition during early and late recovery after stroke.

- Neurorehabil. Neural Repair* **22**, 396-403 (2008).
43. Zhang, Z. G. & Chopp, M. Neurorestorative therapies for stroke: underlying mechanisms and translation to the clinic. *Lancet Neurol.* **8**, 491-500 (2009).
44. Li, Y. *et al.* Gliosis and brain remodeling after treatment of stroke in rats with marrow stromal cells. *Glia* **49**, 407-417 (2005).
45. Levin, M. F., Kleim, J. A. & Wolf, S. L. What do motor "recovery" and "compensation" mean in patients following stroke? *Neurorehabil. Neural Repair* **23**, 313-319 (2009).
46. *Cognitive Neurorehabilitation: Evidence and Application* (eds Stuss, D. T., Winocur, G. & Robertson, I. H.) (Cambridge University Press, Cambridge, 2008).
47. Alexander, A. L. *et al.* Characterization of cerebral white matter properties using quantitative magnetic resonance imaging stains. *Brain Connect.* **1**, 423-446 (2011).
48. Ivanova, M. V. *et al.* Diffusion-tensor imaging of major white matter tracts and their role in language processing in aphasia. *Cortex* **85**, 165-181 (2016).
49. Yu, C. *et al.* A longitudinal diffusion tensor imaging study on Wallerian degeneration of corticospinal tract after motor pathway stroke. *Neuroimage* **47**, 451-458 (2009).
50. Song, S. K. *et al.* Dysmyelination revealed through MRI as increased radial (but unchanged axial) diffusion of water. *Neuroimage* **17**, 1429-1436 (2002).
51. Song, S. K. *et al.* Demyelination increases radial diffusivity in corpus callosum of mouse brain. *Neuroimage* **26**, 132-140 (2005).
52. Harsan, L. A. *et al.* Brain dysmyelination and recovery assessment by noninvasive in vivo diffusion tensor magnetic resonance imaging. *J. Neurosci. Res.* **83**, 392-402 (2006).
53. Bates, E. *et al.* Voxel-based lesion-symptom mapping. *Nat. Neurosci.* **6**, 448-450 (2003).
54. Ashburner, J. & Friston, K. J. Voxel-based morphometry--the methods. *Neuroimage* **11**, 805-821 (2000).
55. Rogalsky, C. *et al.* Speech repetition as a window on the neurobiology of auditory-motor integration for speech: A voxel-based lesion symptom mapping study. *Neuropsychologia* **71**, 18-27 (2015).
56. Geva, S., Baron, J. C., Jones, P. S., Price, C. J. & Warburton, E. A. A comparison of VLSM and VBM in a cohort of patients with post-stroke aphasia. *Neuroimage Clin.* **1**, 37-47 (2012).
57. Fridriksson, J., Fillmore, P., Guo, D. & Rorden, C. Chronic Broca's aphasia is caused by damage to

- Broca's and Wernicke's areas. *Cereb. Cortex* **25**, 4689-4696 (2015).
58. Dronkers, N. F., Wilkins, D. P., Van Valin, R. D., Jr, Redfern, B. B. & Jaeger, J. J. Lesion analysis of the brain areas involved in language comprehension. *Cognition* **92**, 145-177 (2004).
59. Mirman, D. *et al.* Neural organization of spoken language revealed by lesion-symptom mapping. *Nat. Commun.* **6**, 6762 (2015).
60. Henseler, I., Regenbrecht, F. & Obrig, H. Lesion correlates of patho-linguistic profiles in chronic aphasia: comparisons of syndrome-, modality- and symptom-level assessment. *Brain* **137**, 918-930 (2014).
61. Xing, S. *et al.* Right hemisphere grey matter structure and language outcomes in chronic left hemisphere stroke. *Brain* **139**, 227-241 (2016).
62. Moon, H. I., Pyun, S. B., Tae, W. S. & Kwon, H. K. Neural substrates of lower extremity motor, balance, and gait function after supratentorial stroke using voxel-based lesion symptom mapping. *Neuroradiology* **58**, 723-731 (2016).
63. Moon, H. I., Lee, H. J. & Yoon, S. Y. Lesion location associated with balance recovery and gait velocity change after rehabilitation in stroke patients. *Neuroradiology* **59**, 609-618 (2017).
64. Lo, R., Gitelman, D., Levy, R., Hulvershorn, J. & Parrish, T. Identification of critical areas for motor function recovery in chronic stroke subjects using voxel-based lesion symptom mapping. *Neuroimage* **49**, 9-18 (2010).
65. Yin, D. *et al.* Secondary degeneration detected by combining voxel-based morphometry and tract-based spatial statistics in subcortical strokes with different outcomes in hand function. *AJNR Am. J. Neuro-radiol.* **34**, 1341-1347 (2013).
66. Stebbins, G. T. *et al.* Gray matter atrophy in patients with ischemic stroke with cognitive impairment. *Stroke* **39**, 785-793 (2008).
67. Chechlacz, M. *et al.* Common and distinct neural mechanisms of visual and tactile extinction: A large scale VBM study in sub-acute stroke. *Neuroimage Clin.* **2**, 291-302 (2013).
68. Perani, D. *et al.* Functional specializations for music processing in the human newborn brain. *Proc. Natl. Acad. Sci. U. S. A.* **107**, 4758-4763 (2010).
69. Virtala, P., Huotilainen, M., Partanen, E., Fellman, V. & Tervaniemi, M. Newborn infants' auditory system is sensitive to Western music chord categories. *Front. Psychol.* **4**, 492 (2013).

70. Zentner, M. & Eerola, T. Rhythmic engagement with music in infancy. *Proc. Natl. Acad. Sci. U. S. A.* **107**, 5768-5773 (2010).
71. Sacks, O. The power of music. *Brain* **129**, 2528-2532 (2006).
72. Zatorre, R. & McGill, J. Music, the food of neuroscience? *Nature* **434**, 312-315 (2005).
73. Hahn, J. & Münzel, S. Knochenflöten aus den Aurignacien des Geissenklösterle bei Blaubeuren, Alb-Donau-Kreis. *Fundberichte aus Baden-Württemberg, 20 (1995)* **20**, 1-12 (1995).
74. Mithen, S. in *The Singing Neanderthals: The Origins of Music, Language, Mind, and Body* 384 (Harvard University Press, 2007).
75. Samson, F., Zeffiro, T. A., Tous-saint, A. & Belin, P. Stimulus complexity and categorical effects in human auditory cortex: an activation likelihood estimation meta-analysis. *Front. Psychol.* **1**, 241 (2011).
76. Schmithorst, V. J. Separate cortical networks involved in music perception: preliminary functional MRI evidence for modularity of music processing. *Neuroimage* **25**, 444-451 (2005).
77. Griffiths, T. D., Büchel, C., Frackowiak, R. S. & Patterson, R. D. Analysis of temporal structure in sound by the human brain. *Nat. Neurosci.* **1**, 422-427 (1998).
78. Patterson, R. D., Uppenkamp, S., Johnsrude, I. S. & Griffiths, T. D. The processing of temporal pitch and melody information in auditory cortex. *Neuron* **36**, 767-776 (2002).
79. Gutschalk, A., Patterson, R. D., Rupp, A., Uppenkamp, S. & Scherg, M. Sustained magnetic fields reveal separate sites for sound level and temporal regularity in human auditory cortex. *Neuroimage* **15**, 207-216 (2002).
80. Tramo, M. J., Shah, G. D. & Braid, L. D. Functional role of auditory cortex in frequency processing and pitch perception. *J. Neurophysiol.* **87**, 122-139 (2002).
81. Hyde, K. L., Peretz, I. & Zatorre, R. J. Evidence for the role of the right auditory cortex in fine pitch resolution. *Neuropsychologia* **46**, 632-639 (2008).
82. Zatorre, R. J. & Belin, P. Spectral and temporal processing in human auditory cortex. *Cereb. Cortex* **11**, 946-953 (2001).
83. Jamison, H. L., Watkins, K. E., Bishop, D. V. & Matthews, P. M. Hemispheric specialization for processing auditory nonspeech stimuli. *Cereb. Cortex* **16**, 1266-1275 (2006).
84. Bendor, D. & Wang, X. Neural response properties of primary, rostral, and rostrotemporal core fields in the auditory cortex of marmoset

- monkeys. *J. Neurophysiol.* **100**, 888-906 (2008).
85. Warren, J. D., Jennings, A. R. & Griffiths, T. D. Analysis of the spectral envelope of sounds by the human brain. *Neuroimage* **24**, 1052-1057 (2005).
86. Foster, N. E., Halpern, A. R. & Zatorre, R. J. Common parietal activation in musical mental transformations across pitch and time. *Neuroimage* **75**, 27-35 (2013).
87. Royal, I. *et al.* Activation in the Right Inferior Parietal Lobule Reflects the Representation of Musical Structure beyond Simple Pitch Discrimination. *PLoS One* **11**, e0155291 (2016).
88. Jerde, T. A., Childs, S. K., Handy, S. T., Nagode, J. C. & Pardo, J. V. Dissociable systems of working memory for rhythm and melody. *Neuroimage* **57**, 1572-1579 (2011).
89. Schulze, K., Zysset, S., Mueller, K., Friederici, A. D. & Koelsch, S. Neuroarchitecture of verbal and tonal working memory in nonmusicians and musicians. *Hum. Brain Mapp.* **32**, 771-783 (2011).
90. Albouy, P., Weiss, A., Baillet, S. & Zatorre, R. J. Selective Entrainment of Theta Oscillations in the Dorsal Stream Causally Enhances Auditory Working Memory Performance. *Neuron* **94**, 193-206.e5 (2017).
91. Janata, P. *et al.* The cortical topography of tonal structures underlying Western music. *Science* **298**, 2167-2170 (2002).
92. Chen, J. L., Penhune, V. B. & Zatorre, R. J. Listening to musical rhythms recruits motor regions of the brain. *Cereb. Cortex* **18**, 2844-2854 (2008).
93. Grahn, J. A. & Brett, M. Rhythm and beat perception in motor areas of the brain. *J. Cogn. Neurosci.* **19**, 893-906 (2007).
94. Sakai, K. *et al.* Neural representation of a rhythm depends on its interval ratio. *J. Neurosci.* **19**, 10074-10081 (1999).
95. Xu, D., Liu, T., Ashe, J. & Bushara, K. O. Role of the olivo-cerebellar system in timing. *J. Neurosci.* **26**, 5990-5995 (2006).
96. Koelsch, S. Neural substrates of processing syntax and semantics in music. *Curr. Opin. Neurobiol.* **15**, 207-212 (2005).
97. Tillmann, B. *et al.* Cognitive priming in sung and instrumental music: activation of inferior frontal cortex. *Neuroimage* **31**, 1771-1782 (2006).
98. Bianco, R. *et al.* Neural networks for harmonic structure in music perception and action. *Neuroimage* **142**, 454-464 (2016).

99. Peretz, I. *et al.* Music lexical networks: the cortical organization of music recognition. *Ann. N. Y. Acad. Sci.* **1169**, 256-265 (2009).
100. Halpern, A. R. & Zatorre, R. J. When that tune runs through your head: a PET investigation of auditory imagery for familiar melodies. *Cereb. Cortex* **9**, 697-704 (1999).
101. Platel, H., Baron, J. C., Desgranges, B., Bernard, F. & Eustache, F. Semantic and episodic memory of music are subserved by distinct neural networks. *Neuroimage* **20**, 244-256 (2003).
102. Salimpoor, V. N., Benovoy, M., Larcher, K., Dagher, A. & Zatorre, R. J. Anatomically distinct dopamine release during anticipation and experience of peak emotion to music. *Nat. Neurosci.* **14**, 257-262 (2011).
103. Blood, A. J. & Zatorre, R. J. Intensely pleasurable responses to music correlate with activity in brain regions implicated in reward and emotion. *Proc. Natl. Acad. Sci. U. S. A.* **98**, 11818-11823 (2001).
104. Brown, S., Martinez, M. J. & Parsons, L. M. Passive music listening spontaneously engages limbic and paralimbic systems. *Neuroreport* **15**, 2033-2037 (2004).
105. Koelsch, S., Fritz, T., V Cramon, D. Y., Muller, K. & Friederici, A. D. Investigating emotion with music: an fMRI study. *Hum. Brain Mapp.* **27**, 239-250 (2006).
106. Blood, A. J., Zatorre, R. J., Bermudez, P. & Evans, A. C. Emotional responses to pleasant and unpleasant music correlate with activity in paralimbic brain regions. *Nat. Neurosci.* **2**, 382-387 (1999).
107. Baumgartner, T., Esslen, M. & Jancke, L. From emotion perception to emotion experience: emotions evoked by pictures and classical music. *Int. J. Psychophysiol.* **60**, 34-43 (2006).
108. LaCroix, A. N., Diaz, A. F. & Rogalsky, C. The relationship between the neural computations for speech and music perception is context-dependent: an activation likelihood estimate study. *Front. Psychol.* **6**, 1138 (2015).
109. Özdemir, E., Norton, A. & Schlaug, G. Shared and distinct neural correlates of singing and speaking. *Neuroimage* **33**, 628-635 (2006).
110. Callan, D. E. *et al.* Song and speech: brain regions involved with perception and covert production. *Neuroimage* **31**, 1327-1342 (2006).
111. Saito, Y. *et al.* Neural substrates for semantic memory of familiar songs: is there an interface between lyrics and melodies? *PLoS One* **7**, e46354 (2012).

112. Sammler, D. *et al.* The relationship of lyrics and tunes in the processing of unfamiliar songs: a functional magnetic resonance adaptation study. *J. Neurosci.* **30**, 3572-3578 (2010).
113. Bonnel, A. M., Fäita, F., Peretz, I. & Besson, M. Divided attention between lyrics and tunes of operatic songs: evidence for independent processing. *Percept. Psychophys.* **63**, 1201-1213 (2001).
114. Besson, M., Fäita, F., Peretz, I., Bonnel, A. - & Requin, J. Singing in the Brain: Independence of Lyrics and Tunes. *Psychol. Sci.* **9**, 494-498 (1998).
115. Poulin-Charronnat, B., Bigand, E., Madurell, F. & Peereman, R. Musical structure modulates semantic priming in vocal music. *Cognition* **94**, B67-78 (2005).
116. Särkämö, T., Tervaniemi, M. & Huotilainen, M. Music perception and cognition: development, neural basis, and rehabilitative use of music. *Wiley Interdisciplinary Reviews: Cognitive Science* **4**, 441-451 (2013).
117. Catani, M., Howard, R. J., Pajevic, S. & Jones, D. K. Virtual in vivo interactive dissection of white matter fasciculi in the human brain. *Neuroimage* **17**, 77-94 (2002).
118. Kier, E. L., Staib, L. H., Davis, L. M. & Bronen, R. A. MR imaging of the temporal stem: anatomic dissection tractography of the uncinat fasciculus, inferior occipitofrontal fasciculus, and Meyer's loop of the optic radiation. *AJNR Am. J. Neuro-radiol.* **25**, 677-691 (2004).
119. Martino, J., Brogna, C., Robles, S. G., Vergani, F. & Duffau, H. Anatomic dissection of the inferior fronto-occipital fasciculus revisited in the lights of brain stimulation data. *Cortex* **46**, 691-699 (2010).
120. Turken, A. U. & Dronkers, N. F. The neural architecture of the language comprehension network: converging evidence from lesion and connectivity analyses. *Front. Syst. Neurosci.* **5**, 1 (2011).
121. Sarubbo, S., De Benedictis, A., Maldonado, I. L., Basso, G. & Duffau, H. Frontal terminations for the inferior fronto-occipital fascicle: anatomical dissection, DTI study and functional considerations on a multi-component bundle. *Brain Struct. Funct.* **218**, 21-37 (2013).
122. Dohn, A. *et al.* Gray- and white-matter anatomy of absolute pitch possessors. *Cereb. Cortex* **25**, 1379-1388 (2015).
123. Zamm, A., Schlaug, G., Eagleman, D. M. & Loui, P. Pathways to seeing music: enhanced structural connectivity in colored-music synesthesia. *Neuroimage* **74**, 359-366 (2013).

124. Schmithorst, V. J. & Wilke, M. Differences in white matter architecture between musicians and non-musicians: a diffusion tensor imaging study. *Neurosci. Lett.* **321**, 57-60 (2002).
125. Bengtsson, S. L. *et al.* Extensive piano practicing has regionally specific effects on white matter development. *Nat. Neurosci.* **8**, 1148-1150 (2005).
126. Oechslin, M. S., Imfeld, A., Loenneker, T., Meyer, M. & Jancke, L. The plasticity of the superior longitudinal fasciculus as a function of musical expertise: a diffusion tensor imaging study. *Front. Hum. Neurosci.* **3**, 76 (2010).
127. Halwani, G. F., Loui, P., Ruber, T. & Schlaug, G. Effects of practice and experience on the arcuate fasciculus: comparing singers, instrumentalists, and non-musicians. *Front. Psychol.* **2**, 156 (2011).
128. Schlaug, G., Jancke, L., Huang, Y., Staiger, J. F. & Steinmetz, H. Increased corpus callosum size in musicians. *Neuropsychologia* **33**, 1047-1055 (1995).
129. Han, Y. *et al.* Gray matter density and white matter integrity in pianists' brain: a combined structural and diffusion tensor MRI study. *Neurosci. Lett.* **459**, 3-6 (2009).
130. Ruber, T., Lindenberg, R. & Schlaug, G. Differential adaptation of descending motor tracts in musicians. *Cereb. Cortex* **25**, 1490-1498 (2015).
131. Abdul-Kareem, I. A. *et al.* Plasticity of the superior and middle cerebellar peduncles in musicians revealed by quantitative analysis of volume and number of streamlines based on diffusion tensor tractography. *Cerebellum* **10**, 611-623 (2011).
132. Gaser, C. & Schlaug, G. Brain structures differ between musicians and non-musicians. *J. Neurosci.* **23**, 9240-9245 (2003).
133. Elbert, T., Pantev, C., Wienbruch, C., Rockstroh, B. & Taub, E. Increased cortical representation of the fingers of the left hand in string players. *Science* **270**, 305-307 (1995).
134. Vaquero, L. *et al.* Structural neuroplasticity in expert pianists depends on the age of musical training onset. *Neuroimage* **1**, 106-119 (2016).
135. Fauvel, B. *et al.* Morphological brain plasticity induced by musical expertise is accompanied by modulation of functional connectivity at rest. *Neuroimage* **90**, 179-188 (2014).
136. Sluming, V. *et al.* Voxel-based morphometry reveals increased gray matter density in Broca's area in male symphony orchestra musicians. *Neuroimage* **17**, 1613-1622 (2002).

137. Bailey, J. A., Zatorre, R. J. & Penhune, V. B. Early musical training is linked to gray matter structure in the ventral premotor cortex and auditory-motor rhythm synchronization performance. *J. Cogn. Neurosci.* **26**, 755-767 (2014).
138. Tillmann, B., Albouy, P. & Caclin, A. Congenital amusias. *Handb. Clin. Neurol.* **129**, 589-605 (2015).
139. Peretz, I. Neurobiology of Congenital Amusia. *Trends Cogn. Sci.* **20**, 857-867 (2016).
140. Whiteford, K. L. & Oxenham, A. J. Auditory deficits in amusia extend beyond poor pitch perception. *Neuropsychologia* **99**, 213-224 (2017).
141. Kalmus, H. & Fry, D. B. On tune deafness (dysmelodia): frequency, development, genetics and musical background. *Ann. Hum. Genet.* **43**, 369-382 (1980).
142. Henry, M. & McAuley, J. On the Prevalence of Congenital Amusia. *Music Perception* **27**, 413-418 (2010).
143. Peretz, I. & Vuvar, D. T. Prevalence of congenital amusia. *Eur. J. Hum. Genet.* **25**, 625-630 (2017).
144. Hyde, K. L., Zatorre, R. J., Griffiths, T. D., Lerch, J. P. & Peretz, I. Morphometry of the amusic brain: a two-site study. *Brain* **129**, 2562-2570 (2006).
145. Albouy, P. *et al.* Impaired pitch perception and memory in congenital amusia: the deficit starts in the auditory cortex. *Brain* **136**, 1639-1661 (2013).
146. Hyde, K. L. *et al.* Cortical Thickness in Congenital Amusia: When Less Is Better Than More. *J Neurosci* **27**, 13028-13032 (2007).
147. Mandell, J., Schulze, K. & Schlaug, G. Congenital amusia: an auditory-motor feedback disorder? *Restor. Neurol. Neurosci.* **25**, 323-334 (2007).
148. Omigie, D., Müllensiefen, D. & Stewart, L. The Experience of Music in Congenital Amusia. *Music Percept.* **30**, 1-18 (2012).
149. Good, C. D. *et al.* A voxel-based morphometric study of ageing in 465 normal adult human brains. *Neuroimage* **14**, 21-36 (2001).
150. Keller, S. S., Wilke, M., Wieshmann, U. C., Sluming, V. A. & Roberts, N. Comparison of standard and optimized voxel-based morphometry for analysis of brain changes associated with temporal lobe epilepsy. *Neuroimage* **23**, 860-868 (2004).
151. Loui, P., Alsop, D. & Schlaug, G. Tone deafness: a new disconnection syndrome? *J. Neurosci.* **29**, 10215-10220 (2009).
152. Chen, J. L. *et al.* Detection of the arcuate fasciculus in congenital

- amusia depends on the tractography algorithm. *Front. Psychol.* **6**, 9 (2015).
153. Zhao, Y. *et al.* Abnormal topological organization of the white matter network in Mandarin speakers with congenital amusia. *Sci. Rep.* **6**, 26505 (2016).
154. Hyde, K. L., Zatorre, R. J. & Peretz, I. Functional MRI evidence of an abnormal neural network for pitch processing in congenital amusia. *Cereb. Cortex* **21**, 292-299 (2011).
155. Norman-Haignere, S. V. *et al.* Pitch-Responsive Cortical Regions in Congenital Amusia. *J. Neurosci.* **36**, 2986-2994 (2016).
156. Leveque, Y. *et al.* Altered intrinsic connectivity of the auditory cortex in congenital amusia. *J. Neurophysiol.* **116**, 88-97 (2016).
157. Zendel, B. R., Lagrois, M. E., Robitaille, N. & Peretz, I. Attending to pitch information inhibits processing of pitch information: the curious case of amusia. *J. Neurosci.* **35**, 3815-3824 (2015).
158. Peretz, I., Brattico, E. & Tervaniemi, M. Abnormal electrical brain responses to pitch in congenital amusia. *Ann. Neurol.* **58**, 478-482 (2005).
159. Peretz, I., Brattico, E., Järvenpää, M. & Tervaniemi, M. The amusic brain: in tune, out of key, and unaware. *Brain* **132**, 1277-1286 (2009).
160. Omigie, D., Pearce, M. T., Williamson, V. J. & Stewart, L. Electrophysiological correlates of melodic processing in congenital amusia. *Neuropsychologia* **51**, 1749-1762 (2013).
161. Zhou, L., Liu, F., Jing, X. & Jiang, C. Neural differences between the processing of musical meaning conveyed by direction of pitch change and natural music in congenital amusia. *Neuropsychologia* **96**, 29-38 (2017).
162. Anderson, S., Himonides, E., Wise, K., Welch, G. & Stewart, L. Is there potential for learning in amusia? A study of the effect of singing intervention in congenital amusia. *Ann. N. Y. Acad. Sci.* **1252**, 345-353 (2012).
163. Wilbiks, J. M., Vuvan, D. T., Girard, P. Y., Peretz, I. & Russo, F. A. Effects of vocal training in a musicophile with congenital amusia. *Neurocase* **22**, 526-537 (2016).
164. Loui, P., Guenther, F. H., Mathys, C. & Schlaug, G. Action-perception mismatch in tone-deafness. *Curr. Biol.* **18**, R331-2 (2008).
165. Ayotte, J., Peretz, I. & Hyde, K. Congenital amusia: A group study of adults afflicted with a music-specific disorder. *Brain* **125**, 238-251 (2002).

166. Price, C. J. & Friston, K. J. Degeneracy and cognitive anatomy. *Trends Cogn. Sci.* **6**, 416-421 (2002).
167. McFarland, H. R. & Fortin, D. Amusia due to right temporoparietal infarct. *Arch. Neurol.* **39**, 725-727 (1982).
168. Griffiths, T. D. *et al.* Spatial and temporal auditory processing deficits following right hemisphere infarction. A psychophysical study. *Brain* **120 (Pt 5)**, 785-794 (1997).
169. Münte, T. F. *et al.* Brain potentials in patients with music perception deficits: evidence for an early locus. *Neurosci. Lett.* **256**, 85-88 (1998).
170. Kohlmetz, C., Altenmüller, E., Schuppert, M., Wieringa, B. M. & Münte, T. F. Deficit in automatic sound-change detection may underlie some music perception deficits after acute hemispheric stroke. *Neuropsychologia* **39**, 1121-1124 (2001).
171. Murayama, J., Kashiwagi, T., Kashiwagi, A. & Mimura, M. Impaired pitch production and preserved rhythm production in a right brain-damaged patient with amusia. *Brain Cogn.* **56**, 36-42 (2004).
172. Satoh, M., Takeda, K., Nagata, K., Hatazawa, J. & Kuzuhara, S. The anterior portion of the bilateral temporal lobes participates in music perception: a positron emission tomography study. *AJNR Am. J. Neuroradiol.* **24**, 1843-1848 (2003).
173. Terao, Y. *et al.* Vocal amusia in a professional tango singer due to a right superior temporal cortex infarction. *Neuropsychologia* **44**, 479-488 (2006).
174. Johannes, S., Jobges, M. E., Dengler, R. & Münte, T. F. Cortical auditory disorders: a case of non-verbal disturbances assessed with event-related brain potentials. *Behav. Neurol.* **11**, 55-73 (1998).
175. Särkämö, T. *et al.* Cognitive deficits associated with acquired amusia after stroke: a neuropsychological follow-up study. *Neuropsychologia* **47**, 2642-2651 (2009).
176. Hochman, M. S. & Abrams, K. J. Amusia for pitch caused by right middle cerebral artery infarct. *J. Stroke Cerebrovasc Dis.* **23**, 164-165 (2014).
177. Mazzoni, M. *et al.* A case of music imperception. *J. Neurol. Neurosurg. Psychiatry.* **56**, 322 (1993).
178. Kohlmetz, C., Müller, S. V., Nager, W., Münte, T. F. & Altenmüller, E. Selective loss of timbre perception for keyboard and percussion instruments following a right temporal lesion. *Neurocase* **9**, 86-93 (2003).
179. Hofman, S., Klein, C. & Arlazoroff, A. Common hemisphericity

- of language and music in a musician. A case report. *J. Commun. Disord.* **26**, 73-82 (1993).
180. Mavlov, L. Amusia due to rhythm agnosia in a musician with left hemisphere damage: a non-auditory supramodal defect. *Cortex* **16**, 331-338 (1980).
181. Di Pietro, M., Laganaro, M., Leemann, B. & Schnider, A. Receptive amusia: temporal auditory processing deficit in a professional musician following a left temporo-parietal lesion. *Neuropsychologia* **42**, 868-877 (2004).
182. Wilson, S. J., Pressing, J. L. & Wales, R. J. Modelling rhythmic function in a musician post-stroke. *Neuropsychologia* **40**, 1494-1505 (2002).
183. Yoo, H. J., Moon, H. I. & Pyun, S. B. Amusia After Right Temporo-parietal Lobe Infarction: A Case Report. *Ann. Rehabil. Med.* **40**, 933-937 (2016).
184. Särkämö, T. *et al.* Auditory and cognitive deficits associated with acquired amusia after stroke: a magnetoencephalography and neuropsychological follow-up study. *PLoS One* **5**, e15157 (2010).
185. Hirel, C. *et al.* Verbal and musical short-term memory: Variety of auditory disorders after stroke. *Brain Cogn.* **113**, 10-22 (2017).
186. Zatorre, R. J., Belin, P. & Penhune, V. B. Structure and function of auditory cortex: music and speech. *Trends Cogn. Sci.* **6**, 37-46 (2002).
187. Rauschecker, J. P. Is there a tape recorder in your head? How the brain stores and retrieves musical melodies. *Front. Syst. Neurosci.* **8**, 149 (2014).
188. Sammler, D., Grosbras, M. H., Anwander, A., Bestelmeyer, P. E. & Belin, P. Dorsal and Ventral Pathways for Prosody. *Curr. Biol.* **25**, 3079-3085 (2015).
189. Loui, P. A Dual-Stream Neuroanatomy of Singing. *Music. Percept.* **32**, 232-241 (2015).
190. Musso, M. *et al.* A single dual-stream framework for syntactic computations in music and language. *Neuroimage* **117**, 267-283 (2015).
191. Kummerer, D. *et al.* Damage to ventral and dorsal language pathways in acute aphasia. *Brain* **136**, 619-629 (2013).
192. Särkämö, T. *et al.* Music listening enhances cognitive recovery and mood after middle cerebral artery stroke. *Brain* **131**, 866-876 (2008).
193. Peretz, I., Champod, A. S. & Hyde, K. Varieties of musical disorders. The Montreal Battery of Evaluation of Amusia. *Ann. N. Y. Acad. Sci.* **999**, 58-75 (2003).

194. Peretz, I. & Coltheart, M. Modularity of music processing. *Nat. Neurosci.* **6**, 688-691 (2003).
195. Goodglass, H. & Kaplan, E. in *Boston Diagnostic Aphasia Examination (BDAE)* (Lea & Febiger, Philadelphia, PA, USA, 1983).
196. Lezak, M., Howieson, D., Bigler, E. & Tranel, D. in *Neuropsychological Assessment* (Oxford University Press, New York, NY, USA, 2012).
197. De Renzi, E. & Faglioni, P. Normative data and screening power of a shortened version of the Token Test. *Cortex* **14**, 41-49 (1978).
198. Laine, M. *et al.* Adaptation of the Boston Diagnostic Aphasia Examination and the Boston Naming Test into Finnish. *Scand. J. Log. Phon.* **18**, 83-92 (1993).
199. Brett, M., Leff, A. P., Rorden, C. & Ashburner, J. Spatial normalization of brain images with focal lesions using cost function masking. *Neuroimage* **14**, 486-500 (2001).
200. Ripollés, P. *et al.* Analysis of automated methods for spatial normalization of lesioned brains. *Neuroimage* **60**, 1296-1306 (2012).
201. Rorden, C. & Brett, M. Stereotaxic display of brain lesions. *Behav. Neurol.* **12**, 191-200 (2000).
202. Ashburner, J. & Friston, K. J. Unified segmentation. *Neuroimage* **26**, 839-851 (2005).
203. Crinion, J. *et al.* Spatial normalization of lesioned brains: performance evaluation and impact on fMRI analyses. *Neuroimage* **37**, 866-875 (2007).
204. Andersen, S. M., Rapcsak, S. Z. & Beeson, P. M. Cost function masking during normalization of brains with focal lesions: still a necessity? *Neuroimage* **53**, 78-84 (2010).
205. Smith, S. M. *et al.* Tract-based spatial statistics: voxelwise analysis of multi-subject diffusion data. *Neuroimage* **31**, 1487-1505 (2006).
206. Smith, S. M. *et al.* Advances in functional and structural MR image analysis and implementation as FSL. *Neuroimage* **23 Suppl 1**, S208-19 (2004).
207. Leemans, A. & Jones, D. K. The B-matrix must be rotated when correcting for subject motion in DTI data. *Magn. Reson. Med.* **61**, 1336-1349 (2009).
208. Smith, S. M. Fast robust automated brain extraction. *Hum. Brain Mapp.* **17**, 143-155 (2002).
209. Rueckert, D. *et al.* Nonrigid registration using free-form deformations: application to breast MR images. *IEEE Trans. Med. Imaging* **18**, 712-721 (1999).

210. Conturo, T. E. *et al.* Tracking neuronal fiber pathways in the living human brain. *Proc. Natl. Acad. Sci. U. S. A.* **96**, 10422-10427 (1999).
211. Basser, P. J., Pajevic, S., Pierpaoli, C., Duda, J. & Aldroubi, A. In vivo fiber tractography using DT-MRI data. *Magn. Reson. Med.* **44**, 625-632 (2000).
212. Catani, M., Jones, D. K. & ffytche, D. H. Perisylvian language networks of the human brain. *Ann. Neurol.* **57**, 8-16 (2005).
213. Glasser, M. F. & Rilling, J. K. DTI tractography of the human brain's language pathways. *Cereb. Cortex* **18**, 2471-2482 (2008).
214. Vaquero, L., Rodriguez-Fornells, A. & Reiterer, S. M. The Left, The Better: White-Matter Brain Integrity Predicts Foreign Language Imitation Ability. *Cereb. Cortex* (2016).
215. Francois, C. *et al.* Language learning and brain reorganization in a 3.5-year-old child with left perinatal stroke revealed using structural and functional connectivity. *Cortex* **77**, 95-118 (2016).
216. Sierpowska, J. *et al.* Words are not enough: nonword repetition as an indicator of arcuate fasciculus integrity during brain tumor resection. *J. Neurosurg.* **126**, 435-445 (2017).
217. Burks, J. D. *et al.* Anatomy and white matter connections of the orbitofrontal gyrus. *J. Neurosurg.*, 1-8 (2017).
218. Catani, M. & Thiebaut de Schotten, M. A diffusion tensor imaging tractography atlas for virtual in vivo dissections. *Cortex* **44**, 1105-1132 (2008).
219. Lopez-Barroso, D. *et al.* Word learning is mediated by the left arcuate fasciculus. *Proc. Natl. Acad. Sci. U. S. A.* **110**, 13168-13173 (2013).
220. Huang, H. *et al.* DTI tractography based parcellation of white matter: application to the mid-sagittal morphology of corpus callosum. *Neuroimage* **26**, 195-205 (2005).
221. Sierpowska, J. *et al.* Morphological derivation overflow as a result of disruption of the left frontal aslant white matter tract. *Brain Lang.* **142**, 54-64 (2015).
222. Catani, M. *et al.* A novel frontal pathway underlies verbal fluency in primary progressive aphasia. *Brain* **136**, 2619-2628 (2013).
223. Calhoun, V. D., Kiehl, K. A. & Pearlson, G. D. Modulation of temporally coherent brain networks estimated using ICA at rest and during cognitive tasks. *Hum. Brain Mapp.* **29**, 828-838 (2008).
224. Calhoun, V. D., Liu, J. & Adali, T. A review of group ICA for fMRI data and ICA for joint inference of

- imaging, genetic, and ERP data. *Neuroimage* **45**, S163-72 (2009).
225. Smith, S. M. The future of fMRI connectivity. *Neuroimage* **62**, 1257-1266 (2012).
226. Smith, S. M. *et al.* Correspondence of the brain's functional architecture during activation and rest. *Proc. Natl. Acad. Sci. U. S. A.* **106**, 13040-13045 (2009).
227. Forn, C. *et al.* Task-load manipulation in the Symbol Digit Modalities Test: an alternative measure of information processing speed. *Brain Cogn.* **82**, 152-160 (2013).
228. Lopez-Barroso, D. *et al.* Multiple brain networks underpinning word learning from fluent speech revealed by independent component analysis. *Neuroimage* **110**, 182-193 (2015).
229. Bell, A. J. & Sejnowski, T. J. An information-maximization approach to blind separation and blind deconvolution. *Neural Comput.* **7**, 1129-1159 (1995).
230. Chao, L. L. & Knight, R. T. Contribution of Human Prefrontal Cortex to Delay Performance. *J. Cogn. Neurosci.* **10**, 167-177 (1998).
231. Dronkers, N. F. A new brain region for coordinating speech articulation. *Nature* **384**, 159-161 (1996).
232. Dovern, A. *et al.* Apraxia impairs intentional retrieval of incidentally acquired motor knowledge. *J. Neurosci.* **31**, 8102-8108 (2011).
233. Timpert, D. C., Weiss, P. H., Vossel, S., Dovern, A. & Fink, G. R. Apraxia and spatial inattention dissociate in left hemisphere stroke. *Cortex* **71**, 349-358 (2015).
234. Tzourio-Mazoyer, N. *et al.* Automated anatomical labeling of activations in SPM using a macroscopic anatomical parcellation of the MNI MRI single-subject brain. *Neuroimage* **15**, 273-289 (2002).
235. Smith, S. M. & Nichols, T. E. Threshold-free cluster enhancement: addressing problems of smoothing, threshold dependence and localisation in cluster inference. *Neuroimage* **44**, 83-98 (2009).
236. Nichols, T. E. & Holmes, A. P. Nonparametric permutation tests for functional neuroimaging: a primer with examples. *Hum. Brain Mapp.* **15**, 1-25 (2002).
237. Colby, J. B. *et al.* Along-tract statistics allow for enhanced tractography analysis. *Neuroimage* **59**, 3227-3242 (2012).
238. Chechlacz, M., Rotshtein, P. & Humphreys, G. W. Neuroanatomical Dissections of Unilateral Visual Neglect Symptoms: ALE Meta-Analysis of Lesion-Symptom Mapping. *Front Hum Neurosci* **6** (2012).

239. Sihvonen, A. J. *et al.* Neural Basis of Acquired Amusia and Its Recovery after Stroke. *Journal of Neuroscience* **36**, 8872-8881 (2016).
240. Sihvonen, A. J. *et al.* Tracting the neural basis of music: Deficient structural connectivity underlying acquired amusia. *Cortex* (2017).
241. Sihvonen, A. J. *et al.* Functional neural changes associated with acquired amusia across different stages of recovery after stroke. *Sci. Rep.* **7**, 11390-017-11841-6 (2017).
242. Sidtis, J. J. & Volpe, B. T. Selective loss of complex-pitch or speech discrimination after unilateral lesion. *Brain Lang.* **34**, 235-245 (1988).
243. Piccirilli, M., Sciarma, T. & Luzzi, S. Modularity of music: evidence from a case of pure amusia. *J. Neurol. Neurosurg. Psychiatry.* **69**, 541-545 (2000).
244. Mendez, M. F. Generalized auditory agnosia with spared music recognition in a left-hander. Analysis of a case with a right temporal stroke. *Cortex* **37**, 139-150 (2001).
245. Maess, B., Koelsch, S., Gunter, T. C. & Friederici, A. D. Musical syntax is processed in Broca's area: an MEG study. *Nat. Neurosci.* **4**, 540-545 (2001).
246. Abrams, D. A. *et al.* Decoding temporal structure in music and speech relies on shared brain resources but elicits different fine-scale spatial patterns. *Cereb. Cortex* **21**, 1507-1518 (2011).
247. Rogalsky, C., Rong, F., Saberi, K. & Hickok, G. Functional anatomy of language and music perception: temporal and structural factors investigated using functional magnetic resonance imaging. *J. Neurosci.* **31**, 3843-3852 (2011).
248. Garcea, F. E. *et al.* Direct Electrical Stimulation in the Human Brain Disrupts Melody Processing. *Curr. Biol.* **27**, 2684-2691.e7 (2017).
249. Seither-Preisler, A., Parncutt, R. & Schneider, P. Size and synchronization of auditory cortex promotes musical, literacy, and attentional skills in children. *J. Neurosci.* **34**, 10937-10949 (2014).
250. Wengenroth, M. *et al.* Increased volume and function of right auditory cortex as a marker for absolute pitch. *Cereb. Cortex* **24**, 1127-1137 (2014).
251. Hau, J. *et al.* Cortical Terminations of the Inferior Fronto-Occipital and Uncinate Fasciculi: Anatomical Stem-Based Virtual Dissection. *Front. Neuroanat.* **10** (2016).
252. Husain, F. T. *et al.* Neuroanatomical changes due to hearing loss and chronic tinnitus: a combined VBM and DTI study. *Brain Res.* **1369**, 74-88 (2011).
253. Loui, P., Li, H. C., Hohmann, A. & Schlaug, G. Enhanced cortical

- connectivity in absolute pitch musicians: a model for local hyperconnectivity. *J. Cogn. Neurosci.* **23**, 1015-1026 (2011).
254. Albouy, P., Mattout, J., Sanchez, G., Tillmann, B. & Caclin, A. Altered retrieval of melodic information in congenital amusia: insights from dynamic causal modeling of MEG data. *Front. Hum. Neurosci.* **9**, 20 (2015).
255. Andoh, J., Matsushita, R. & Zatorre, R. J. Asymmetric Interhemispheric Transfer in the Auditory Network: Evidence from TMS, Resting-State fMRI, and Diffusion Imaging. *J. Neurosci.* **35**, 14602-14611 (2015).
256. Westerhausen, R., Gruner, R., Specht, K. & Hugdahl, K. Functional relevance of interindividual differences in temporal lobe callosal pathways: a DTI tractography study. *Cereb. Cortex* **19**, 1322-1329 (2009).
257. Burunat, I. *et al.* Action in Perception: Prominent Visuo-Motor Functional Symmetry in Musicians during Music Listening. *PLoS One* **10**, e0138238 (2015).
258. Tillmann, B., Janata, P. & Bharucha, J. J. Activation of the Inferior Frontal Cortex in Musical Priming. *Ann. N. Y. Acad. Sci.* **999**, 209-211 (2003).
259. Altenmüller, E., Siggel, S., Mohammadi, B., Samii, A. & Münte, T. F. Play it again, Sam: brain correlates of emotional music recognition. *Front. Psychol.* **5**, 114 (2014).
260. Tabei, K. Inferior Frontal Gyrus Activation Underlies the Perception of Emotions, While Precuneus Activation Underlies the Feeling of Emotions during Music Listening. *Behav. Neurol.* **2015**, 529043 (2015).
261. Sammler, D., Koelsch, S. & Friederici, A. D. Are left fronto-temporal brain areas a prerequisite for normal music-syntactic processing? *Cortex* **47**, 659-673 (2011).
262. Grahn, J. A. & Rowe, J. B. Feeling the beat: premotor and striatal interactions in musicians and non-musicians during beat perception. *J. Neurosci.* **29**, 7540-7548 (2009).
263. Schaal, N. K., Javadi, A. H., Halpern, A. R., Pollok, B. & Banissy, M. J. Right parietal cortex mediates recognition memory for melodies. *Eur. J. Neurosci.* **42**, 1660-1666 (2015).
264. Lappe, C., Steinstrater, O. & Pantev, C. Rhythmic and melodic deviations in musical sequences recruit different cortical areas for mismatch detection. *Front. Hum. Neurosci.* **7**, 260 (2013).
265. Limb, C. J., Kemeny, S., Ortigoza, E. B., Rouhani, S. & Braun, A. R. Left hemispheric lateralization of brain activity during passive rhythm perception in musicians.

- Anat. Rec. A. Discov. Mol. Cell. Evol. Biol.* **288**, 382-389 (2006).
266. Janata, P., Tillmann, B. & Bharucha, J. J. Listening to polyphonic music recruits domain-general attention and working memory circuits. *Cogn. Affect. Behav. Neurosci.* **2**, 121-140 (2002).
267. Penhune, V. B., Zattore, R. J. & Evans, A. C. Cerebellar contributions to motor timing: a PET study of auditory and visual rhythm reproduction. *J. Cogn. Neurosci.* **10**, 752-765 (1998).
268. Grahn, J. A. & Brett, M. Impairment of beat-based rhythm discrimination in Parkinson's disease. *Cortex* **45**, 54-61 (2009).
269. Peretz, I. Processing of local and global musical information by unilateral brain-damaged patients. *Brain* **113 (Pt 4)**, 1185-1205 (1990).
270. Ross, E. D. Cerebral localization of functions and the neurology of language: fact versus fiction or is it something else? *Neuroscientist* **16**, 222-243 (2010).
271. Catani, M. & Mesulam, M. The arcuate fasciculus and the disconnection theme in language and aphasia: history and current state. *Cortex* **44**, 953-961 (2008).
272. Thiebaut de Schotten, M. *et al.* Visualization of disconnection syndromes in humans. *Cortex* **44**, 1097-1103 (2008).
273. Perani, D. *et al.* Neural language networks at birth. *Proc. Natl. Acad. Sci. U. S. A.* **108**, 16056-16061 (2011).
274. Thiebaut de Schotten, M., Dell'Acqua, F., Valabregue, R. & Catani, M. Monkey to human comparative anatomy of the frontal lobe association tracts. *Cortex* **48**, 82-96 (2012).
275. Rauschecker, J. P. & Tian, B. Mechanisms and streams for processing of "what" and "where" in auditory cortex. *Proc. Natl. Acad. Sci. U. S. A.* **97**, 11800-11806 (2000).
276. Hickok, G. & Poeppel, D. The cortical organization of speech processing. *Nat. Rev. Neurosci.* **8**, 393-402 (2007).
277. Rauschecker, J. P. & Scott, S. K. Maps and streams in the auditory cortex: nonhuman primates illuminate human speech processing. *Nat. Neurosci.* **12**, 718-724 (2009).
278. Lopez-Barroso, D. *et al.* Language learning under working memory constraints correlates with microstructural differences in the ventral language pathway. *Cereb. Cortex* **21**, 2742-2750 (2011).
279. Mitchell, R. L. & Ross, E. D. fMRI evidence for the effect of verbal complexity on lateralisation of the neural response associated with decoding prosodic emotion. *Neuropsychologia* **46**, 2880-2887 (2008).

-
280. Cox, A. M., McKeivitt, C., Rudd, A. G. & Wolfe, C. D. Socioeconomic status and stroke. *Lancet Neurol.* **5**, 181-188 (2006).
281. Pan, S. L., Wu, S. C., Wu, T. H., Lee, T. K. & Chen, T. H. Location and size of infarct on functional outcome of noncardioembolic ischemic stroke. *Disabil. Rehabil.* **28**, 977-983 (2006).
282. Thompson, W. F., Marin, M. M. & Stewart, L. Reduced sensitivity to emotional prosody in congenital amusia rekindles the musical proto-language hypothesis. *Proc. Natl. Acad. Sci. U. S. A.* **109**, 19027-19032 (2012).
283. Lima, C. F. *et al.* Impaired socio-emotional processing in a developmental music disorder. *Sci. Rep.* **6**, 34911 (2016).
284. Sihvonen, A. J. *et al.* Music-based interventions in neurological rehabilitation. *Lancet Neurol.* **16**, 648-660 (2017).

Annales Universitatis Turkuensis



Turun yliopisto
University of Turku

ISBN 978-951-29-7262-3 (PRINT)
ISBN 978-951-29-7263-0 (PDF)
ISSN 0355-9483 (Print)
ISSN 2343-3213 (Online)